The mannose receptor influences antigen-presenting cells by direct interaction with CD45R0

Dissertation

zur

Erlangung des Doktorgrades (Dr. rer. nat.)

der

Mathematisch-Naturwissenschaftlichen Fakultät

der

Rheinischen Friedrich-Wilhelms-Universität Bonn

vorgelegt von

Maria Katharina Embgenbroich

Bonn, Januar 2017

Angefertigt mit Genehmigung der Mathematisch-Naturwissenschaftlichen Fakultät
der Rheinischen Friedrich-Wilhelms-Universität Bonn

1. Gutachter: Prof. Dr. Sven Burgdorf
2. Gutachter: PD Dr. Heike Weighardt
Tag der Promotion: 06.04.2017
Erscheinungsjahr: 2017

Table of content

1. Abstract

The immune system has to manage the critical decision to induce either immunity or tolerance. Cells that take part in the regulatory processes of the immune system are amongst others antigen presenting cells (APCs), especially dendritic cells (DCs) and macrophages (MΦs). Recently, it was shown that the mannose receptor (MR), known as an endocytic receptor expressed by specific APCs, is responsible for the induction of T cell tolerance. Under non-inflammatory conditions, the MR expressed by DCs can bind to CD45 on $CD8^+$ T cells. The interaction of MR and CD45 induces the inhibition of CD45 phosphatase activity. Thereby, transcriptional T cell re-programming and up-regulation of CTLA-4 in T cells are initiated resulting in T cell tolerance.
As CD45 is not only expressed by T cells but by all hematopoietic cells including APCs, the aim of this thesis was to investigate a putative influence of the MR on APCs by interaction with CD45.

We could show that GM-CSF induced, bone marrow derived APCs (BM(GM-CSF) cells) express the lowest molecular isoform of CD45, CD45R0, that interacted with a recombinant MR construct comprising the CR, FN II, and CTLD1-2 domains of the MR (FcMR). This interaction impaired CD45 phosphatase activity in BM(GM-CSF) cells and altered intracellular signalling pathways. The capacity of APCs to stimulate antigen-specific T cells was altered by binding of FcMR to CD45. Antigen-specific T cells primed by FcMR pre-stimulated APCs showed reduced cytokine secretion of $CD4^+$ T cells determined by IFN-γ levels and diminished cytotoxic activity of $CD8^+$ T cells, although, proliferation of T cells remained unaffected.
In addition, the application of supernatant containing soluble mannose receptor (sMR), that is shed by MR-positive cells, to stimulate BM(GM-CSF) cells also decreases CD45 phosphatase activity but in contrast supports an immunstimulatory phenotype of activated antigen-specific T cells.
Recently, sMR was found to be highly elevated in several diseases. Here, we could show enhanced sMR serum levels after high-fat died or obesity in mice and human, respectively, pointing out a direct correlation of sMR expression and inflammatory metabolic processes.

2. Introduction

2.1. The immune system

The human body has to constantly manage the invasion of a multitude of different microbes e.g. bacteria, viruses, fungi, and parasites, to maintain a certain state of health [1]. Thereby, discriminating between healthy and infected cells, while pathogens evolve and adapt rapidly to circumvent the detection and neutralization by the immune system, is the main challenge for the host organism [1–3]. Due to this evolutionary pressure, a complex network of interacting cell types with various effector functions has developed [3]. Two different systems, the innate and the adaptive immune system, can be distinguished in regard to speed and specificity of their responses [4].

2.1.1. The innate immune system

An innate immune system is found in all multicellular organisms [3]. It acts at early stages of infection [5] when pathogens break through the physical and chemical barriers of the skin. The innate immune system is composed of different cell types (e.g. neutrophils, macrophages, and natural killer cells) [4,6] as well as immunoregulatory components (e.g. the complement, cytokines like interferons, and acute phase proteins) [4,7]. It reacts fast and thereby prevents antigen-spreading but it is antigen-nonspecific [6]. Cells of the innate immune system recognize pathogens by germline-encoded pathogen recognition receptors (PRRs) [1,3,5]. PRRs recognize highly conserved structures associated and shared by a large group of pathogens [1,5]. These so-called pathogen associated molecular patterns (PAMPs) differ between microbes. E.g. gram-positive and gram-negative bacteria are recognized by bacterial wall components like LPS [3,6,7] or by bacterial DNA with unmethylated CpG motifs [1]. In contrast, viruses are recognized by double-stranded RNA [3,6] and yeasts by carbohydrates like cell wall mannan [3,6].

2.1.2. The adaptive immune system

An adaptive immune system is a hallmark of higher vertebrates [4]. It consists mainly of B and T cells bearing high affinity receptors, which enable the host organism to the antigen-specific recognition and elimination of pathogens [4,5] but also depends on antigen presenting cells (APCs), especially dendritic cells (DCs) and macrophages (MΦs), at the interface of innate and adaptive immune system [4]. The antigen-specific receptors of B and T cells are not germline-encoded but rather a result of random gene arrangement

and splicing leading to a repertoire of over 10^{10} antibody specificities [4]. The APCs take up pathogens at the side of invasion, migrate to secondary lymphoid organs, where the clonal selection and expansion of B and T cells is carried out, and present pathogen-related antigens on their surface to activate antigen-specific T cells [3–5]. The clonal expansion is the explosive increase in lymphocytes where all progeny bear the same antigen specificity. Due to the whole activation cascade, the adaptive immune response is time-consuming [4] and has the ability of an immunological memory [6]. DCs play a unique role because they are able to prime naive T cells and thereby induce the primary immune response [6,7].

2.2. Dendritic cells

DCs develop from progenitors in the bone marrow. As precursors they circulate through blood, lymphatics, and lymphoid tissues. Some DCs remain in peripheral tissues, where they have a high endocytic and phagocytic capacity important for example after tissue damage [6–8]. Once danger signals like microbial products, infectious agents, or inflammatory products are recognized by DCs, they start to mature [8,9]. This maturation is crucial for the initiation of immunity [8]. Surface molecules like major histocompatibility complex (MHC) and costimulatory molecules (cluster of differentiation (CD) 40, CD80, CD86) for antigen presentation and T cell activation are upregulated whereas endocytic and phagocytic capacity is downregulated. During maturation, DCs migrate to secondary lymphoid organs where they present antigens and thereby activate $CD4^+$ and $CD8^+$ T cells [7,8]. Afterwards, T cells are able to leave the lymphoid organs, migrate to the site of infection and start to eliminate invading pathogens (see Figure 1).

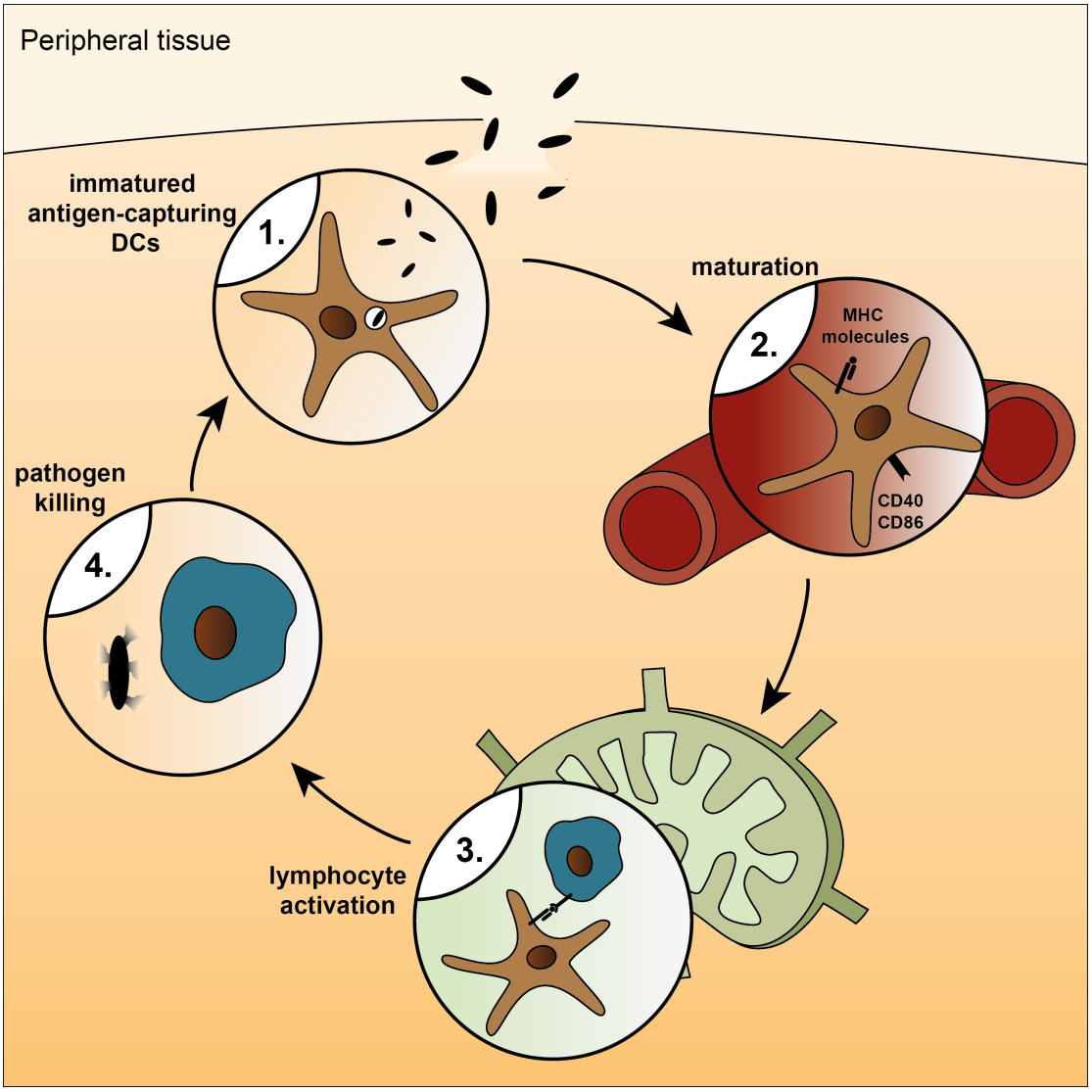

Figure 1: Initiation of adaptive immunity by the example of CD8$^+$ T cells. Immature DCs capture and process antigen in peripheral tissues if pathogens enter the body. Afterwards, DCs start to mature while they migrate to secondary lymphoid organs, that means upregulation of MHC and costimulatory (CD40, CD80, CD86) molecules and downregulation of endocytotic capacity. In the lymphoid organ, DCs activate antigen-specific naïve CD8$^+$ T cells. Activated T cells start to proliferate and leave the secondary lymphoid organ to eliminate pathogens in the peripheral tissues.

DCs are initiator as well as modulator of the adaptive immune response [8]. Multiple subsets of DCs exist generating a heterogeneous cell population [7]. Each DC subgroup expresses distinct surface molecules and secretes different cytokines [9]. Thereby, DCs can not only induce immunity but also confer to the host's tolerance preventing autoimmunity [6,8]. The immune stimulatory and inhibitory potential of DCs contributes to disease pathogenesis (e.g. organ transplantation, allergy, and autoimmunity) [7]. Therefore, DCs are of special interest as targets for clinical trials [8].

2.3. Antigen presentation

To activate naïve T cells, antigens need to be processed and presented on MHC molecules by APCs [8]. The process of antigen presentation comprises the uptake, degradation, and loading of antigen on MHC molecules [9].

APCs incorporate particles or soluble antigens by phagocytosis or macropinocytosis, respectively. Furthermore, they express a wide range of surface receptors e.g. Fc-receptors or C-type lectins like the mannose receptor (MR) for receptor-mediated antigen uptake [7,9]. Both, endogenous and exogenous antigens are degraded by the proteasome in the cytosol or by enzymes via the endocytic and phagocytic pathway [7,10].

Proteins degraded by proteasomal proteolysis are loaded onto MHC class I molecules in the endoplasmic reticulum (ER). The antigens result from intracellular proteins such as viral proteins, as well as from phagocytosis [10]. A process called cross-presentation also enables the uptake, degradation, and loading of extracellular antigens on MHC I molecules in stable early endosomes (SEE) or the ER after receptor-mediated endocytosis e.g. by the mannose receptor (see Figure 2). This plays an important role for the recognition of transplant- and tumor-derived antigens as well as antigens from viruses that cannot infect APCs [8,11]. Only MHC I-bound peptides are recognized by cytotoxic $CD8^+$ T cells and this recognition is essential for their activation [4,7,8].

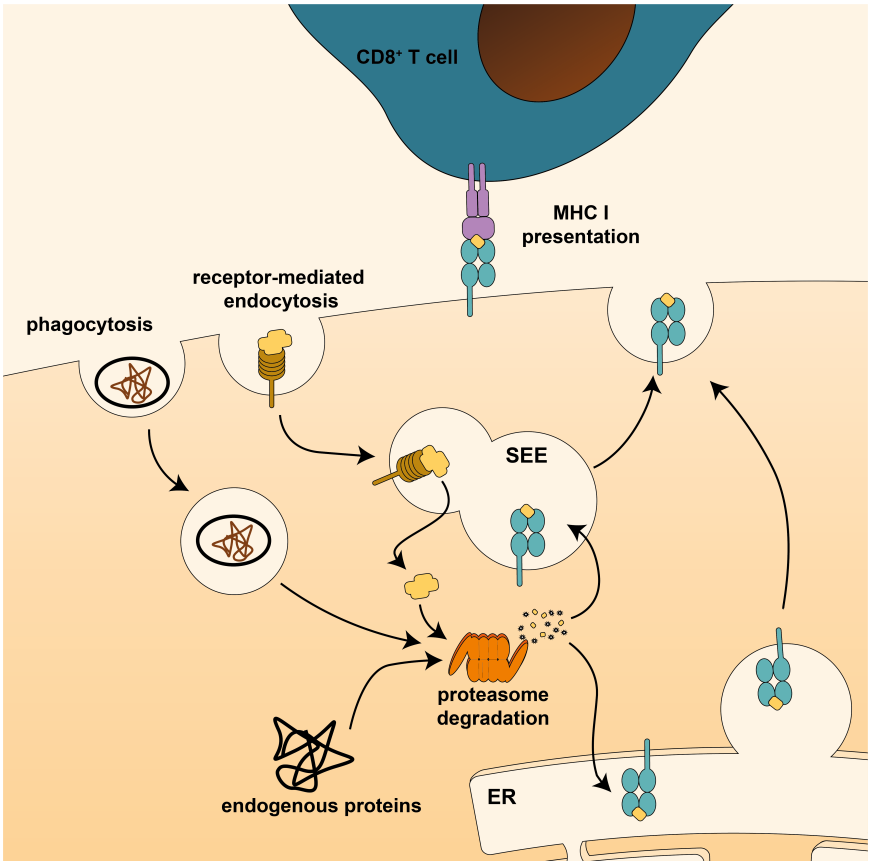

Figure 2: Antigen processing for MHC class I presentation. Intracellular proteins or antigens from phagocytosis are degraded in the cytoplasm by the proteasome, transported to the ER and loaded onto MHC I molecules. Peptide/MHC I complexes are transmitted to the cell surface where they can activate $CD8^+$ T cells. Exogenous antigens taken up by receptor-mediated endocytosis e.g. by the mannose receptor, are transported to stable early endosomes (SEE) from where they are translocated to the cytoplasm and also degraded by the proteasome. Peptides are reimported in the SEE or in the ER for loading onto MHC I molecules and the MHC I/peptide complexes are transported to the cell surface. This process is called cross-presentation.

Antigens of lysosomal proteolysis are loaded onto MHC II molecules. These peptide-MHC complexes are recognized by $CD4^+$ T helper cells [4,7,8]. Exogenous antigens taken up by macropinocytosis and endocytosis are delivered to late endosomal structures but also endogenous antigens can be transported to endosomal compartments by macroautophagy and chaperone-mediated autophagy [10,12] (**Figure 3**).

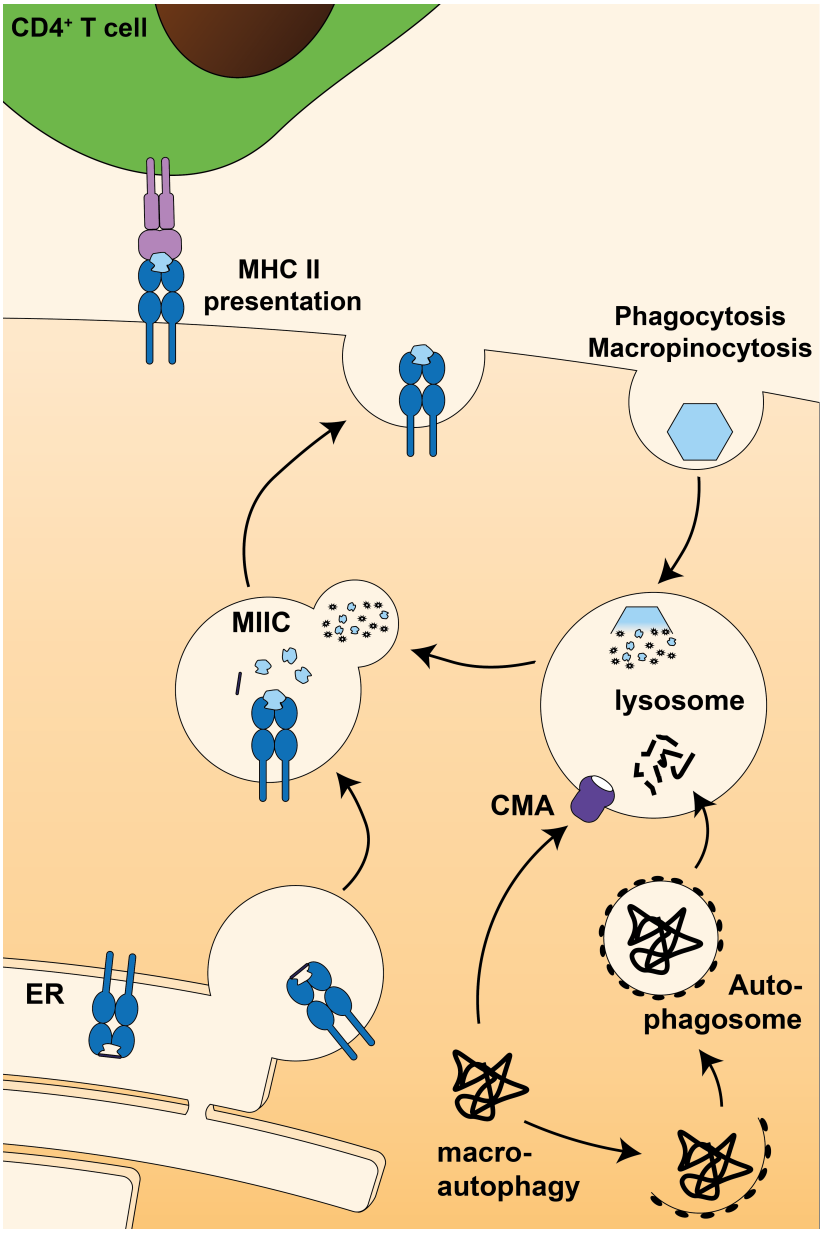

Figure 3: Antigen processing for MHC class II presentation. Antigens for MHC II presentation are generated by proteolysis in lysosomes and reach these compartments through different pathways. (i) Exogenous antigens captured by phagocytosis or macropinocytosis are transported to lysosomes. (ii) Endogenous antigens are engulfed by an isolated membrane generating an autophagosome. These vesicles readily fuse to lysosomes. (iii) Endogenous proteins can be recognized by heat shock proteins that guide antigens for membrane translocation and entry into lysosomes via chaperone-mediated autophagy (CMA). In lysosomes, proteases facilitate the digestion of captured antigens. These late-endosomale structures fuse with MHC class II-rich compartments (MIIC) coming from the ER. Peptides are loaded onto MHC II molecules, transported to the cell surface and activate $CD4^+$ T cells.

2.4. Three signals for T cell activation

The productive activation of naïve T cells needs three signals from APCs.

First, the recognition of MHC/peptide complexes on the cell surface of APCs by antigen-specific T cell receptor (TCR) of T cells [3,7].

Second, the interaction of costimulatory molecules expressed by APCs (CD40, CD80, CD86) with ligands and counterreceptors on T cells (CD28, CD40L) [1,3,7]. Off note, the presentation of antigens in the absence of costimulatory molecules leads to the permanent inactivation of T cells [3].

Third, cytokines released by APCs (e.g. interleukin (IL)-12) can induce different classes of immune response and are critical for T cell differentiation [7] (see Figure 4).

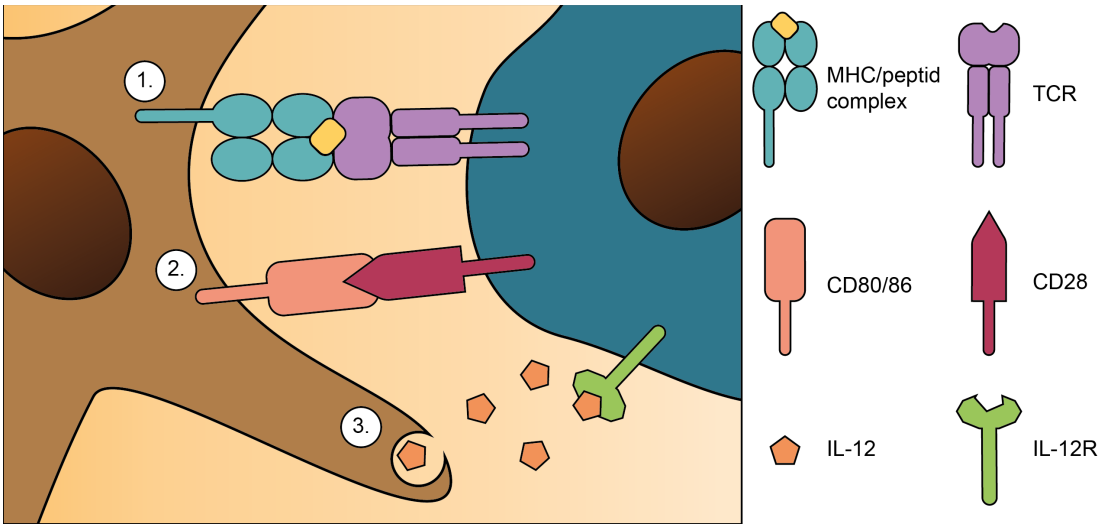

Figure 4: Three signals crucial for T cell activation. Three signals are important for full activation of T cells. Signal one is the binding of MHC/peptid complex to T cell receptor (TCR). Signal two is the interaction of costimulatory molecules (e.g. CD80/86) of APCs with its counterreceptor of T cells (e.g. CD28). For signal three APCs release cytokines (e.g. IL-12) that bind to cytokine receptors (e.g. IL-12R) on T cells.

The combination of the three signals leads to the clonal expansion and differentiation of T cells into effector and memory cells [13].

2.5. Initiation of T cell activation

To maintain the healthy state of the body a proper function of T cells is essential. This function is mediated by a direct cell-cell interaction or via the secretion of various cytokines. Deviations in the function of T cells lead to immunological diseases e.g. autoimmunity, allergies, or immunodeficiencies [14].

2.5.1. CD4$^+$ T cell effector mechanisms

CD4$^+$ T helper cells recognize foreign antigens presented by MHC class II molecules on APCs [4]. Once activated, CD4$^+$ T cells produce cytokines important for activating other cells of the cell-mediated immune response, e.g. MΦs or B cells. Due to the function of CD4$^+$ T cells to activate a wide range of effector cells, the stimulation of CD4$^+$ T cells is highly controlled. Thus, only a small number of cells express MHC II molecules [4].

The cytokine environment secreted by APCs mainly dictates the development of specialized effector T helper cells (see Figure 5). Depending on the production of signature cytokines that are secreted by effector T cells, CD4$^+$ T cells are subdivided into Th1, Th2, Th9, Th17, T follicular-helper (T_{FH}), and T-regulatory (T_{reg}) cells [15]. All subsets show diverse functions. Th1 cells secrete among other IFN-γ facilitating clearance of intracellular pathogens. Th2 cells secrete e.g. IL-4, IL-5, and IL-13, and thereby promoting clearance of extracellular organisms especially parasites [15]. Th17 and T_{reg} cells contribute to tissue inflammation, whereas Th17 cells induce autoimmune tissue injury by secreting IL-17. T_{reg} cells inhibit autoimmunity and tissue injury. Furthermore, T_{reg} cells also suppress other T cell subsets by secreting IL-10 [16]. Th9 and T_{FH} cell function is not entirely clear but the cells might contribute to both protective immunity and immune-mediated inflammatory diseases [15,17].

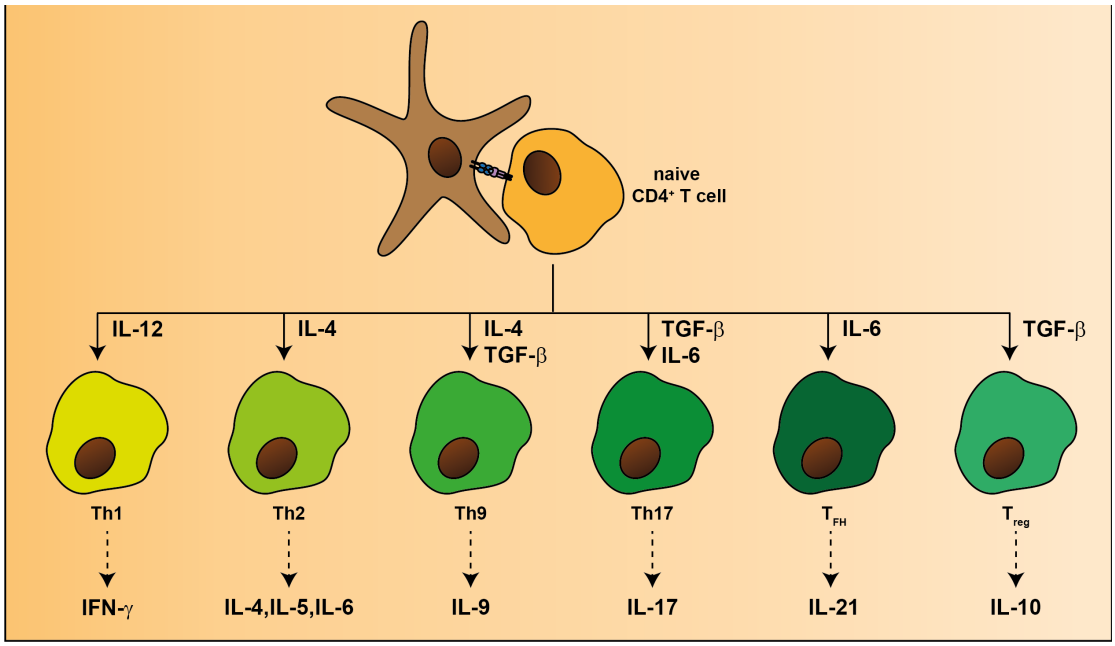

Figure 5: CD4$^+$ T cell effector mechanisms. Binding of T cell receptor to the MHC II/peptide complex presented by APCs activates naïve CD4$^+$ T cells. The cytokine environment generated by APCs promotes the development of effector CD4$^+$ T helper cells. Once activated, T helper cell subsets are identified by their signature cytokine production facilitating diverse effector functions.

2.5.2. CD8$^+$ T cell effector mechanisms

Cytotoxic CD8$^+$ T cells are activated by peptides presented on MHC class I molecules which are expressed on all nucleated cells [4]. Via MHC class I molecules, these cells present endogenous self-antigens as well as virus, intracellular pathogens, and abnormal tumor antigens. Cells presenting the T cell-specific pathogen-related peptide get directly eliminated by CD8$^+$ T cells [4,8]. The cytotoxic T cells secrete perforin and granzymes to penetrate the membrane and induce DNA fragmentation and cell apoptosis, respectively (see Figure 6). Additionally, cytotoxic T cells express Fas molecules that bind to Fas receptors on target cells and promote also apoptosis [4].

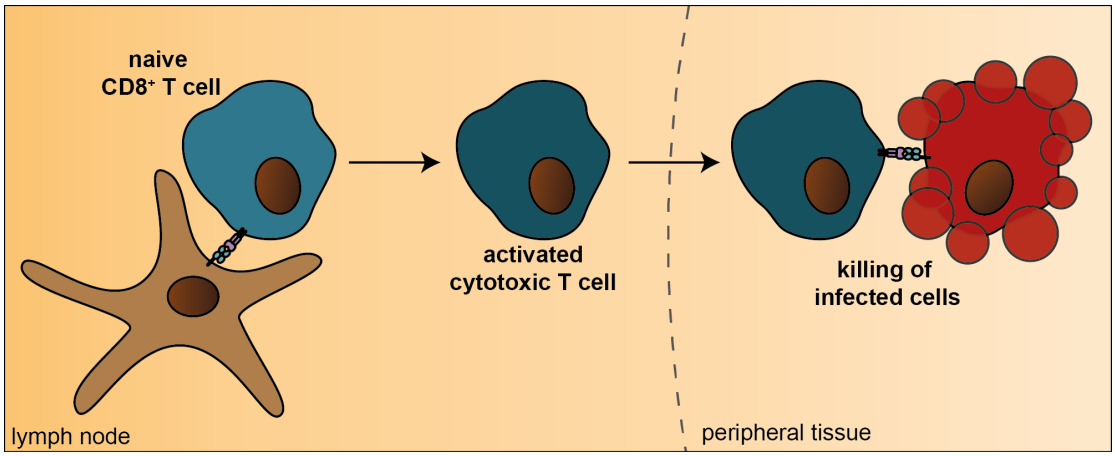

Figure 6: CD8$^+$ T cell effector mechanism. Binding of T cell receptor to MHC I/peptide complex presented by APCs in the lymph node activates naïve CD8$^+$ T cells. Once activated, cytotoxic T cell (CTL) recognize infected cells by bearing foreign peptides on MHC I in peripheral tissues. CTLs secrete perforin and granzymes that induce DNA fragmentation and apoptosis of the target cell. Furthermore, the Fas/Fas ligand pathway gets activated in the target cell also leading to apoptosis.

2.6. TCR signaling

The activation of T cells is initiated by a signal transduction induced by binding of TCR to peptide-MHC complex [18].

The TCR is a transmembrane receptor comprised of two different subunits: The α and β chain. In <10% of T cells the TCR is made up from a γ and a δ chain, a subgroup of T cells which specific function is still elusive [4]. The TCR is associated with CD3 which consists of two ε, a γ and a δ chain and two ζ chains that are important for the transduction of the signal generated by ligand binding [14,19].

After interaction of TCR with peptid/MHC complex, coreceptor CD4 or CD8 binds to MHC molecules and thereby brings the Src family protein tyrosine kinase (PTK) Lck into the proximity of cytoplasmic domains of the TCR. Lck phosphorylates

immunoreceptor tyrosine-based activation motifs (ITAMs) of the TCR [14] that provides docking sites for the SH2 domains of ZAP-70. The Syk family PTK ZAP-70 gets phosphorylated and activated by Lck and can then phosphorylates the adaptor proteins SLP-76 and LAT. This leads to the phosphorylation and activation of multiple downstream effectors resulting in calcium mobilization, activation of mitogen-activated protein kinases (MAPKs), transcriptional regulation and cytoskeletal rearrangement (Figure 7) [14,18,20,21].

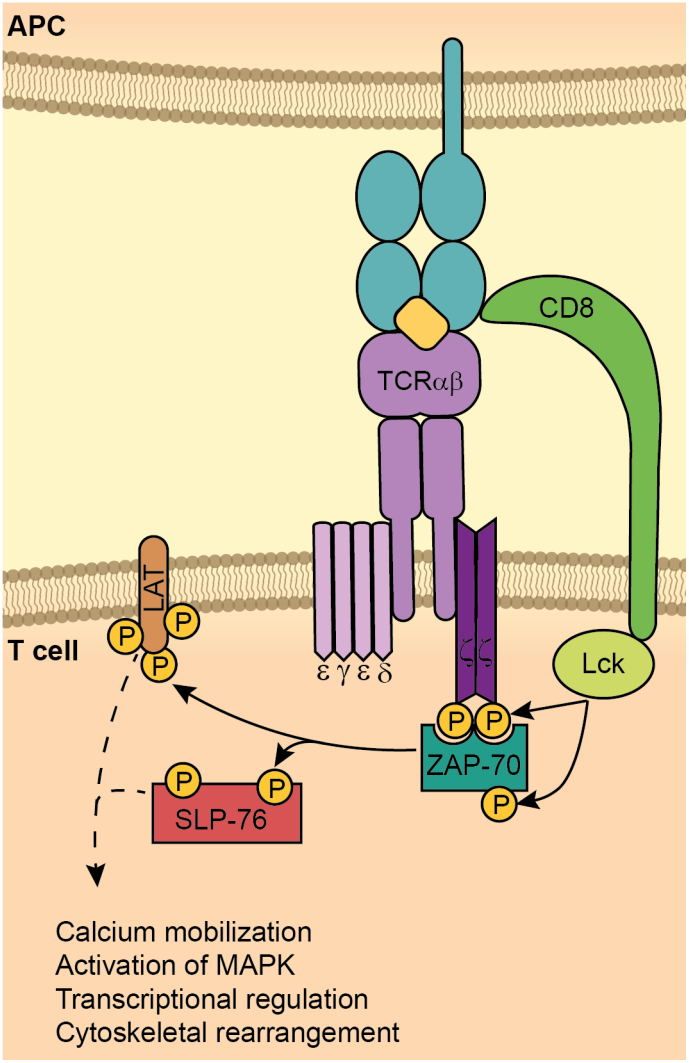

Figure 7: T cell receptor signaling. The T cell receptor (TCR) on T cells binds to peptide/MHC I complex on APCs. The interaction enables the binding of CD8 to MHC molecules whereby Lck comes in close proximity to TCR. Lck phosphorylates ITAMs in ζ chains of TCR whereby ZAP-70 could be recruited to TCR. ZAP-70 gets activated by phosphorylation through Lck and could then phosphorylates LAT and SLP-76. Phosphorylation of these molecules initiates downstream signaling cascades leading to calcium mobilization, activation of MAPKs, transcriptional regulation and cytoskeletal rearrangement.

The natural counterparts of PTKs are protein tyrosine phosphatases (PTPs). PTPs dephosphorylate proteins and reduce or enhance their function depending on the phosphorylation site and signalling context [18]. The activity of Lck, the first PTK downstream of TCR, is highly regulated by PTPs. An inhibitory C-terminal site of Lck (Y505) can be phosphorylated by Csk and dephosphorylated by CD45. Furthermore, the PTPs LYP and SHP-1 can dephosphorylate an activating tyrosine (Y394) within the catalytic domain. The balance between the activities of PTPs and PTKs is responsible for the initiation of signalling [18].

2.7. CD45

CD45 is a leukocyte-specific high-molecular-weight surface glycoprotein. It covers ~10% of the cell surface and is, thereby, the most abundant cell surface glycoprotein in leukocytes. The glycosylation pattern varies between cell types and depends on developmental and activation state as well as differential spliced exons. The differences in carbohydrate structures imply a functional consequence [22].

CD45 is encoded by 34 exons. Different isoforms are generated by alternative splicing of three exons (4, 5 and 6). To date, five isoforms have been detected at the protein level in human leukocytes. CD45 consists of a large cytoplasmic domain, a single membrane-spanning domain and an N-terminal, external domain of variable length [22] (see Figure 8).

The intracellular part of CD45 has two tandemly duplicated PTPase homology domains. The membrane-proximal domain D1 has enzymatic activity [23] and is necessary for TCR-mediated signal transduction shown by experiments in a CD45-deficient cell line [24]. The function of the second intracellular domain D2 remains elusive. Some studies have indicated that the D2 domain might be essential for D1 PTP activity [25,26].

The extracellular part of CD45 consists of a cysteine-rich region, three fibronectin type III repeats and the alternatively spliced exons [23,27]. The molecular weight of CD45 differs between 180-240 kDa depending on the isoform.

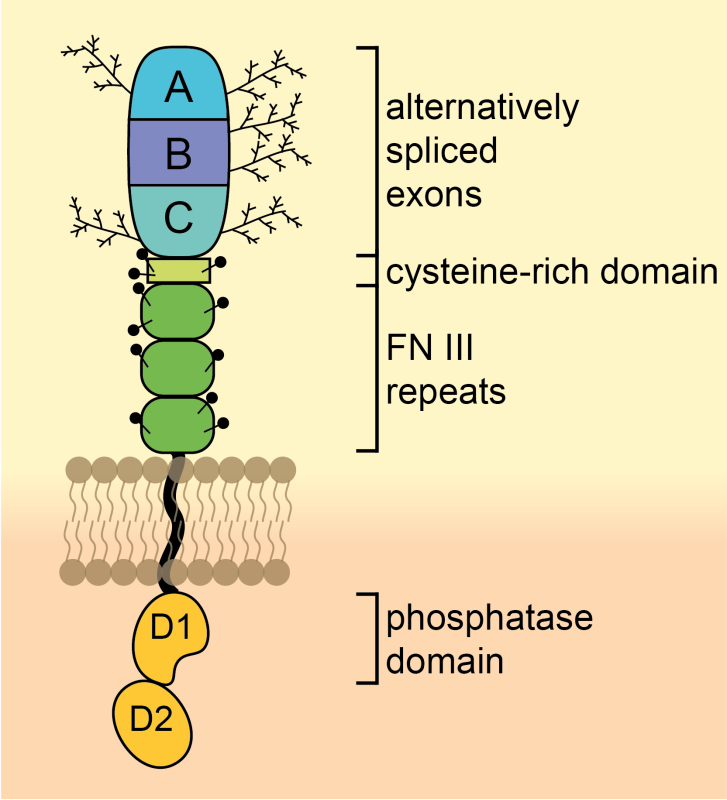

Figure 8: Structure of CD45. The protein tyrosine phosphatase (PTPase) CD45 consists of a large cytoplasmic domain, a single membrane-spanning domain and an external domain of variable length. Intracellular, the D1 domain, one of two tandemly duplicated PTPase homology domains, has phosphatase activity. The D2 domain is thought to be essential for D1 PTPase activity. The extracellular, highly glycosylated part of CD45 consists of three fibronectin type III (FN III) repeats, a cysteine-rich domain and three alternatively spliced exons.

The extracellular conserved part of CD45 is heavily N-glycosylated with sugars of tetra- and triantennary complex-type as well as poly (N-acetyllactosamine) groups and α-2,6-linked sialic acid residues. The exterior domain has multiple sites for core 1 and 2 O-linked carbohydrates variable modified by sialic acid. Therefore, the various isoforms differ in size, shape, and charge [22,23].

A specific juxtamembrane 'wedge' motif seems to be involved in trans-dimerization of CD45 leading to inhibition of activity [18,23]. An inactivating point mutation (CD45E613R) in the inhibitory wedge motif generates a constitutively active form resulting in an autoimmune syndrome resembling human systemic lupus erythematosus (SLE) [28]. Although all isoforms show identical PTPase activity, *in vitro*, the isoforms homodimerize differently [23].

The function of CD45 differs between leukocytes. In B cells, CD45 is a critical regulator of BCR signalling. In mast cells, CD45 is important in histamine degranulation after IgE receptor cross-linking [23] and in neutrophils CD45 influences chemotaxis [29].

CD45-deficient MΦs revealed a role of CD45 in integrin-mediated adhesion and in regulation of Hck and Lyn activity [30].

Reduction of CD45 activity in DCs lead to enhanced adhesion due to strong cell cluster [31,32]. However, Prickett et al. (1989) showed reduced cluster stability in the presence of a CD45 antibody [33]. Furthermore, in DCs, CD45 has a positive as well as negative effect on TLR-induced cytokine secretion [34–36].

In T cells, CD45 has a pivotal role in signal transduction by acting as a positive and negative regulator of Src family protein tyrosine kinases (SFKs). In $CD45^{-/-}$ mice the majority of peripheral T cells are self-reactive due to hyporesponsiveness to antigen stimulation [37]. Furthermore, CD45-deficient humans [38,39] or mice [40–42] develop a severe-combined immunodeficiency (SCID) phenotype due to defects in thymic development [23]. Other data of CD45-deficient mice suggest also a negative regulatory function of CD45 [43–46]. CD45 can indirectly inhibit T cell function by upregulating the expression of the inhibitory co-receptor CTLA-4 [47]. Janus kinases (JAKs) are other substrates of CD45, which dephosphorylated by CD45 negatively regulate cytokine and interferon receptor activation [48–50].

Ligands of CD45 are e.g. Galectin-1 [51] or the C-type lectin MGL [52]. In 1999 Martinez-Pomares et al. published the MΦ mannose receptor (MR) as counter-receptor of CD45 [53].

2.8. Mannose receptor (MR)

The MR is a 180 kDa transmembrane, carbohydrate-specific PRR expressed by diverse subpopulations of MΦs and DCs as well as nonvascular endothelium [54,55]. It is part of the C-type lectin family of PRRs [56] and shares the same overall structure: extracellular a N-terminal cysteine-rich (CR) domain, a single fibronectin type II (FN) domain, and multiple C-type lectin-like domains (CTLDs); a type I membrane domain; intracellular a short cytoplasmic domain (see Figure 9). Other members of this family are e.g. DEC205, phospholipase A2 and Endo180.

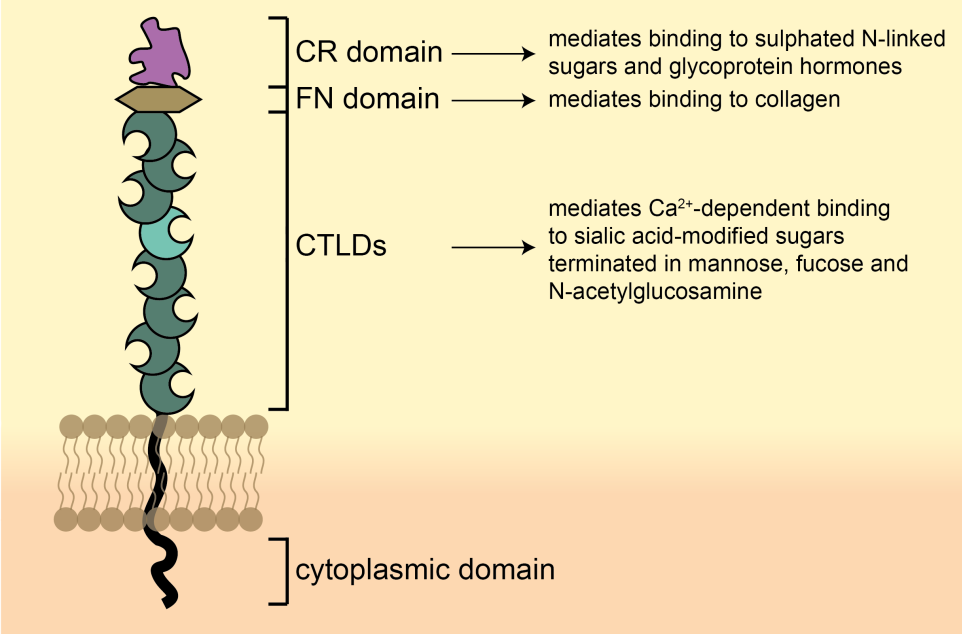

Figure 9: Structure and binding properties of MR. The MR is a type I transmembrane protein with a large extracellular part containing three different types of domains. A cysteine-rich (CR) domain is followed by a fibronectin type II (FN) domain and eight C-type lectin-like domains (CTLDs). The CR domain mediates the binding to sulphated N-linked carbohydrates and glycoprotein hormones like lutropin and thyrotropin. The FN domain binds collagen and of the eight CTLDs only 4 and 5 has carbohydrate-binding capacity. In a calcium-dependent manner, the CTLD 4 recognizes sialic acid-modified carbohydrates terminated in mannose, fucose and N-acetylglucosamine. The cytoplasmic domain contains a motif important for endocytic function.

The CR region of the MR is capable to bind sulphated sugars like N-acetylgalactosamine [57] and glycoprotein hormones like lutropin and thyrotropin [55] in a calcium-independent manner. Its binding capacity is enhanced by multimerization [58]. The CR domain also binds to ligands expressed by the marginal zone metallophilic MΦs in the spleen and subcapsular sinus MΦs in lymph nodes [59]. Investigated ligands are e.g. sulphated forms of sialoadhesin and CD45 [53].

The FN II domain is known for its binding of collagen. In human and mouse, MΦs [60,61] as well as in liver sinusoidal endothelial cells [62] collagen is endocytosed through the MR.

The MR has eight CTLDs. Nevertheless, only CTLD4 and 5 have carbohydrate-binding ability [55]. In a calcium-dependent manner, the CTLDs recognize carbohydrates terminated in mannose, fucose and N-acetylglucosamine that are modified with sialic acid [54].

A tyrosine-based motif in the cytoplasmic domain is required for receptor internalization and recycling [63,64].

The MR undergoes proteolytic processing resulting in a functional, soluble form of the MR (sMR) [54]. The sMR consist of the complete extracellular region and is generated after

cleavage by metalloproteases [65]. Fungal pathogens such as *Candida albicans*, *Aspergillus fumigatus* and *Pneumocystis carinii* can enhance the production of the sMR [66,67]. The binding capacity of sMR is still functional but recognition of sulphated carbohydrates by the CR domain requires protein multimerization [54]. sMR is found in supernatant of MR-positive cells as well as in mouse [65] and human serum [68]. In several diseases including sepsis, liver disease, and multiple myeloma, sMR is strongly elevated and, therefore sMR is seen as a new biomarker [68–70].

The well-known function of the MR is the internalization of glycoconjugates of pathogenic origin as well as self-molecules. Under inflammatory conditions, mannosylated proteins are taken up by the MR and conducted in compartments specialized for cross-presentation. These SEEs allow the export of proteins to the cytoplasm for degradation by the proteasome and the relocation in the SEEs for loading on MHC I molecules. The MHC I/peptid complex is translocated to the cell membrane to activate antigen-specific $CD8^+$ T cells (see Figure 2) [71]. Due to this mechanism, the MR facilitates the immune response against pathogens.

Under non-inflammatory conditions, the MR has also an immunregulatory function. The MR is expressed by a multitude of tolerogenic APCs. Its expression is upregulated by anti-inflammatory cytokines like IL-4 and IL-10 [72,73]. As it was shown by various studies, the MR-dependent antigen uptake can lead to tolerance. For example, the treatment of experimental autoimmune encephalomyelitis (EAE) mice with a soluble mannosylated epitope of proteolipid protein ($M\text{-}PLP_{139\text{-}151}$) generates antigen-specific tolerogenic T cells [74]. Additionally, monocyte-derived DCs that are treated with an anti-MR crosslinking antibody secrete an anti-inflammatory cytokine profile resulting in regulatory T cells and T cell anergy [75]. MR-expressing $CD11b^+CD11c^-$ cells in the mucosa generated suppressive $CD4^+$ T cells after sublingual immunotherapy (SLIT) [76]. Furthermore, tumoral mucins that are taken up by the MR as well as anti-MR antibodies result in an immune suppressive cytokine profile in human tumor-associated MΦs [77]. In line with this, systemically circulating tumor antigens processed in a MR-dependent manner by liver sinusoidal endothelial cells (LSECs) promote $CD8^+$ T cell tolerance [78].

Besides the tolerogenic properties due to MR-dependent antigen uptake, the MR can directly initiate T cell tolerance. The presence of MR on the surface of APCs directly impairs the cytotoxic activity of $CD8^+$ T cells *in vitro* and *in vivo*.

Under non-inflammatory conditions, $CD8^+$ T cells activated by APCs in the presence of MR display decreased cytotoxic activity and IFN-γ secretion compared to T cells activated in the absence of MR. These diminished effector functions are due to a direct interaction of the MR with CD45 on T cells. The interaction impairs CD45 phosphatase activity leading to an active reprogramming of T cells. The crucial step of inactivating CD45 enables a signalling pathway in addition to T cell receptor signalling that reduces the expression of Bcl-6 facilitating the up-regulation of CTLA-4. High protein levels of CTLA-4 in T cells activated by MR-bearing APCs lead to $CD8^+$ T cell tolerance [79] (Figure 10).

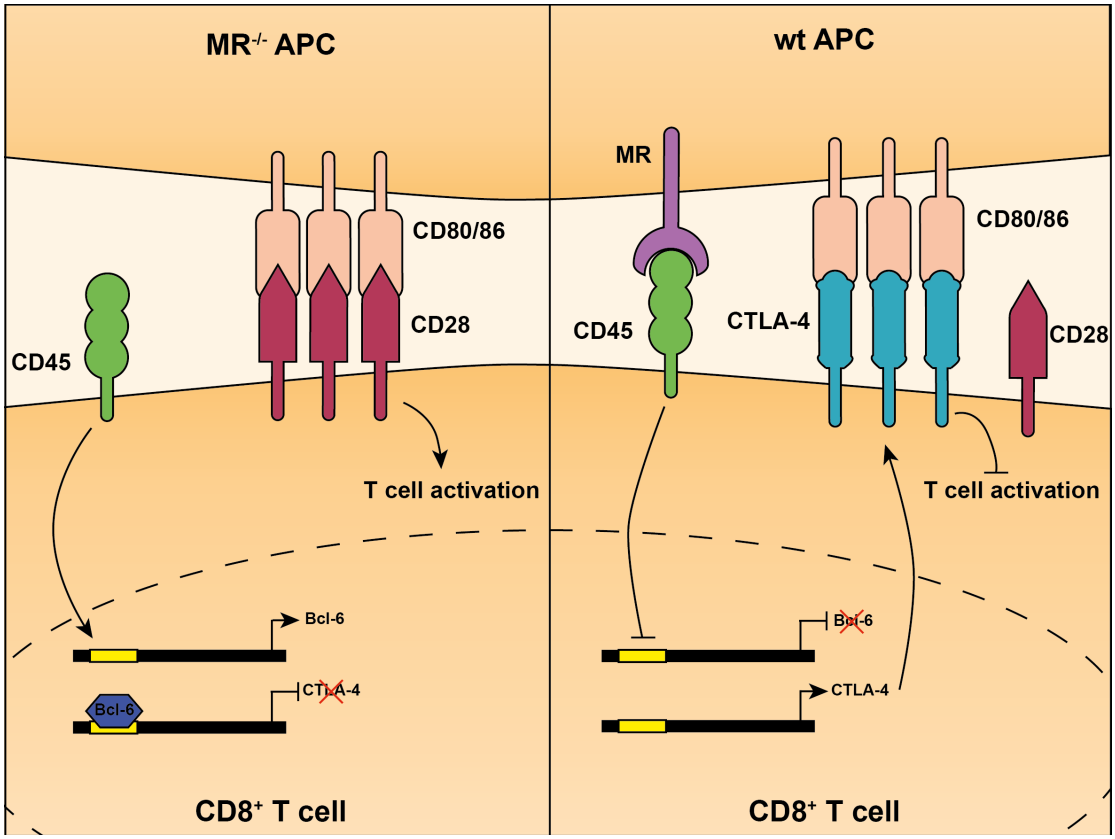

Figure 10: MR-mediated induction of T cell tolerance in $CD8^+$ T cells via inhibition of CD45 and up-regulation of CTLA-4. In the absence of the MR CD45 phosphatase of $CD8^+$ T cells is active and facilitate expression of Bcl-6. Bcl-6 is a repressor of transcription and inhibits transcription of CTLA-4. Reduced expression of CTLA-4 enables costimulation via CD80/86 binding to CD28 and promotes T cell activation (left panel). In the presence of MR, MR binds to CD45 on $CD8^+$ T cells and inhibits CD45 phosphatase activity. Expression of Bcl-6 is inhibited that enables transcription of CTLA-4. Up-regulation of CTLA-4 on the surface of $CD8^+$ T cells interrupts costimulation via CD28 and thereby, inhibits T cell activation (right panel).

3. Aim of the thesis

The MR in a cell-bound form is able to induce T cell tolerance by up-regulation of CTLA-4 in $CD8^+$ T cells through direct binding of CD45 [79]. CD45 is expressed by all lymphocytes including antigen presenting cells (APCs) [23]. APCs take part in the regulation of critical decisions of the immune system to induce either T cell activation or tolerance. We hypothesized an MR-mediated influence on the function of APCs by interaction of MR with CD45 on APCs. The aim of the following study was to analyse an effect of the MR on APC capacity.

As a model, GM-CSF-induced, bone-marrow derived APCs (BM(GM-CSF)) were used. First, the expression of CD45 on these cells as well as the expressed isoform should be analysed. To investigate an influence of MR on APC function a recombinant mannose receptor (MR) construct comprising the CR, FN II, and CTLD1-2 domain of the MR fused to a human IgG1 Fc part (FcMR) was used. By using FcMR an interaction with CD45 on APCs as well as an influence on CD45 phosphatase activity should be investigated. Furthermore, the stimulation of APCs with FcMR should elucidate an effect of MR on APCs by analysing the effector function of $CD4^+$ as well as $CD8^+$ T cells activated by pre-stimulated APCs.

Beside the cell-bound form of the MR, a soluble protein (sMR) is generated by proteolytic cleavage through metalloproteases [65]. The secretion of sMR by BM(GM-CSF) cells in cell supernatant should be analysed. Additionally, this natural source of MR should also be used to investigate an influence of MR on APCs performing CD45 phosphatase activity assays and effector functions of activated $CD4^+$ and $CD8^+$ T cells.

This sMR is also found in the serum of mice [65] and human [68] and is strongly elevated in several diseases [68–70]. Therefor, the levels of sMR *in vivo* in serum of mice fed a low-fat diet (LFD) or high-fat diet (HFD) as well as of lean and obese humans should be analysed.

4. Material and Methods

4.1. Material

4.1.1. Mouse strains

Strain	Description	Background	Haplotyp
C57BL/6JCrl	Wild type mouse strain	C57BL/6JCrl	H-2K^b
DesTCR	Transgenic mouse strain with a K^b-specific T cell receptor (KB5.C20 TCR) in CD8$^+$ thymocytes. T cells recognize endogenous processed peptides presented on H-2K^b in an allogenic reaction [80]	B10.BR	H-2K^k
MR-KO	Transgenic mouse strain with an insertion of a stop-codon in exon 1 of mannose receptor preventing its expression [81]	C57BL/6JCrl	H-2K^b
OT-I/RAG-KO	Transgenic mouse strain with expression of an OVA$_{257-264}$ CD8$^+$ specific MHC class I H-2K^b TCR [82,83]	C57BL/6	H-2K^b
OT-II	Transgenic mouse strain with expression of an OVA$_{323-339}$ CD4$^+$ specific MHC class II I-Ab-restricted TCR [84]	C57BL/6	H-2^b

4.1.2. Cell lines

Cell line	Description	Culture medium
HEK293T	Human embryonic kidney cell line immortalized by adenovirus type 5 DNA [85]	HEK medium
J558L	Murine BALB/c myeloma cell line transduced with murine GM-CSF sequence [86]	BM(GM-CSF) survey medium
RMA	Murine T cell tumor cell line derived from C57BL/6 mice [87]	T cell medium
RMA-S	Mutagenized RMA cell line with mutated TAP gene. Procession and expression of endogenous peptides on MHC class I molecules are impossible. [87]	T cell medium
YBM42.2.2	Murine rat hybridoma producing anti-mouse CD45 antibody [88]	YBM medium

4.1.3. Consumables

Consumable	Company
15 mL / 50 mL PP tubes	Sarstedt
24-well cell culture plate, flat bottom	Sarstedt
26G x 1" disposable hypodermic needle	B. Braun
41 µm polyamide mesh	Labomedic
6-well cell culture plate, flat bottom	Sarstedt
96-well tissue culture plate, flat bottom	TPP
BD Plastipak^{TM} 50 mL syringe	Becton Dickinson
Bottle-top filter, 0.22 µm	Corning

Cell culture dish 100 x 20 mm	Sarstedt
Cell culture dish 150 x 20 mm	Sarstedt
Cell scraper 25 cm	Sarstedt
EASYstrainer™ 40 µm cell strainer	Greiner Bio-One
ELISA-plate Microlon® 96W, flat bottom, high binding	Greiner Bio-One
FACS tubes, 5 mL	Sarstedt
Petri dish 92 x 16 mm	Sarstedt
Protran BA83 nitrocellulose membrane, 0.2 µm	Amersham
Rotilabor-blotting papers, 1.5 mm	Roth
Spin-X® UF 6 concentrator (50k MWCO)	Corning
T75 tissue cell culture flask	Sarstedt
Whatman™ sterile 0.45 µm cellulose acetate membrane syringe	GE Healtcare

4.1.4. Chemicals, reagents and commercial kits

Reagent	Company
4-Nitrophenyl phosphate disodium salt hexahydrate (4-NPP)	Sigma-Aldrich
Albumin egg (ovalbumin)	Serva Electrophoresis
Albumin Fraction V (BSA)	Roth
Ammonium persulfate	Sigma-Aldrich
Calciumchlorid ($CaCl_2$)	Roth
CFSE Proliferation Dye	eBioscience
ColorPlus Prestained Protein Ladder	New England BioLabs
Complete EDTA-free protease inhibitor cocktail tablets	Roche
Dephostatin	Santa Cruz
Dulbecco's Modified Eagle's Medium (DMEM)	Pan Biotech
DyNAmo ColorFlash SYBR Green qPCR Kit	Thermo Scientific
Ethylenediamintetraacetic acid (EDTA)	Roth
Fetal Bovine Serum PAA Clone	PAA
Fetal Bovine Serum Standard Quality	PAA
Ficoll-Paque™ Premium 1.084	GE Healthcare
Glycin Pufferan®	Roth
Hoechst 33258	Invitrogen
Iscove's Modified Dulbecco's Medium (IMDM)	Pan Biotech
L-Glutamine (200 mM)	PAA
Lipopolysaccharides from Escherichia coli	Sigma-Aldrich
Methyl-3,4-dephostatin	Sigma-Aldrich
MHCI Peptid OVA (257-264)	AnaSpec Inc.
MHCII Peptid OVA (323-339)	AnaSpec Inc.
Mouse IFN-γ recombinant protein (ELISA Standard)	eBioscience
Mouse IL-2 recombinant protein (ELISA Standard)	eBioscience
Mouse serum	Pan Biotech
Natriumazid	Roth
Natriumchlorid	Roth
NeutrAvidin™ Horseradish Peroxidase Conjugate	Thermo Scientific
Nonfat dried milk powder	Appli Chem
OneComp eBeads	eBioscience
OPTI-MEM® I	Gibco
Ovalbumin (OVA)-Alexa Fluor® 647 conjugate	Invitrogen

PBS Dulbecco w/o Ca^{2+} w/o Mg^{2+}	Biochrom
PD-10 Desaltin Columns, Sephadex G-25 Medium	GE Healthcare
Penicillin/Streptomycin (10,000 units/mL/ 10 mg/mL)	Pan Biotech
phosphorylated biotin-conjugated TATEGQYQPY peptid	PSL
PhosStop phosphatase inhibitor cocktail tablets	Roche
Pierce® BCA Protein Assay Kit	Thermo Scientific
Pierce® Chromatography Cartridges Protein G	Thermo Scientific
Pierce® ECL Western Blotting Substrate	Thermo Scientific
Protein A/G Plus-Agarose	Santa Cruz
PTP CD45 Inhibitor SF1670	Calbiochem
Restore™ PLUS Western Blot Stripping Buffer	Thermo Scientific
RNeasy® Mini Kit	Qiagen
Roswell Park Memorial Institute 1640 (RPMI 1640)	Pan Biotech
Roti®-Stock 20% SDS	Roth
Sodium Pyruvate (100 mM)	Pan Biotech
Streptavidin Agarose	Merck Millipore
SuperScript® II Reverse Transcriptase	Invitrogen
SuperSignal® West Pico Chemiluminescent Substrate	Thermo Scientific
TMB One	Kementec
Transferrin-Alexa Fluor® 647 conjugate	Invitrogen
Tris Pufferan®	Roth
β-Mercaptoethanol	Roth

4.1.5. Buffers and solutions

Common buffer

FACS buffer 0.1% (w/v) BSA, 0.1% (w/v) NaN_3 in 1x PBS; stored at 4 °C
2 mM EDTA 0.5 M EDTA diluted 1:250 in 1x PBS; stored at 4 °C
2x BBS buffer 50 mM BES, 280 mM NaCl, 1.425 mM Na_2HPO_4 in H_2O; adjusted to pH 7.05; sterile filtered; stored at 4 °C
0.3% BSA 0.3% (w/v) BSA in 1x PBS; stored at 4 °C
0.5 M EDTA 500 mM EDTA in H_2O; adjusted with NaOH to pH 8; stored at 4 °C

Media

BM(GM-CSF) culture medium IMDM, 10% FCS Clone, 100 units/mL Penicillin, 0.1 mg/mL Streptomycin, 50 mM β-Mercaptoethanol, 2.5% J558 supernatant
BM(GM-CSF) survey medium IMDM, 10% FCS Clone, 100 units/mL Penicillin, 0.1 mg/mL Streptomycin, 50 mM β-Mercaptoethanol
T cell medium RPMI 1640, 10% FCS Standard, 100 units/mL Penicillin, 0.1 mg/mL Streptomycin, 50 mM β-Mercaptoethanol

HEK cell medium DMEM, 10% FCS Standard, 100 units/mL Penicillin, 0.1 mg/mL Streptomycin, 1mM Sodium Pyruvate
YBM medium IMDM, 5% FCS Standard, 2 mM L-glutamine, 100 units/mL Penicillin, 0.1 mg/mL Streptomycin

Buffers for FcMR generation

0.02% NaN_3 0.02% (w/v) NaN_3 in H_2O; stored at 4 °C
Binding buffer for Protein G column 50 mM sodium acetate in H_2O; adjusted to pH 5.0; stored at 4 °C
Elution buffer for Protein G column 0.1 M glycine in H_2O; adjusted to pH 2.5; stored at 4 °C
Neutralisation buffer for Protein G column 1 M Tris in H_2O; adjusted to pH 7.5; stored at 4 °C
Protein G column storage buffer 0.05% NaN_3 (w/v) in H_2O; stored at 4 °C

SDS-PAGE and Western Blot buffer

10% APS 1 g APS in 10 mL H_20; stored at -20 °C
1x TBS 50 mM Tris, 150 mM NaCl in H_2O; adjusted to pH 7.6; stored at RT
1x SDS-Running buffer 150 mM Glycin, 25 mM Tris, 0.1% SDS (v/v) in H_2O; stored at RT
1x Towbin buffer 25 mM Tris, 192 mM Glycin in H_2O; stored at RT
4x SDS Protein Sample buffer/Laemmli buffer 40% Glycerol (v/v), 240 mM Tris/HCl (pH 6.8), 8% SDS (v/v), 0.04% Bromphenolblue (v/v) in H_2O, if necessary 5% β-Mercaptoethanol (v/v); stored at RT
Triethanolamine-buffered (TEA) lysis buffer 10 mM Triethanolamine (pH 8.2), 150 mM NaCl, 1 mM $MgCl_2$, 1 mM $CaCl_2$, 1% Triton (v/v) in H_2O; stored at 4 °C fresh added: 1x EDTA-free protease inhibitor cocktail
PBST 0.1% TWEEN®20 (v/v) in 1x PBS; stored at RT
TBST 0.1% TWEEN®20 (v/v) in 1x H_2O; stored at RT

ELISA buffer

ABTS buffer 0.1 M Citric acid in H_2O; adjusted to pH 4.35; stored at 4 °C
ELISA Coating buffer 0.1 M $NaHCO_3$ in H_2O; adjusted to pH 8.2; stored at 4 °C
ELISA Wash Buffer 0.05% TWEEN®20 (v/v) in 1x PBS; stored at RT
ELISA Blocking Buffer 1% BSA (w/v) in 1x PBS; stored at 4 °C

ABTS substrate solution 1 mg/mL ABTS, 15 µL H_2O_2 in 10 mL ABTS buffer; prepared freshly

Phosphatase assay buffer

Phosphatase assay lysis buffer 20 mM HEPES (pH 7.2), 2 mM EDTA, 1% Nonident P-40 (v/v), 10% Glycerol (v/v) in H_2O; stored at 4 °C fresh added: 1x EDTA-free protease inhibitor cocktail, 2 mM Dithiothreitol (DTT)
Phosphatase assay Buffer 20 mM HEPES (pH 7.2), 2 mM EDTA in H_2O; stored at 4 °C fresh added: 2 mM Dithiothreitol (DTT)
100 mM HEPES 100 mM HEPES in H_2O; stored at 4 °C

4.1.6. Antibodies

Primary antibodies for flow cytometry

Antigen	Clone	Species	Company	Conjugate	Conc. (ng/mL)
anti-CD206	MR5D3	rat	AbD Serotec	Alexa Fluor® 647	125
anti-CD11b	M1/70	rat	eBioscience	FITC	1250
anti-CD11c	N418	rat	eBisocience	eFluor® 450	500
anti-F4/80	BM8	rat	eBioscience	eFluor® 660	500
anti-CD45	30-F11	rat	BioLegend	PerCP/Cy5.5	500
anti-CD45R/B220	RA3-6B2	rat	BioLegend	APC/Cy7	500
anti-CD45RB	16A	rat	Santa Cruz	FITC	500
anti-CD45RC	C455.1F	rat	Santa Cruz	PE	250
anti-CD40	3/23	rat	Abd Serotec	PE	250
anti-CD4	GK1.5	rat	BioLegend	PerCP/Cy5.5	500
anti-CD8	53-6.7	rat	eBioscience	PerCP/Cy5.5	500
anti-CD80	16-10A1	rat	eBioscience	PE	500
anti-CD86	PO3	rat	Abd Serotec	Alexa Fluor® 488	250
anti-MHCI	AF6-120.1	mouse	BioLegend	Alexa Fluor® 647	500
anti-MHCII	M5/114.15.2	rat	eBioscience	PerCP/Cy5.5	500
anti-B7H1	MIH5	rat	eBioscience	PE	500
anti-B7H2	HK5.3	rat	BioLegend	PE	500

Primary antibodies for complexation, phosphatase assay, IP and Western Blot

Antigen	Clone	Species	Company	Conjugate	Conc. (ng/mL)
anti-GAPDH	6C5	mouse	Millipore	purified	100
anti-Vinculin	-	rabbit	Sigma	purified	1000
anti-CD206	MR5D3	rat	AbD Serotec	purified	1000
anti-CD206	MR5D3	rat	AbD Serotec	Biotin	100
anti-human CD206	7-450	mouse	Acris	purified	500
anti-human CD206	15-2	mouse	BioLegend	Biotin	100
anti-human IgG	-	rabbit	Santa Cruz	HRP	4000
anti-CD45	30-F11	rat	BioLegend	Biotin	500
anti-CD45	30-F11	rat	BioLegend	purified	500
anti-CD45RA	14.8	rat	Santa Cruz	purified	1000

anti-CD45RB	C363-16A	rat	Abd Serotec	purified	500
anti-CD45RC	C455.1F	rat	Santa Cruz	purified	500
anti-Phosphotyrosine	4G10	mouse	Millipore	purified	200
anti-Calnexin	-	rabbit	Abcam	purified	1000

Secondary antibodies

Antigen	Species	Company	Conjugate	Conc. (ng/mL)
anti-rat	goat	Jackson Immuno	HRP	160
anti-rabbit	goat	Santa Cruz	HRP	80
anti-mouse	goat	Dianova	HRP	-

ELISA antibodies (used concentration 0.5 µg/mL)

Antigen	Clone	Species	Company	Conjugate
anti-IFN-γ	AN-18	rat	eBioscience	purified
anti-IFN-γ	RA-6A2	rat	eBioscience	Biotin
anti-IL-2	JES6-1A12	rat	eBioscience	purified
anti-IL-2	JES6-5H4	rat	eBioscience	Biotin
anti-IL-6	MP5-20F3	rat	eBioscience	purified
anti-IL-6	MP5-32C11	rat	eBioscience	Biotin
anti-IL-10	JES5-16E3	rat	eBioscience	purified
anti-IL-10	JES5-2A5	rat	eBioscience	Biotin
anti-IL-12 p35/p70	C18.2	rat	eBioscience	purified
anti-IL-12/IL-23 p40	C17.8	rat	eBioscience	Biotin
anti-IL-4	11B11	rat	eBioscience	purified
anti-IL-4	BVD6-24G2	rat	eBioscience	Biotin

Cell stimulation antibodies

Antigen	Clone	Species	Company	Conjugate	Conc.
anti-CD3ε	17A2	rat	eBioscience	purified	5 µg/mL

4.1.7. Primers

All primers were purchased from Life technologies

cDNA production

Primer	Sequence
OligodT	TTTTTTTTTTTTTTTT

RT-PCR

Primer	Sequence
HPRT_for	TCCCAGCGTCGTGATTAGCGATGA
HPRT_rev	AATGTGATGGCCTCCCATCTCCTTCATGACAT
PPIA_for	GCGTCTCCTTCGAGCTGTT
PPIA_rev	RAAGTCACCACCCTGGCA
SOCS3_for	ATTTCGCTTCGGGACTAGC
SOCS3_rev	AACTTGCTGTGGGTGACCAT
STAT1_for	AAATGTGAAGGATCAAGTCATGTG
STAT1_rev	CATCTTGTAATTCTTCTAGGGTCTTGA

STAT3_for	GTTCCTGGCACCTTGGATT
STAT3_rev	CAACGTGGCATGTGACTCTT
STAT6_for	CCTTTGAGGAGAGCCTAGCA
STAT6_rev	CTGCTGCAGCTGGGAATAA
TBP_for	CCAATGACTCCTATGACCCCTA
TBP_rev	CAGCCAAGATTCACGGTAGAT

4.1.8. Equipment

Device	Company
BioLogic LP System (peristaltic pump)	Bio-Rad Laboratories
ChemiDoc™ MP System	Bio-Rad Laboratories
Flow Cytometer LSR II	BD Biosciences
Infinite F200PRO plate reader	Tecan
iQ™5-Real-time PCR Detection System	Bio-Rad Laboratories
Mini-PROTEAN® Tetra and Mini Trans-Blot® Cell System	Bio-Rad Laboratories
NanoDrop 2000 spectrophotometer	Thermo Scientific
QuadroMACS™ Separation Unit and MACS Multi Stand	Miltenyi Biotec
Thermo MultiscanEX Plate reader	Thermo Scientific

4.1.9. Software

Software	Company
Adobe Acrobat Pro Version 10.1.14	Adobe System
Adobe Illustrator CS5 Version 15.0.0	Adobe System
BD FACSDiva™	BD Biosciences
BioLogic™ LP Data View™	Bio-Rad Laboratories
FlowJo Version 9.6.4	FlowJo Enterprise
GraphPad Prism 5 for Mac OS X Version 5.0c	GraphPad Software
Image Lab™ Version 5.1	Bio-Rad Laboratories
iQ5 Optical System Software	Bio-Rad Laboratories
Microsoft® Office for Mac 2011	Microsoft
NanoDrop 2000/2000c	Thermo Scientific
TECAN plate reader software i-control 1.10	Tecan

4.2. Methods

4.2.1. Generation and stimulation of BM(GM-CSF) cells

4.2.1.1 Standard cell culture conditions

Cells were cultured under standard cell culture conditions at 37 °C at levels of 5% CO_2 and a relative humidity of 90%. If not mentioned otherwise, cells were detached by incubation with 2 mM EDTA in PBS for 5 min at 37 °C followed by gently pipetting. BM(GM-GSF) and HEK293 T cells were centrifuged 5 min at 300 rcf whereas splenocytes were centrifuged 10 min at 450 rcf.

4.2.1.2 Production of GM-CSF-containing cell supernatant

GM-CSF for BM(GM-CSF) cell differentiation was produced by J558L cells. This mouse BALB/c B myeloma cell line is able to secrete GM-CSF into its supernatant. Cells were thawed, expanded and then, 10^6 cells were plated in 30 mL survey medium on a 15 cm cell culture dish. After 8-10 days of incubation, supernatant was centrifuged 5 min at 300 rcf and sterile filtered using bottle-top filter from Corning. GM-CSF-containing cell supernatant was aliquoted and stored at -20 °C.

4.2.1.3 Differentiation of BM(GM-CSF) cells

A mouse was euthanized, killed by cervical dislocation and tibiae and femurs were taken out. Under sterile conditions and in 1x PBS, bones were opened on both ends and bone marrow was flushed out with PBS and a 26G x 1" gauge needle. Cells were separated by pipetting, filtered through a 40 µm nylon mesh and centrifuged for 5 min at 300 rcf. Supernatant was discarded and cells were resuspended in 45 mL BM(GM-CSF) culture medium comprising 2.5% GM-CSF-containing cell supernatant. 15 mL cell suspension per 10 cm petri dish was plated and incubated for 3-4 days at 37 °C. Then, supernatant with swimming cells of 3 plates was collected in a 50 mL reaction tube, adherent cells were detached with 2 mM EDTA (see. 4.2.1.1) and combined with the supernatant. Cells were centrifuged for 5 min at 300 rcf, supernatant was discarded and cells were resuspended in double volume (90 mL) fresh culture medium. Again, 15 mL cell solution were plated per 10 cm petri dish and incubated 3-4 days. BM(GM-CSF) cells were used on day 7 or 8.

4.2.1.4 FcMR and sMR stimulation

For stimulation with FcMR or sMR, MR-KO BM(GM-CSF) cells were plated on day 7 at a concentration of 10^6 cells/mL in sMR-containing supernatant (production see 4.2.3) or survey medium supplemented with complexed MR proteins (complexation see 4.2.2.5). Cells were incubated O/N at 37 °C.

4.2.2. Generation of recombinant MR protein

4.2.2.1 Recombinant MR vectors

The chimeric MR construct consists of the CR domain, FN domain and CTLD 1-2 of the MR fused to a human Fc part of IgG1. It was cloned in the backbone of plgplus vector that has an ampicillin and kanamycin resistance as well as an IL-2 signal sequence fot he secretion of the chimeric protein. (Figure 12) The plasmid were cloned and kindly provided by Luisa Martinez-Pomares [60]. As isotype control the pFuse-hIgG1-Fc2 vector from InvivoGen was used. The plasmid contains an IL-2 signal sequence for secretion and the human IgG1 Fc part equal to plgplus-CR-FN-CTLD1-2 (Figure 11).

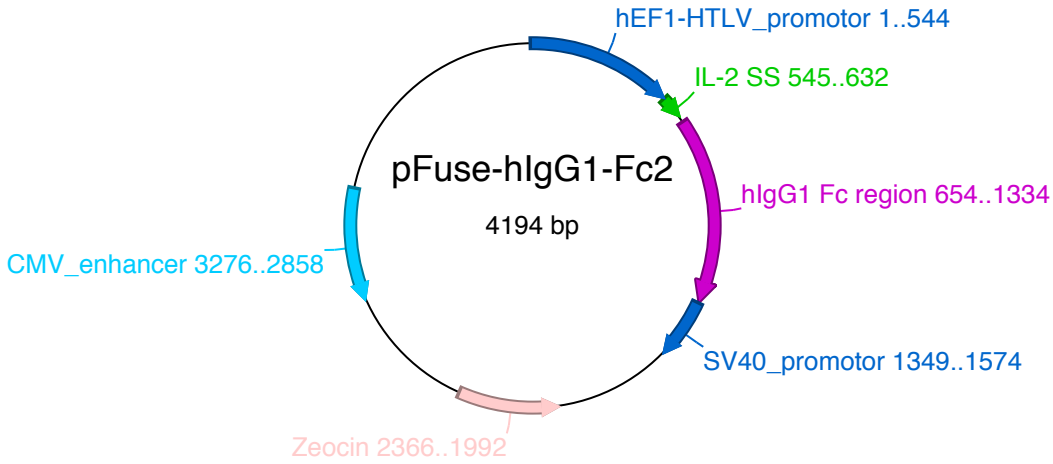

Figure 11: Vector map of pFuse-hIgG1-Fc2. The vector was purchased from InvivoGen and served as isotype control.

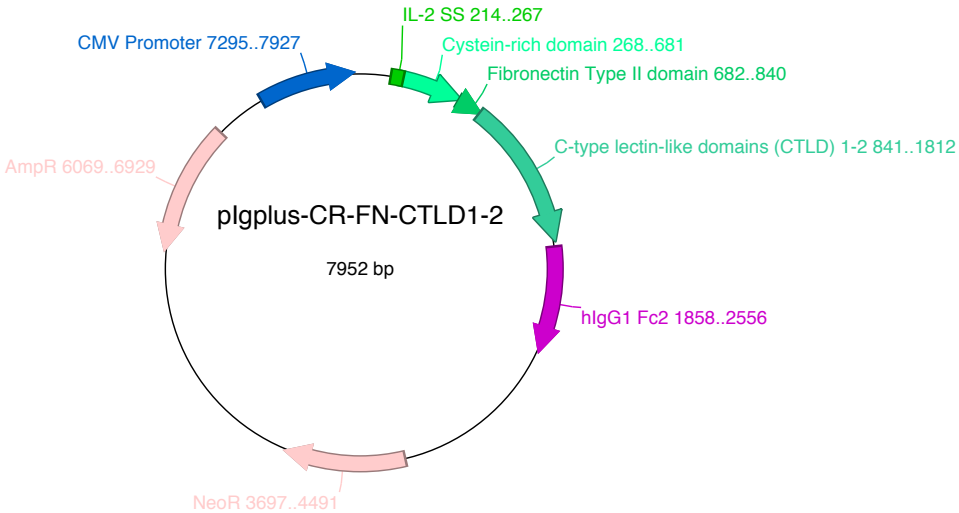

Figure 12: Vector map of plgplus-CR-FN-CTLD1-2. The vector was cloned and provided by Luisa Martinez-Pomares [60]. The plasmid encodes the chimeric protein FcMR containing cysteine-rich (CR), fibronectin (FN) type II, and C-type lectin-like domains (CTLD) 1-2 of the MR fused to a human IgG1 Fc part.

4.2.2.2 Transfection of HEK293T cells

$3*10^6$ HEK293T cells were plated on a T75 cell culture flask in 10 mL HEK cell medium one day prior transfection. 10 µg DNA per T75 cell culture flask were mixed with 2.5 mM $CaCl_2$ and water. This mixture was added to an equal amount of 2x BBS buffer during constant airflow. After 5 min incubation, the transfection preparation was distributed over the cells. On the following day, medium was changed to 20 mL OPTI-MEM. Transfected cells were cultured 4-5 days at 37 °C and 5% CO_2.

4.2.2.3 Protein purification via Protein G column

Recombinant MR constructs were purified from transfected HEK cells by affinity chromatography using a Protein G column from Pierce and BioLogic LP system from Bio-Rad. Procedure was done according to the manufacturer's instructions. Briefly, cell supernatant was centrifuged 5 min at 300 rcf to remove cell debris. Supernatant was filtered with sterile 0.45 µm cellulose acetate membrane syringe and then mixed in a ratio 1:2 with binding buffer. Column was equilibrated with 10 mL binding buffer with a flow rate of 1.5 mL/min. Sample was run over the column with a constant flow rate of 1 mL/min. Afterwards, column was washed with 10 mL binding buffer and protein was eluted with elution buffer. For both the flow rate was enhanced to 1.5 mL/min. Eluated fraction were mixed with neutralization buffer in a ratio of 1:9. Finally, column was washed with 5 mL storage buffer for repeated application. Protein concentration of eluted fractions was measured at 280 nm with NanoDrop.

4.2.2.4 Protein concentration via spin column

Eluted fractions containing protein were combined. Buffer exchange as well as concentration was done by centrifugation at 3200 rcf using a VivaSpin column with a cut-off 30k. Protein concentration of concentrated fraction was measured at 280 nm with NanoDrop. Recombinant proteins were enriched with 1x protease inhibitor cocktail mix and 0.02% NaN_2 for long time storage.

4.2.2.5 Complexation of MR protein

10 µg MR protein (final concentration; normally 10 µg MR protein per 10^6 cells or per mL medium were used) was mixed with 1x protease inhibitor cocktail mix, 1:100 anti-human-HRP antibody and 0.3% BSA in PBS in a total volume not less than 100 µL. The complexation took place 1 h at RT.

4.2.3. Generation of soluble mannose receptor (sMR)-containing cell supernatant

Wt and $MR^{-/-}$ BM (GM-CSF) cells were plated on day 7 at a concentration of $2*10^6$ cell/mL survey medium on a 10 cm cell culture plate. After 5-7 days incubation at 37 °C and 5% CO_2, cell supernatant was centrifuged at 300 rcf for 5 min. Supernatant was stored at 4 °C. Quality of sMR was analyzed by SDS-PAGE and western blot (see 4.2.4).

4.2.4. Sodium dodecyl sulfate polyacrylamide gel electrophorese (SDS-PAGE) and Western Blot

4.2.4.1 Cell lysis

Cells were plated and incubated differently for the individual experiments.

After incubation, BM(GM-CSF) cells were scraped off, transferred to a reaction tube and centrifuged 5 min at 300 rcf. Supernatant was discarded and cell pellet was lysed in Triethanolamine-buffered (TEA) lysis buffer supplemented with protease and phosphatase inhibitor mix. Lysis was performed on ice for 5-30 min. Lysate was centrifuged 5 min at full speed to remove cell debris. Supernatant was transferred to a new tube and stored at -20 °C until further analysis.

4.2.4.2 SDS-PAGE

Separation of proteins was done using the MiniProtean® Tetra cell system from Bio-Rad. Handling of equipment was according to the manufacturer's instructions. Percentage of resolving gel was geared to the separation range of analyzed proteins. Percentage of the stacking gel was 5%. SDS-PAGE was performed at 30 mA const., 120 V and 100 W in 1x SDS running buffer.

4.2.4.3 Western Blot

To analyze proteins, SDS polyacrylamide gel with separated proteins was transferred on a nitrocellulose membrane using the Mini Trans-Blot® wet transfer cell system from Bio-Rad. Assembling of the blot chamber was done according to the manufacturer's instructions. Wet blot transfer was carried out 1 h at 350 mA const., 100 V and 300 W in 1x Towbin buffer.

Next, membrane was blocked with 5% milk powder or 5% BSA in TBST or PBST for 1 h at RT. In most cases, membrane was incubated in primary antibody diluted in blocking solution 1 h at RT followed by three washing steps of 5 min each with TBST or PBST. Then, secondary antibody incubation was performed in TBST or PBST for 1 h at RT

followed by three washing steps of 5 min each with TBST or PBST. The staining procedure was performed under rocking conditions. Detection of the protein of interest was done by chemiluminescence with SuperSignal® West Pico Chemiluminescent substrate from Pierce® and ChemiDoc™ MP Imaging System from Bio-Rad.

4.2.5. Immunprecipitation of CD45

4.2.5.1 Preparation and pre-clearance of protein lysates

For generation of CD45-containing cell lysate see 4.2.4.1. First, unspecific binding of samples was removed by pre-clearance. 10 µL protein A/G beads were washed twice with PBS by centrifugation at 6800 rcf for 30 sec. Beads were incubated with cell lysates for 1 h at 4 °C on a rotation wheel. Subsequently, beads were centrifuged (6800 rcf 30 sec) and supernatant was transferred in a new tube.

4.2.5.2 Pull-down

Cell lysates were incubated with 0.5 µg anti-CD45 (clone 30-F11) antibody for 1 h at 4 °C on a rotation wheel. In the meantime, 20 µL protein A/G beads per sample were washed twice with PBS. Samples were loaded to the beads and incubated for 1 h at 4 °C on a rotation wheel. Beads were spun down (6800 rcf for 30 sec) and supernatant were discarded. Beads were washed twice with lysis buffer or PBS in case of cell lysate or cell supernatant, respectively. 1x Laemmli buffer (LB) w/o β-mercaptoethanol was added to the beads and samples were boiled 5 min at 97 °C. Supernatant was loaded on SDS-PAGE.

4.2.5.3 Western blot analysis

Immunoprecipitated proteins were analyzed by SDS-PAGE (see 4.2.4.2) and western blot (see 4.2.4.3)

Blocking was done with 5% BSA in TBST and all washing steps were performed with TBST. Rat anti-CD45 biotin-labeled (clone 30-F11) antibody was used 1:1000 followed by detection with NeutrAvidin horseradish peroxidase (NaPOX) 1:5000.

4.2.6. CD45 phosphatase assay

For stimulation with FcMR, $3.5*10^6$ $MR^{-/-}$ BM(GM-CSF) cells were plated in a 6-well plate in survey medium. After 1 h, complexed MR constructs (for complexation see 4.2.2.5) (10 µg/10^6 cells) were added to the medium and cells were incubated for 1 h at 37 °C.

For stimulation with sMR, $5*10^6$ $MR^{-/-}$ BM(GM-CSF) cells were plated in a 6-well plate in supernatant of wt or $MR^{-/-}$ BM(GM-CSF) cells (for generation see 4.2.3) and incubated for 1 h at 37 °C.

After MR incubation, supernatant of cells was discard and cells were lysed in 600 µL phosphatase assay lysis buffer for 15-30 min on ice. After this point, samples were handled separately depending on phosphatase activity detection by 4-NPP substrate or phospho-TATEGQYQPY peptid.

4-NPP substrate: 10 µL protein A/G beads per sample were washed twice with 1x PBS (6800 rcf for 30 sec). Cells were scraped off, added to the prepared beads and incubated for 1 h at 4 °C on a rotation wheel. Beads were centrifuged for 30 sec at 680 rcf and supernatant was split into three equal fractions. anti-CD45 antibody was added and samples were incubated for 1 h at 4 °C with rotation. In the meantime, 20 µL protein A/G beads per sample were washed twice with 1x PBS (6800 rcf for 30 sec). Antibody-coupled lysates were added to the prepared beads and incubated for 1 h at 4 °C on a rotation wheel. Beads were washed twice with 100 mM HEPES solution. Before second washing step, each sample was split in two fractions. 70 µL CD45 substrate (4-NPP)-containing phosphatase assay buffer supplemented with or without 2 µM CD45 inhibitor SF1670 was added to the beads. Samples were incubated O/N at 37 °C and 500 1/min in the dark. Beads were centrifuged for 1 min at 6800 rcf and supernatant were transferred to an ELISA plate. Analysis of substrate conversion was measured by colorimetry at 405 nm.

phospho-TATEGQYQPY peptid: Lysates were centrifuged for 5 min at full speed to remove cell debris. Supernatant was split into three equal fractions and 1.25 µg anti-CD45 antibody per sample was added. Samples were incubated for 1 h at 4 °C with rotation. In the meantime, 20 µL protein A/G beads per sample were washed twice with 1x PBS (6800 rcf for 30 sec). Antibody-coupled lysates were added to the prepared beads and incubated for 1 h at 4 °C on a rotation wheel. Beads were washed twice with 1x PBS. 70 µL phosphatase assay buffer supplemented with 0.25 µg/mL phospho-TATEGQYQPY peptid was added to the beads. Samples were incubated O/N at 37 °C and 500 1/min in the dark. 25 µL streptavidin agarose per sample were washed twice with 1x PBS (6800 rcf for 30 sec). O/N-incubated samples were filled up with 500 µl 1x PBS and centrifuged for 30 sec at 6800 rcf. 500 µl supernatant were transferred to streptavidin agarose and incubated for 1 h at 4 °C with rotation. Agarose beads were centrifuged for 30 sec at 6800 rcf and supernatant was discarded. 500 µl 3% BSA in PBS

supplemented with 1:10,000 anti-phosphotyrosine antibody (clone 4G10) were added to the beads. Samples were incubated for 1 h at 4 °C with rotation. Beads were centrifuged for 30 sec at 6800 rcf and supernatant was discarded. 500 µl 3% BSA in PBS supplemented with 1:10,000 anti-mouse-HRP antibody were added to the beads. Samples were incubated for 30 min at 4 °C with rotation. Beads were washed twice with 1x PBS and once with H_2O. Dephosphorylation of peptide was analyzed with TMB substrate and measured by colorimetry at 450 nm.

4.2.7. Detection of phosphotyrosine levels

$2*10^6$ $MR^{-/-}$ BM(GM-CSF) cells were plated in a 6-well plate. Next day, cells were washed with 1x PBS and stimulated with 10 µg FcMR or 1 mL sMR for 30 min at 37 °C. Afterwards, cells were lysed as described in 4.2.4.1. Protein concentration was determined by bicinchoninic acid (BCA) assay. 15 µg protein lysate/sample was loaded on SDS-PAGE and detected by immunoblotting (see 4.2.4.3). Membranes were blocked with 5% BSA in TBST for 1 h at RT.

Next, membranes were incubated in phosphotyrosine-specific antibody (clone 4G10) diluted in blocking solution O/N at 4 °C followed by three washing steps of 5 min with TBST, followed by incubation with anti-mouse-HRP antibody in TBST for 1 h at RT. After extensive washing, membranes were detected with ECL reagent followed by membrane stripping with Restore™ PLUS Western Blot stripping buffer and restaining with anti-GAPDH antibody.

4.2.8. Quantitative Real-time polymerase chain reaction (qRT-PCR)

$3*10^6$ $MR^{-/-}$ BM(GM-CSF) cells were plated in a 6-well plate and stimulated with 10 µg complexed FcMR/10^6 cells for 4 h or 12 h at 37 °C. After incubation, cells were scraped off and RNA was isolated using RNeasy® Mini Kit (Qiagen). Subsequently, 500 ng total RNA was used to generate cDNA using SuperScript® II Reverse Transcriptase (Invitrogen). Afterwards, analysis of gene expression was performed with DyNAmo ColorFlash SYBR Green qPCR Kit (Thermo Scientific) on an iQ™5 Real-time Detection System (BioRad). All kits were used according to the manufactures instructions. PCR was prepared and run with the following mix and program.

PCR Mix	final
2x Master Mix	1x
5 µM Primer Mix	0.5 µM each
40x Yellow sample buffer	1x
Template cDNA	1 µl
H_2O	up to 15 µl

PCR Programm	Time	Temperature	
Denaturation	7 min	95 °C	
Denaturation	10 sec	95 °C	44 cycles
Annealing	15 sec	60°C	
Extension	30 sec	72 °C	
Melting curve	each 30 sec	55-95 °C in 0.5 °C steps	

4.2.9. Flow cytometry analysis of cell surface molecules

BM(GM-CSF) cells were stimulated on day 7 with FcMR or sMR (see 4.2.1.4). After 24 h, cells were scraped off and transferred to FACS tubes. 2 mL FACS buffer were added per tube and samples were centrifuged for 5 min at 300 rcf. Supernatant were discarded and cells were stained with fluorescent-labeled antibodies in a ratio of 1:400 for 20 min at 4 °C in the dark. Mouse serum was added (final ratio 1:100) to block unspecific antibody binding.

After incubation, cells were washed once with 2 mL FACS buffer by centrifugation for 5 min at 300 rcf and analyzed by flow cytometry on LSRII.

4.2.10. Antigen uptake assay

After stimulation with FcMR or sMR (see 4.2.1.4), $4*10^5$ BM(GM-CSF) cells were plated in a 24-well plate and incubated for 45 min. Medium was changed to medium containing 250 ng/mL ovalbumin-Alexa Fluor® 647 or 5 µg/mL transferrin-Alexa Fluor® 647 and incubated for 15, 30, or 60 min at 37 °C. After incubation, cells were scraped off, transferred to a FACS tube and washed once with FACS buffer by centrifugation at 300 rcf for 5 min. Supernatant was discarded and cells were resuspended in 500 µL FACS buffer. Antigen uptake was analyzed by flow cytometry on LSR II.

4.2.11. T cell function assays

4.2.11.1 Isolation of primary splenocytes

Mice were killed by cervical dislocation. Spleen was taken out and stored in 1x PBS on ice. Under sterile conditions and in 1x PBS, spleen was shredded through a 100 µm metal mesh with a plunger of a syringe. Cells were further singularized by pipetting and filtered through a 40 µm nylon mesh. Cells were counted and used directly for co-culturing (see 4.2.11.4) or stained with CFSE (see 4.2.11.2).

4.2.11.2 CFSE-staining of splenocytes

To analyze proliferation of T cells, splenocytes were stained with CFSE. Isolated splenocytes (see 4.2.11.1) were centrifuged for 10 min at 450 rcf and resuspended in 10 mL 1x PBS. Cell solution was mixed 1:2 with 10 mL 2 µM CFSE in PBS (final concentration of 1 µM CFSE). Cells were incubated for 15 min at 37 °C in the dark. Staining was stopped through addition of 20 mL T cell medium. Unbound CFSE was removed by washing three times with 10 mL T cell medium by centrifugation for 7 min at 450 rcf. Cells were counted and resuspended at a concentration of 10^6 cells/mL in T cell medium.

4.2.11.3 Ovalbumin (OVA) preparation

As an extracellular antigen for T cell activation OVA was used. OVA was dissolved in 1x PBS to a final concentration of 100 mg/mL. After centrifugation for 5 min at full speed to remove unsolved OVA, it was purified from small OVA fragments by gel filtration via a PD10 column. Final concentration was measured at 280 nm with NanoDrop. OVA was always prepared freshly for each experiment.

4.2.11.4 BM(GM-CSF)/T cell co-culture

FcMR- or sMR-prestimulated BM(GM-CSF) cells (see 4.2.1.4) were plated for IL-2 secretion and proliferation at a density of $5*10^4$ cells/well in a 96-well plate and for *in vitro* cytotoxicity assay and restimulation at a density of $4*10^5$ cells/well in a 24-well plate. Cells were incubated for 1-2 h at 37 °C. For the priming of $CD4^+$ OT-II T cells, medium of BM(GM-CSF) wells were changed to medium supplemented with 1 mg/mL OVA and cells were incubated 3 h at 37 °C.

Afterwards, BM(GM-CSF) cells were co-cultured with 10^5 splenocytes/96-well or $5*10^5$ splenocytes/24-well at 37 °C for indicated time points.

For IL-2 secretion, *in vitro* cytotoxicity assays, and restimulation, unlabeled DesTCR or OT-II splenocytes were used, for proliferation CFSE-labeled splenocytes (see 4.2.11.2) were used. All experiments were performed in triplicates.

4.2.11.5 IL-2 secretion

24 h after co-culturing of BM(GM-CSF) cells with DesTCR or OT-II splenocytes, supernatant of cells were centrifuged for 7 min at 450 rcf to remove cells and stored at -80 °C. Secretion of IL-2 were analyzed by ELISA (see 4.2.12).

4.2.11.6 Proliferation assay

For analysis of proliferation, BM(GM-CSF) cells and CFSE-stained DesTCR or OT-II splenocytes were co-cultured 3 days. Next, cells were washed once with 1x FACS buffer by centrifugation at 450 rcf for 5 min. Antigen-specific OT-II and DesTCR T cells were stained with anti-CD4 (1:400) or anti-CD8 (1:400) antibody, respectively. Staining was performed for 20 min at 4 °C. Cells were washed again with 1x FACS buffer by centrifugation and analyzed by flow cytometry on LSR II. Washing, staining and analysis was performed in 96-well plate format.

4.2.11.7 T cell purification by density gradient centrifugation

For *in vitro* cytotoxicity assay and restimulation, T cells have to be separated from BM(GM-CSF) cells after priming. DesTCR splenocytes were primed 3 days, OT-II splenocytes were primed 5 days. Primed cells were isolated by density gradient centrifugation. T cells were resuspended by gently pipetting and transferred to a 15 mL reaction tube. Triplicates were combined. Cells were centrifuged for 10 min at 450 rcf, supernatant was discarded and cells were resuspended in 5 mL T cell medium. Cell solution was carefully underlaid with 2 mL Ficoll. Samples were centrifuged for 20 min at 800 rcf with acceleration of 7 and without brake. Cells were carefully collected from the interphase and mixed with 8 mL PBS to dilute remaining Ficoll. Samples were centrifuged for 10 min at 450 rcf, supernatant was discarded and cells were resuspended in T cell medium. After counting, cells were diluted to a concentration of $4*10^5$ or $2.5*10^5$ cells/mL for *in vitro* cytotoxicity assay or restimulation respectively.

4.2.11.8 In vitro cytotoxicity assay

RMA and RMA-S cells were used as target and control cells, respectively. The same number of both cell lines was centrifuged for 10 min at 450 rcf and cells were resuspended in 1 μM or 0.1 μM CFSE (RMA and RMA-S, respectively). Cells were

incubated for 15 min at 37 °C in the dark. CFSE staining was stopped by adding 10 mL T cell medium. Cells were washed three times with T cell medium by centrifugation for 10 min at 450 rcf. Afterwards, cells were counted and mixed together equally to a final concentration of $8*10^4$ cells/mL. 100 µL CFSE-stained RMA/RMA-S mix per well was plated in a 96-well plated. 100 µL purified, primed DesTCR T cells were added to RMA/RMA-S cells in the ration 5:1 and 2:1 ($2*10^5$ cells/mL and $8*10^4$ cells/mL, respectively) DesTCR/RMA cells. As a control RMA/RMA-S mix without DesTCR T cells was analysed. Cells were incubated O/N at 37 °C.

Next day, killing of RMA cells was analyzed by flow cytometry on LSRII. 10 µg/mL Hoechst 33258 (1:100) was added immediately before analysis to stain death cells.

The percentages of living RMA and RMA-S cells of the co-culturing with (w/) DesTCR T cells versus the control without (w/o) DesTCR T cells were used to calculate the specific cytotoxicity. The following formula was used.

$$\%\ cytotoxicity = 100 - 100 * \left(\frac{\frac{RMA\ cells\ (w/)}{RMA - S\ cells\ (w/)}}{\frac{RMA\ cells\ (w/o)}{RMA - S\ cells\ (w/o)}} \right)$$

4.2.11.9 Restimulation of T cells

To restimulate primed T cells, a 96-well plate was coated with 5 µg/mL anti-CD3 antibody in 1x PBS for 1 h at 37 °C. Next, $5*10^4$ purified T cells/well were plated on CD3-coated 96-well plate. Cells were incubated O/N at 37 °C. Plate was centrifuged for 5min at 450 rcf and supernatant was used for ELISA to analyze secreted cytokines.

4.2.12. Enzyme-linked immune sorbent assay (ELISA)

An ELISA plate was coated for 1 h at 37 °C or O/N at 4 °C with 0.5 µg/mL capture antibody (purified) in ELISA coating buffer. Plate was washed three times with ELISA washing buffer and blocked with ELISA blocking solution for 30 min at RT. Afterwards, plate was washed again three times and 50 µL of samples or protein standard was loaded. Standard range covered 125 ng/mL – 120 pg/mL for IFN-γ and 80 ng/mL – 8 pg/mL for IL-2 in a dilution ratio of 1:2. 50 µL T cell medium was loaded as blank. Plate was incubated for 1 h at 37 °C or O/N at 4 °C. After incubation, plate was washed again and incubated with 0.5 µg/mL detection antibody (biotin-labeled) in blocking solution for 1 h at 37 °C or O/N at 4 °C. Plate was washed again and incubated for 30 min at RT with 1 µg/mL NeutrAvidin-peroxidase (NA-POX) in 1x PBS. ABTS solution was prepared and

after last washing step, 50 µL ABTS solution per well was loaded. Analysis of substrate conversion was measured by colorimetry at 405 nm.

4.2.13. Detection of sMR in serum samples of mice and human

Serum samples of wt mice fed a low-fat died (LFD) or a high-fat died (HFD) as well as of lean and obese humans were kindly provided by Bruno Guigas of the Leiden University Medical Center.

The relative amount of sMR in the serum was determined by pull-down and western blot analysis.

15 µL mouse serum or 200 µL human serum was pre-cleared with 10 µL protein A/G beads for 1-1.5 h at 4 °C under rotating conditions. 1 µg anti-mouse or anti-human MR antibody per sample was coupled to 10-20 µL protein A/G beads. All samples were centrifuged for 30 sec at 4 °C at 6800 rcf and supernatant of pre-cleared beads was added to antibody-coupled beads. Samples were incubated for 1.5-2 h at 4 °C under rotating conditions, centrifuged and the supernatant was discarded. Beads were washed two times with 200 µL TEA lysis buffer. Samples were centrifuged, the supernatant discarded and beads were boiled for 5 min at 99 °C with 15-20 µL 1x Laemmli buffer. Subsequently, supernatant was used for SDS-PAGE and western blot analysis (see 4.2.4.2 and 4.2.4.3). For the detection of human samples, membranes were blocked in 5% BSA in TBST and stained with anti-human CD206-Biotin (1:5000) in blocking solution and in NA-POX (1:8000) in TBST. For detection of murine samples see 4.2.4.3.

5. Results

5.1. CD45 in BM(GM-CSF)

5.1.1. Characterization of GM-CSF generated BM cells

For decades, bone marrow (BM) cells were used to study the role of APC *in vitro*, especially DCs and MΦs, because a huge number of cells can be prepared from BM progenitor cells. In addition, these cells bear many features of primary APCs. They express costimulatory molecules, initiate antigen uptake and processing to activate T cell-mediated immunity, and undergo maturation in response to microbial stimuli [8,89]. The continuous supply of different cytokines influences the development of generated cells. Traditionally, DCs and MΦs were differentiated predominantly by GM-CSF and M-CSF, respectively. To date, it is known that a heterogeneous population of DCs, MΦs, and granulocytes are generated in GM-CSF cultures [90–92]. Due to problem of controversial discussed terms (regarding DCs and MΦs) the cells in the presented experiments were defined based on the origin and the linked activation standards recommended by Murray et al. as BM(GM-CSF) cells [93].

First, the BM(GM-CSF) cells derived from MR knockout mice were characterized by their expression of different surface molecules CD11b, CD11c, and F4/80 of DCs and MΦs. BM(GM-CSF) cells were stained with fluorescent-labeled antibodies against the extracellular surface markers, and analyzed by flow cytometry (Figure 13).

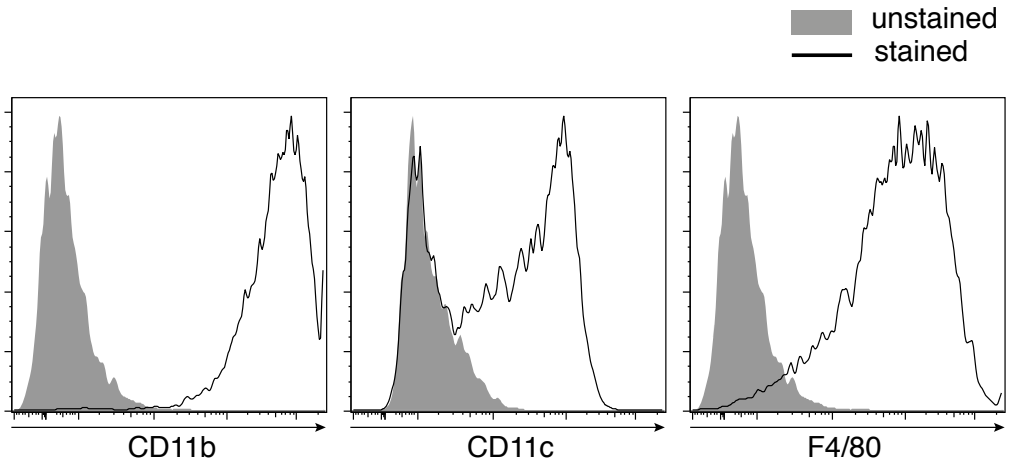

Figure 13: GM-CSF treatment of bone marrow cells led to a heterogeneous cell population of APCs. $MR^{-/-}$ BM(GM-CSF) cells were stained with fluorescent-labeled antibodies against CD11b, CD11c, and F4/80 on day 7 of generation. Expression of surface markers was analyzed by flow cytometry. Unstained cells were used as control (filled gray). Representative graphs from 1 out of 3 independent experiments are shown.

CD11b and F4/80 were expressed by all BM(GM-CSF) cells as it can be seen by the shift compared to unstained cells (left and right panel). A subpopulation of BM(GM-CSF) cells did also express CD11c (middle panel).

5.1.2. CD45R0 was expressed by BM(GM-CSF) cells

CD45 is expressed on the cell surface of all leukocytes. Based on cell type and activation state different isoforms are expressed [94]. Therefore, the CD45 isoforms on BM(GM-CSF) cells were analyzed by western blot and flow cytometry in comparison to spleen cells. Spleen cells are a mixture of mostly B and T cells. According to the literature, B cells express the largest CD45 isoform (comprising all three alternatively spliced exons) termed CD45RABC. Primary naïve T cells express CD45RB whereas activated T cells express CD45R0 [94].

To investigate the isoform expression on BM(GM-CSF) cells, antibodies specific to single isoforms (CD45RA, CD45RB, or CD45RC) as well as an antibody recognizing all isoforms (panCD45) were used. Lysates of BM(GM-CSF) and spleen cells were analyzed by western blotting via staining with CD45 specific antibodies (Figure 14).

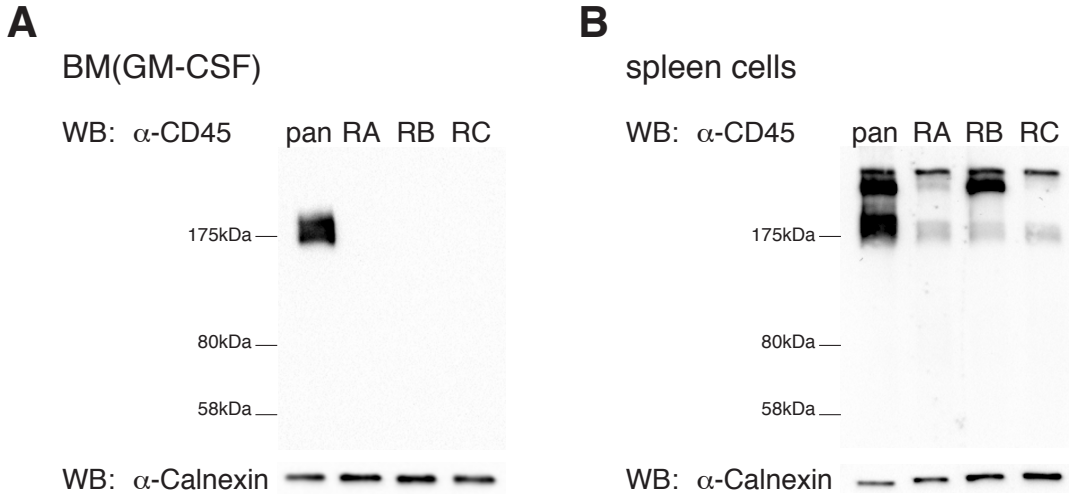

Figure 14 Alternatively spliced exons of CD45 could not be detected on BM(GM-CSF) cells. (A) $MR^{-/-}$ BM(GM-CSF) and (B) $MR^{-/-}$ spleen cells were lysed, separated by SDS-PAGE, and analyzed by western blot using CD45 isoform-specific antibodies against panCD45, CD45RA, CD45RB, and CD45RC. Calnexin was used to check for equal loading. Representative blots from 1 out of 3 independent experiments are shown.

In cell lysates of BM(GM-CSF) cells two bands around 175 kDa appeared if stained with panCD45 antibody that recognize all CD45 isoforms (Figure 14A). No protein was detected with isoform-specific antibodies (CD45RA, -RB, -RC) recognizing alternatively sliced exons of CD45. In spleen cells all isoform-specific antibodies as well as the

panCD45 antibody detected proteins higher than 175 kDa according to the literature [94] (Figure 14B). Because the isoform-specific antibodies did not detect CD45 in BM(GM-CSF) cell lysates this suggest that BM(GM-CSF) cells express CD45R0.

To confirm the data, the surface of BM(GM-CSF) and spleen cells were stained with fluorescent-labeled CD45 antibodies and analyzed by flow cytometry (Figure 15).

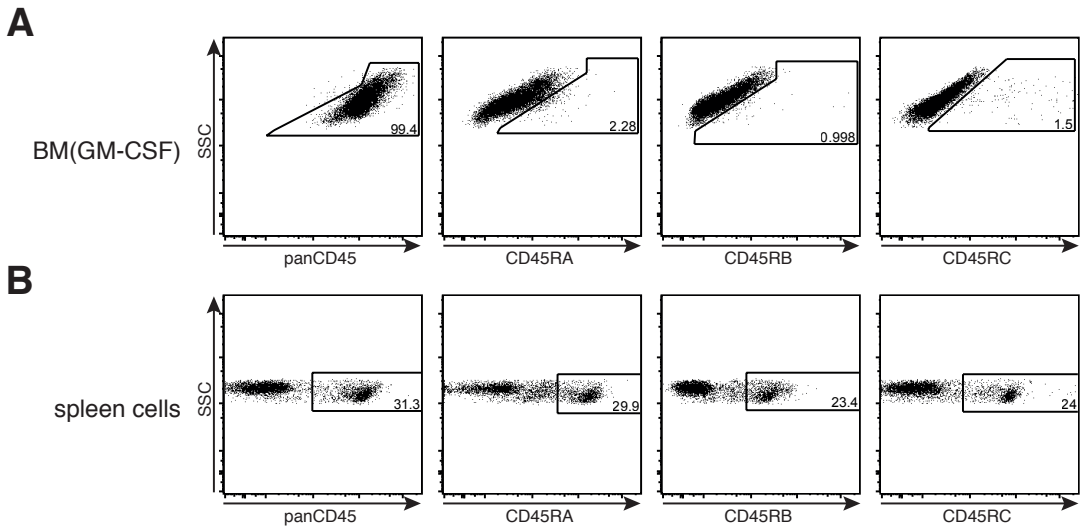

Figure 15: BM(GM-CSF) cells expressed CD45R0. Flow cytometry analysis of (A) $MR^{-/-}$ BM(GM-CSF) and (B) $MR^{-/-}$ spleen cells. Cells of day 7 were stained with fluorescent-labeled CD45 isoform-specific antibodies. Representative dot blots from 1 out of 3 independent experiments are shown.

Whereas in subpopulations of spleen cells all isoforms of CD45 were detected (Figure 15B) only the panCD45 antibody bound on BM(GM-CSF) cells (Figure 15A).
According to the western blot analysis, this indicates that BM(GM-CSF) cells predominantly express the CD45R0 isoform (missing all three alternatively spliced exons).

5.1.3. MR interacted with CD45 on BM(GM-CSF) cells

An interaction of the cysteine-rich region of the MR with CD45 was already described by Martinez-Pomares in 1999 [53]. To date, the isoforms of CD45 can bind the MR are still not defined. To investigate whether the MR could also bind CD45R0 expressed on BM(GM-CSF) cells, a recombinant construct of the MR (FcMR) was used. FcMR comprised the cysteine-rich, fibronectin type II, and C-type lectin 1-2 domains of the MR fused to a human IgG1 Fc part that allowed purification by affinity chromatography, complexation of chimeric protein, and detection by an anti-human antibody.

CD45 of $MR^{-/-}$ BM(GM-CSF) cells was immunoprecipitated and analyzed by SDS-PAGE and western blotting. Protein interaction was detected by far-western blotting using complexed FcMR. As a control immunoprecipitation was performed without antibody (Figure 16, -). To verify the success of the immunoprecipitation, CD45 was also stained on the western blot.

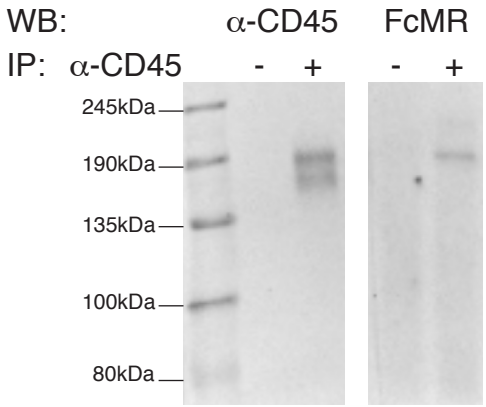

Figure 16: FcMR bound to CD45 of BM(GM-CSF) cells. $MR^{-/-}$ BM(GM-CSF) cells were lysed and CD45 was immunoprecipitated by anti-CD45 antibody and protein A/G beads. Eluates were separated by SDS-PAGE and precipitation of CD45 was stained by anti-CD45 antibody. Binding of FcMR to CD45 in BM(GM-CSF) cells was detected by far-western using complexed FcMR. Representative blot from 1 out of 6 independent experiments are shown.

After immunoprecipitation two CD45-specific bands were detected (Figure 16, left panel) that might be due to posttranscriptional modifications of CD45. An interaction of FcMR with the upper band of CD45 was traceable (Figure 16, right panel). If no antibody was used in the immunoprecipitation neither anti-CD45 nor FcMR detected anything that demonstrated the specificity of the precipitation.

In summary, these initial experiments showed that the BM(GM-CSF) cells are a heterogeneous population of $CD11b^{+}CD11c^{-}F4/80^{+}$ and $CD11b^{+}CD11c^{+}F4/80^{+}$ cells expressing CD45. Based on western blot and flow cytometry analysis this CD45 isoform represents CD45R0. In addition, FcMR interacts with CD45R0 on BM(GM-CSF) cells but only with one of two CD45-specific bands in western blot.

5.2. Interaction with the MR influenced activity of BM(GM-CSF) cells

5.2.1. MR reduced CD45 phosphatase activity

CD45 is a tyrosine phosphatase with a role in TLR-dependent cytokine secretion and integrin-mediated adhesion in APCs [30,32–34,36,95]. In $CD8^+$ T cells, the phosphatase activity of CD45 is inhibited by the interaction with the MR [79].

Because CD45 in BM(GM-CSF) cells was also bound by the MR (Figure 16) it was investigated whether the binding of MR had an influence on phosphatase activity of CD45 in BM(GM-CSF) cells.

$MR^{-/-}$ BM(GM-CSF) cells were incubated with complexed FcMR or isotype control for 1 h. Subsequently, cells were lysed and CD45 was immunoprecipitated using a CD45-specific antibody. Afterwards, CD45 phosphatase activity was measured by the conversion of the alkaline phosphatase substrate 4-nitrophenyl phosphate (4-NPP) into its chromatic dephosphorylated form nitrophenyl in the presence or absence of the phosphatase inhibitor SF1670. The turnover of the substrate was analyzed after 18 h by colorimetry at 405 nm (Figure 17). As a control, the background of the assay was determined by performing the immunoprecipitation without antibody (Ctrl).

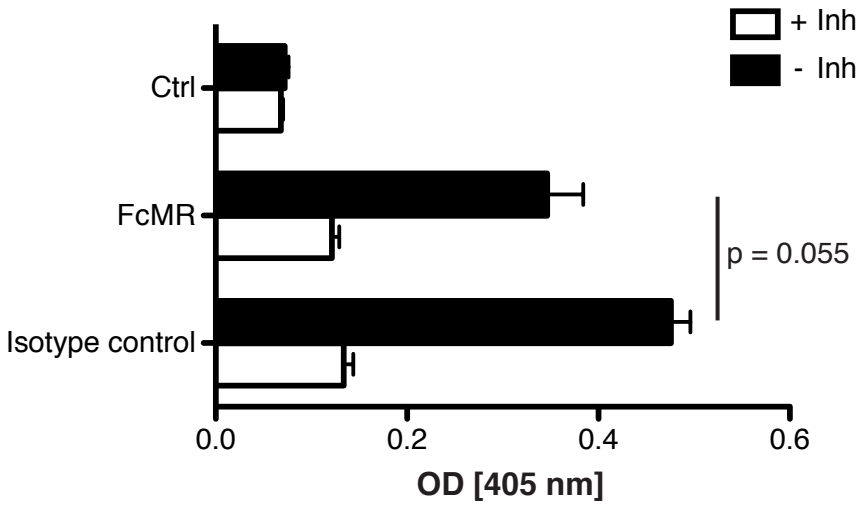

Figure 17: Phosphatase activity of CD45 measured by 4-NPP substrate was reduced by FcMR. CD45 was immunoprecipitated from lysates of FcMR- or isotype control-pretreated $MR^{-/-}$ BM(GM-CSF) cells by an anti-CD45 antibody and protein was coupled to protein A/G beads. Phosphatase activity was measured by substrate conversion of alkaline phosphatase substrate 4-nitrophenyl phosphate. Assay was measured by colorimetry at 405 nm. Activity was blocked by the phosphatase inhibitor SF1670 (Inh; white bars). As a control, no antibody was used for pull-down (Ctrl). Data in the graph represent 1 out of 3 independent experiments ± SEM. *P* values were calculated by student's t-test.

In all samples containing CD45-specific antibody during immunoprecipitation the phosphate substrate 4-NPP was converted and turnover was measured (Figure 17, black bars, FcMR and isotype control). When the activity was blocked by a phosphatase inhibitor nearly no substrate was converted and values of optical densities (ODs) were comparable to the background (Figure 17, white bars), pointing out that measured substrate conversion was due to phosphatase activity. The incubation of BM(GM-CSF) cells with complexed FcMR clearly reduced the phosphatase activity of CD45 in BM(GM-CSF) cell in comparison to the isotype control-treated cells, pointing out that the binding of FcMR and CD45 influences CD45 phosphatase activity.

To validate this result and to exclude dephosphorylation by other (putatively co-precipitated) phosphatases, the phosphatase activity of CD45 was analyzed by dephosphorylation of a biotin-labeled CD45-specific peptide (phospho-TATEGQpYQPY).

Immunoprecipitated CD45 was incubated with phosphorylated peptide for 18 h. Then, peptide was bound to NeutrAvidin beads and tyrosine-phosphorylation was detected by an anti-phosphotyrosine antibody. Conversion of TMB substrate by an HRP-labeled secondary antibody was analyzed by colorimetry at 450 nm (Figure 18).

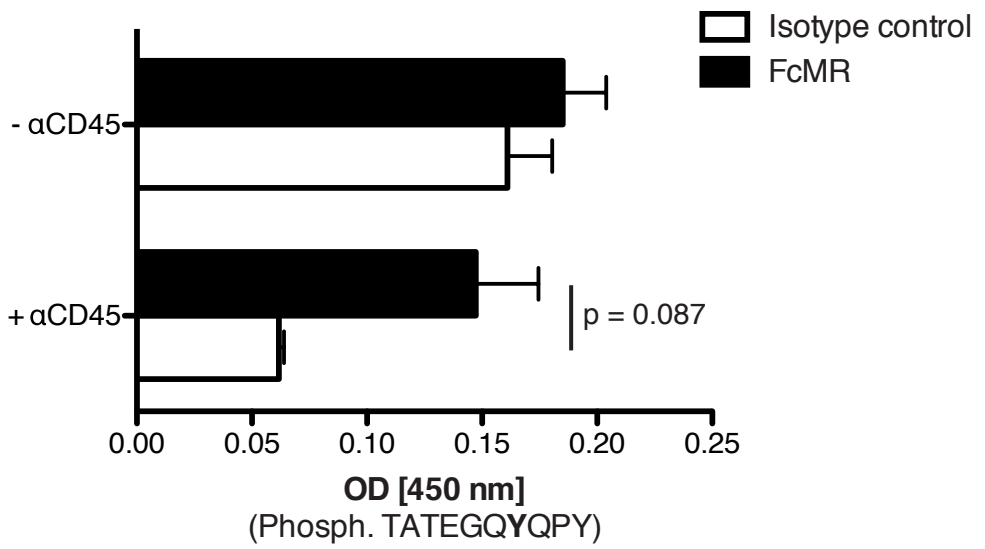

Figure 18: Phosphatase activity of CD45 measured by a CD45-specific peptide was reduced by FcMR. CD45 was immunoprecipitated from lysates of FcMR- (black) or isotype control- (white) pretreated $MR^{-/-}$ BM(GM-CSF) cells by an anti-CD45 antibody and protein was coupled to protein A/G beads. Phosphatase activity was measured by dephosphorylation of a CD45-specific peptide (TATEGQ-pY-QPQ). Phosphorylation of peptide was detected by an anti-phosphotyrosine antibody and substrate conversion of a HRP substrate was analyzed by colorimetry at 450 nm. Data in the graph represent 1 out of 3 independent experiments ± SEM. *P* values were calculated by student's t-test.

The detection maximum of the assay was assessed by performing the assay without CD45 antibody (Figure 18, -αCD45). Since CD45 was not precipitated without antibody, the biotin-labeled CD45-specific peptide could not be dephosphorylated by CD45 and anti-phosphotyrosine antibody staining was high. If CD45 was precipitated by a CD45-specific antibody, the biotin-labeled peptide should be dephosphorylated resulting in reduced phosphotyrosine antibody staining compared to control samples without antibody.

The incubation of BM(GM-CSF) cells with isotype control lead to a clear reduction in phosphotyrosine antibody staining compared to control samples without CD45 antibody (Figure 18, +αCD45, white bar), pointing out that isotype control did not influence CD45 phosphatase activity. CD45 of BM(GM-CSF) cells that were stimulated with FcMR showed an reduced CD45 phosphatase activity compared to isotype control-treated BM(GM-CSF) cells (Figure 18, +αCD45, black bar) depicted by enhanced staining with phosphotyrosine antibody.

Taking together, the interaction of FcMR and CD45 on BM(GM-CSF) cells clearly reduced CD45 phosphatase activity in the stimulated cells.

5.2.2. Binding of MR to CD45 enhanced phosphotyrosine levels

Intracellular substrates of CD45 are SFKs like Hck and Lyn [96] as well as JAKs [48–50]. These kinases are involved in signal transduction pathways regulating a multitude of cellular events like cytokine-mediated proliferation, differentiation, cell growth, survival, and migration [97,98]. The pathways are often regulated by phosphorylation and dephosphorylation of tyrosine residues associated with the activation or inactivation of corresponding enzymes. To investigated whether the binding of the MR to CD45 alters the total phosphotyrosine levels in $MR^{-/-}$ BM(GM-CSF) cells, BM(GM-CSF) cells were stimulated with complexed FcMR or isotype control for 30 min. Immediately cells were lysed, proteins were analyzed by SDS-PAGE and western blotting. Total phosphotyrosine levels were detected with a phosphotyrosine-specific antibody (Figure 19).

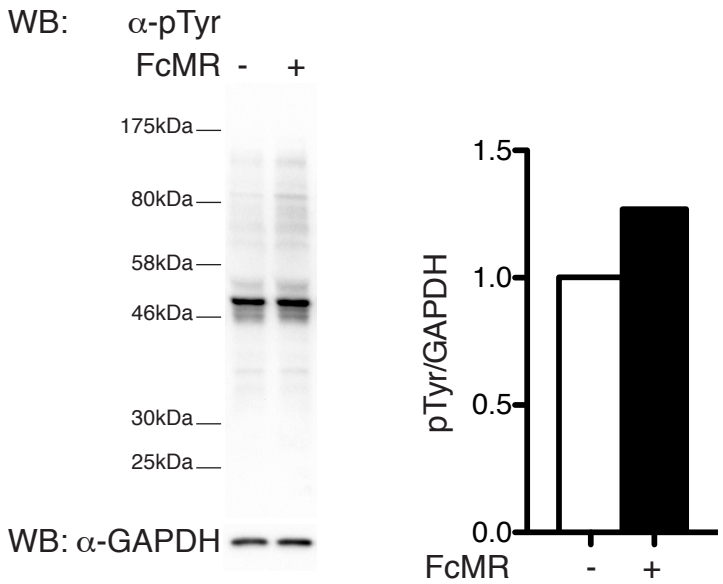

Figure 19: Phosphotyrosine pattern of BM(GM-CSF) cells was altered by the MR/CD45 interaction. $MR^{-/-}$ BM(GM-CSF) cells were stimulated with complexed FcMR (+) or isotype control (-) for 30 min at 37 °C. Afterwards, cells were lysed and total protein content were analyzed by SDS-PAGE and western blot. Phosphotyrosine residues were stained by antibody clone 4G10®. GAPDH was used as loading control. Representative blot from 1 out of 5 independent experiments is shown. Bars indicate mean intensity of phosphotyrosine proteins greater than 40 kDa relative to GAPDH intensity.

Staining of total cell lysates of BM(GM-CSF) cells with a phosphotyrosine-specific antibody generated a huge band pattern over the hole range of the protein standard representing the spectrum of tyrosine-phosphorylated proteins within the cell lysate. After incubation with FcMR the pattern of phosphotyrosine-bearing proteins changed, with a tendency towards an increase in overall phosphorylated proteins. Thus, the

binding of the MR to CD45 inhibited its phosphatase activity leading to modified signal transduction in BM(GM-CSF) cells.

CD45 is known to interact with JAKs and inactivating them by direct dephosphorylation [48]. Activated JAKs are important for activation of the transcriptional factor Signal Transducers and Activators of Transcription (STAT), which are important for cytokine driven signaling [99]. Target genes of STAT proteins are suppressor of cytokine signaling (SOCS) proteins that negatively regulates cytokine signaling [100].

We analyzed a potential influence of the MR on this signaling pathway in BM(GM-CSF) cells. Therefor, BM(GM-CSF) cells were stimulated with complexed FcMR or isotype control for 4 h or 12 h. mRNA of stimulated cells were isolated and analyzed by quantitative Real-time PCR (qRT-PCR) (Figure 20).

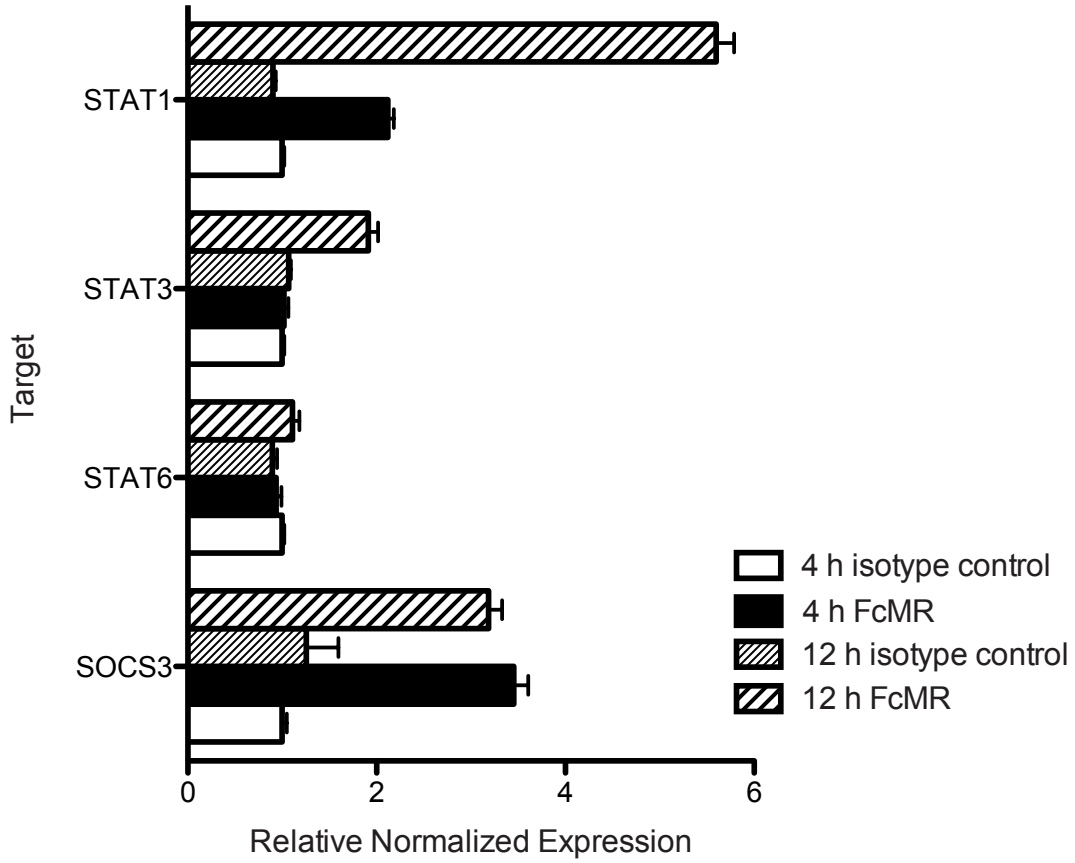

Figure 20: Expression of STAT molecules and target genes were enhanced by FcMR stimulation of BM(GM-CSF) cells. $MR^{-/-}$ BM(GM-CSF) cells were stimulated with complexed FcMR or isotype control for 4 h or 12 h at 37 °C. Afterwards, mRNA of cells were isolated and analyzed by quantitative real-time PCR (qRT-PCR). Relative expression was normalized with ΔΔCT method to housekeeping genes HPRT (hypoxanthine phosphoribosyltransferase), PPIA (peptidylprolyl isomerase A), and TBP (TATA-box binding protein). Representative graph from 1 out of 3 independent experiments is shown ± SEM.

Stimulation of BM(GM-CSF) cells with FcMR for 4 h lead to a 2-fold increase of STAT1 expression compared to isotype control-treated cells. After 12 h, STAT1 expression was further enhanced by FcMR stimulation whereas expression in control cells remained the same (Figure 20, first row). STAT3 expression was only increased after 12 h of FcMR stimulation in BM(GM-CSF) cells (2-fold) compared to controls. Independent of stimulation, expression levels after 4 h were the same (Figure 20, second row). At no time, FcMR-mediated changes in the expression of STAT6 were detectable (Figure 20, third row). Regarding SOCS3, stimulation of BM(GM-CSF) cells with FcMR enhanced expression levels on a 3-fold increase after 4 h as well as after 12 h compared to control cells (Figure 20, fourth row).

In summary, these experiments demonstrate that the inhibition of CD45 phosphatase activity in BM(GM-CSF) cells by interaction with the MR influences the JAK/STAT signaling in BM(GM-CSF) cells.

5.3. FcMR-pretreatment of BM(GM-CSF) cells led to altered effector function of primed T cells

APCs are important for the induction of the adaptive immunity. They process and present endogenous and exogenous peptides on MHC I and II, respectively. Thereby $CD4^+$ and $CD8^+$ naïve T cells get activated [8]. The binding of FcMR to CD45 on BM(GM-CSF) cells altered intracellular signaling pathways by inhibition of CD45 phosphatase activity (see 5.2). Therefore, it was investigated whether FcMR treatment of BM(GM-CSF) cells results in altered T cell effector function.

5.3.1. IFN-γ secretion of $CD4^+$ T cells was impaired by FcMR

$CD4^+$ T cells are necessary for cell-mediated immunity. Once activated, they secrete cytokines to recruit and activate other cells of the immune system [4]. Therefore, the secretion of IFN-γ was analyzed after restimulation of $CD4^+$ T cells that were initially primed with FcMR-pretreated BM(GM-CSF) cells.

$MR^{-/-}$ BM(GM-CSF) cells were pre-treated with complexed FcMR or isotype control and co-cultured with antigen-specific $CD4^+$ OT-II cells. T cells were isolated by density gradient centrifugation and equal cell numbers were restimulated with an anti-CD3 antibody. Secretion of IFN-γ into the cell supernatant was analyzed by ELISA (Figure 21).

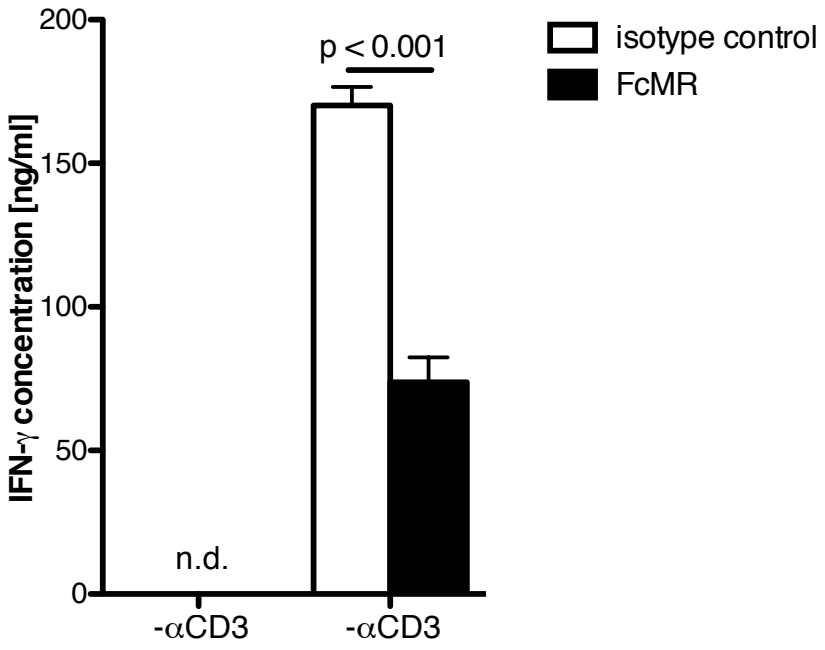

Figure 21: IFN-γ secretion of antigen-specific CD4$^+$ T cells was impaired by priming through FcMR-prestimulated BM(GM-CSF) cells. MR$^{-/-}$ BM(GM-CSF) cells were stimulated O/N with complexed FcMR or isotype control. After stimulation, cells were loaded with OVA antigen and co-cultured with antigen-specific CD4$^+$ OT-II T cells for 5 days. Primed T cells were isolated by density gradient centrifugation and restimulated O/N with or without an anti-CD3 antibody (αCD3). Secretion of IFN-γ by T cells was analyzed in the cell supernatant by ELISA. Data in the graph represent 1 out of 8 independent experiments ± SEM. *P* values were calculated by student's t-test. n.d.: not detectable

Antigen-specific CD4$^+$ T cells primed by BM(GM-CSF) cells that were pre-stimulated with isotype control secrete high amounts of IFN-γ (Figure 21, white bar). A significant reduction ($p < 0.001$) in the amount of secreted IFN-γ was measured if CD4$^+$ T cells were primed by FcMR-prestimulated BM(GM-CSF) cells (Figure 21, black bar).

Taken together, the treatment of BM(GM-CSF) cells with FcMR reduced the activity of antigen-specific CD4$^+$ T cells to secrete IFN-γ compared to T cells activated by control BM(GM-CSF) cells.

5.3.2. Cytotoxicity of CD8$^+$ T cells was reduced by FcMR

Activated CD8$^+$ T cells are cytotoxic and can directly eliminate cells presenting T cell-specific peptides on MHC I molecules [4,8].

To assess the effect of FcMR on effector mechanisms of CD8$^+$ T cells, the killing capacity of CD8$^+$ T cells was analyzed in an *in vitro* cytotoxicity assay.

MR$^{-/-}$ BM(GM-CSF) cells were treated with FcMR or isotype control and co-cultured with antigen-specific CD8$^+$ DesTCR T cells. These cells recognize endogenous processed peptides presented on H-2K^b in an allogenic reaction [80], meaning that the activation of

these T cells is independent of antigen uptake. Primed T cells were isolated by density gradient centrifugation and co-cultured with differently CFSE-labeled target (RMA) and control (RMA-S) cells. Different ratios of T cells and target cells were assessed. The killing of target cells by activated T cells was analyzed by flow cytometry (Figure 22A). To calculate the specific killing, living cells were distinguished from death cells by Hoechst staining.

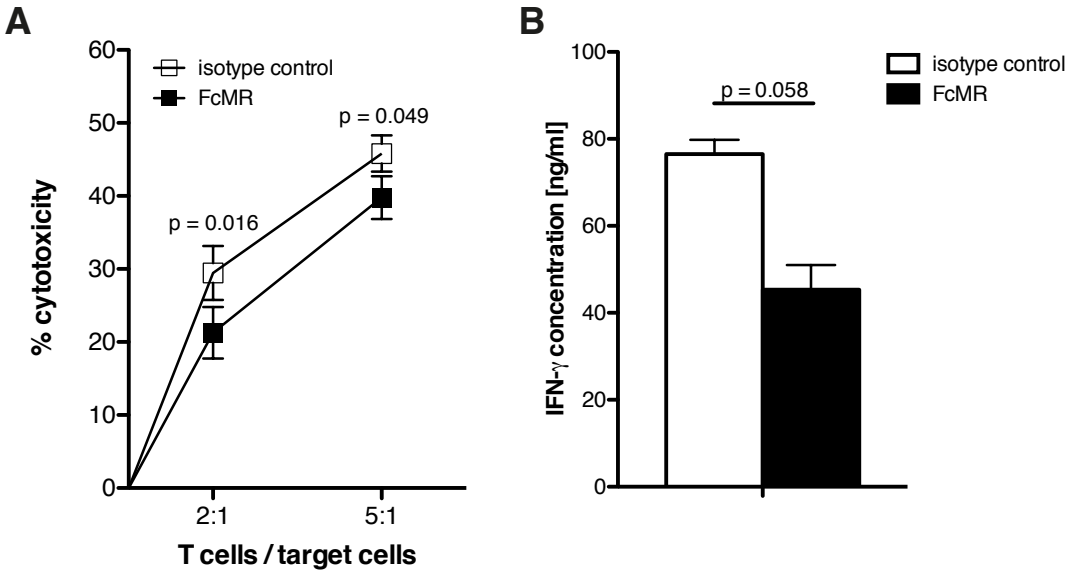

Figure 22: Cytotoxicity and IFN-γ secretion of CD8$^+$ T cells primed by FcMR-prestimulated BM(GM-CSF) cells were decreased. MR$^{-/-}$ BM(GM-CSF) cells were stimulated O/N with complexed FcMR or isotype control. Next day, BM(GM-CSF) cells were co-culture with H-2K^b-specific CD8$^+$ DesTCR T cells for 3 days. Primed T cells were isolated by density gradient centrifugation and used for *in vitro* cytotoxicity assay (A) or restimulation (B). Data in the graphs represent (A) the mean of 3 or (B) 1 representative experiment out of 3 independent experiments ± SEM. *P* values were calculated by student's t-test. *P* values were calculated by student's t-test. (A) Differently CFSE-labeled target (RMA) and control (RMA-S) cells were co-cultured with isolated T cells O/N in different T cell/ target cell ratios. Killing of target cells was analyzed by flow cytometry. Dead cells were stained with Hoechst. (B) Isolated T cells were restimulated O/N with anti-CD3 antibody. Secretion of IFN-γ was analyzed by ELISA using cell supernatant.

The percentage of cytotoxicity was raised with increasing T cell:target cell ratios (Figure 22A). CD8$^+$ T cells primed by FcMR-treated BM(GM-CSF) cells exhibited a significantly reduced cytotoxicity compared to T cells primed by isotype control-treated BM(GM-CSF) cells (Figure 22A, black graph).

The secretion of IFN-γ by primed CD8$^+$ T cells after restimulation was also analyzed. For this purpose, T cells primed by FcMR- or isotype control pretreated BM(GM-CSF) cells were restimulated with an anti-CD3 antibody and IFN-γ cytokine secretion was analyzed by ELISA (Figure 22B). The amount of secreted IFN-γ was reduced when T

cells were primed by FcMR-treated BM(GM-CSF) cells (Figure 22B, black bar) compared to T cells primed by isotype control-teated BM(GM-CSF) cells.

In summary, the activity of antigen-specific $CD8^+$ T cells was inhibited by FcMR treatment of BM(GM-CSF) cells as seen in the overall cytotoxicity as well as in the secreted IFN-γ level.

5.4. Soluble mannose receptor (sMR) was detectable in cell culture supernatant of BM(GM-CSF) cells

Treatment of BM(GM-CSF) cells with the recombinant MR construct (FcMR) reduced CD45 phosphatase activity in BM(GM-CSF) cells *in vitro* causing a reduced IFN-γ secretion of antigen-specific $CD4^+$ T cells and impaired cytotoxic activity of antigen-specific $CD8^+$ T cells that were primed by FcMR-treated BM(GM-CSF) cells (Figure 21 and Figure 22, respectively). These results show that FcMR leds to a tolerogenic effect on BM(GM-CSF) cells presumably via the inhibition of CD45 activity. *In vivo*, an equivalent to the recombinant MR construct might be the soluble MR (sMR). The sMR is generated by cleavage of metalloproteases and comprise the complete extracellular part of the MR in a functional form [65]. The function of the soluble form of the MR is still under investigation. Based on the results of experiments with the recombinant MR a similar role of the sMR was proposed. To further investigate this issue, it was tested first whether the BM(GM-CSF) cells also generate a soluble form of the MR.

BM(GM-CSF) cells were generated from wt and $MR^{-/-}$ mice. On day 7, cells were replated in a defined concentration of $2*10^6$ cells/mL and after 5-7 days the supernatant was collected. Cells were lysed and protein content of cell lysates and supernatants were separated by SDS-PAGE. Western blots were stained with an anti-MR antibody (Figure 23).

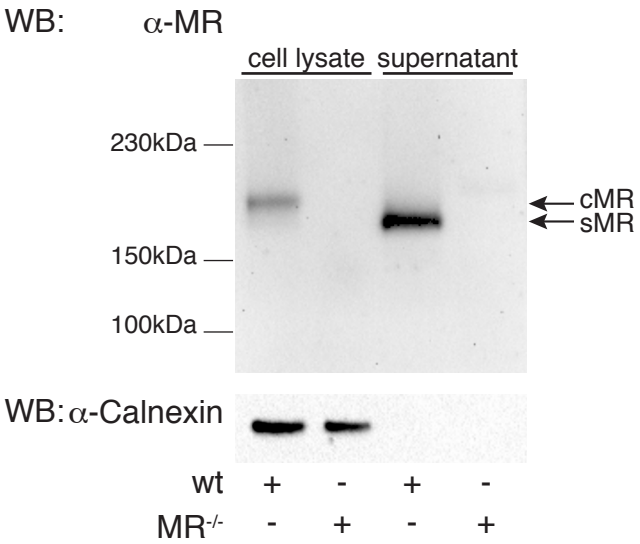

Figure 23: Wt BM(GM-CSF) cells released sMR into the supernatant. BM(GM-CSF) cells of wildtype (wt) and $MR^{-/-}$ mice were cultured for 7 days. Cells were replated in a concentration of $2*10^6$ cells per mL medium for 5 days. Supernatant was collected and cells lysed. Both were analyzed by SDS-PAGE and western blot. Cellular MR (cMR) and soluble MR (sMR) were detected by an antibody specific for the extracellular part of the MR (clone MR5D3). Calnexin was used as loading control for cell lysates. Representative blot from 1 out of 3 independent experiments is shown.

In cell lysates of wt BM(GM-CSF) cells the cellular MR (cMR) could be detected at 170-180 kDa (Figure 23). In the supernatant of these cells a truncated form (~10-20 kDa smaller) of the MR was identified corresponding to the sMR [101]. Neither cMR nor sMR could be detected in cell lysates or supernatant of $MR^{-/-}$ BM(GM-CSF) cells, respectively. These data point out that sMR was generated by MR-expressing BM(GM-CSF) cells *in vitro* as described by Martinez-Pomares (1998) [65].

5.5. Influence of sMR on BM(GM-CSF)

As the recombinant protein of the MR has a tolerogenic effect on $MR^{-/-}$ BM(GM-CSF) cells next it was investigated whether the sMR influenced these cells in a similar manner. For this purpose, $MR^{-/-}$ BM(GM-CSF) cells were incubated with sMR-containing supernatant of wt BM(GM-CSF) cells. As a control, supernatant of $MR^{-/-}$ BM(GM-CSF) cells without sMR was used. We analyzed the CD45 phosphatase activity and total phosphotyrosine levels of the stimulated cells as described in 5.2 (see also 4.2.6 and 4.2.7) (Figure 24).

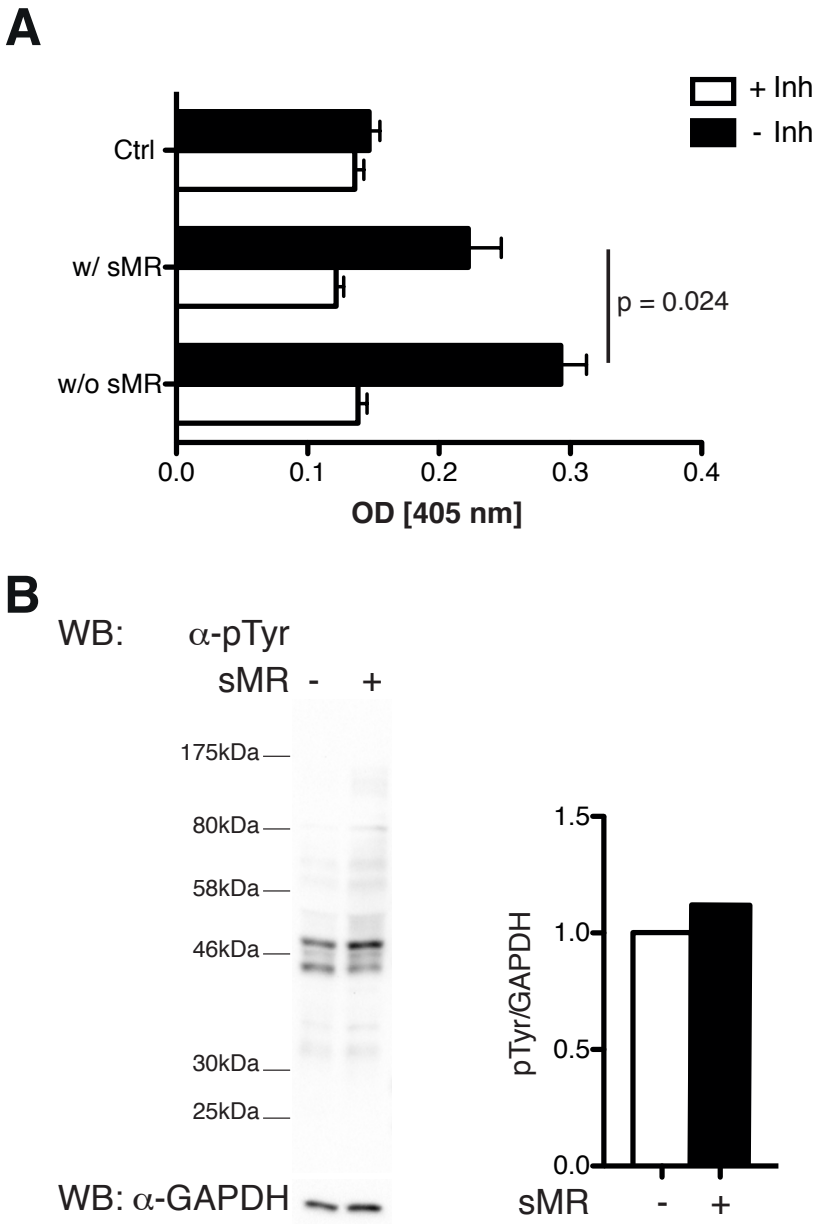

Figure 24: CD45 phosphatase activity was decreased and phosphotyrosine levels were changed by stimulation with sMR-containing supernatant. (A) $MR^{-/-}$ BM(GM-CSF) cells were stimulated with sMR-containing (w/ sMR) or control (w/o sMR) supernatant for 1 h. Cells were lysed and CD45 was immunoprecipitated by an anti-CD45 antibody. Protein was coupled to protein A/G beads and phosphatase activitiy was measured by substrate conversion of alkaline phosphatase substrate 4-nitrophenyl phosphate. Substrate conversion was measured by colorimetry at 405 nm. Activity was blocked by the phosphatase inhibitor SF1670 (inh, white bars). As a control, no antibody was used for immunoprecipitation (Ctrl). Data in the graphs represent the mean of 3 independent experiments ± SEM. *P* values were calculated by student's t-test. (B) $MR^{-/-}$ BM(GM-CSF) cells were stimulated with sMR-containing (+) or control (-) supernatant for 30 min at 37 °C. Afterwards, cells were lysed and total protein content was analyzed by SDS-PAGE and immunoblotting (left). Phosphotyrosine residues were stained by anti-phosphotyrosine antibody (clone 4G10). GAPDH was used as loading control. Representative blot from 1 out of 5 independent experiments is shown. Bars indicate mean intensity of phosphotyrosine proteins greater than 40 kDa relative to GAPDH intensity.

BM(GM-CSF) cells that were stimulated with supernatant containing sMR (w/ sMR) had a reduced CD45 phosphatase activity in comparison to cells stimulated with control (w/o sMR) supernatant (Figure 24A, black bars). Furthermore, the pattern of phosphotyrosine-bearing proteins of BM(GM-CSF) cells stimulated with sMR-containing supernatant was also slightly altered (Figure 24B), demonstrating that the influence of the binding of sMR to CD45 on BM(GM-CSF) cells was comparable to the binding of FcMR to CD45.

5.6. Enhanced T cell effector function after sMR-pretreatment of BM(GM-CSF)

The activity of CD45 and downstream signaling pathways were changed by sMR-containing supernatant in a similar way like the recombinant MR (FcMR) (see Figure 17, Figure 19 and Figure 24). Therefore, it was further analyzed whether the supernatant of wt BM(GM-CSF) cells (including sMR) has also an effect on T cell effector function through pretreatment of BM(GM-CSF) cells.

$MR^{-/-}$ BM(GM-CSF) cells were incubated with supernatant of wt or $MR^{-/-}$ BM(GM-CSF) cells and co-culture with antigen-specific $CD4^+$ OT-II T cells. Primed T cells were isolated by density gradient centrifugation and restimulated O/N with anti-CD3 antibody. IFN-γ secretion of restimulated $CD4^+$ was analyzed by ELISA (Figure 25A)

For $CD8^+$ T cells, $MR^{-/-}$ BM(GM-CSF) cells were incubated with supernatant of wt or $MR^{-/-}$ BM(GM-CSF) cells co-cultured with antigen-specific $CD8^+$ DesTCR T cells. Primed T cells were isolated by density gradient centrifugation and either restimulated O/N with anti-CD3 antibody or used in *in vitro* cytotoxicity assay. IFN-γ secretion of restimulated $CD8^+$ T cells was analyzed by ELISA (Figure 25C) and killing capacity by flow cytometry (Figure 25B).

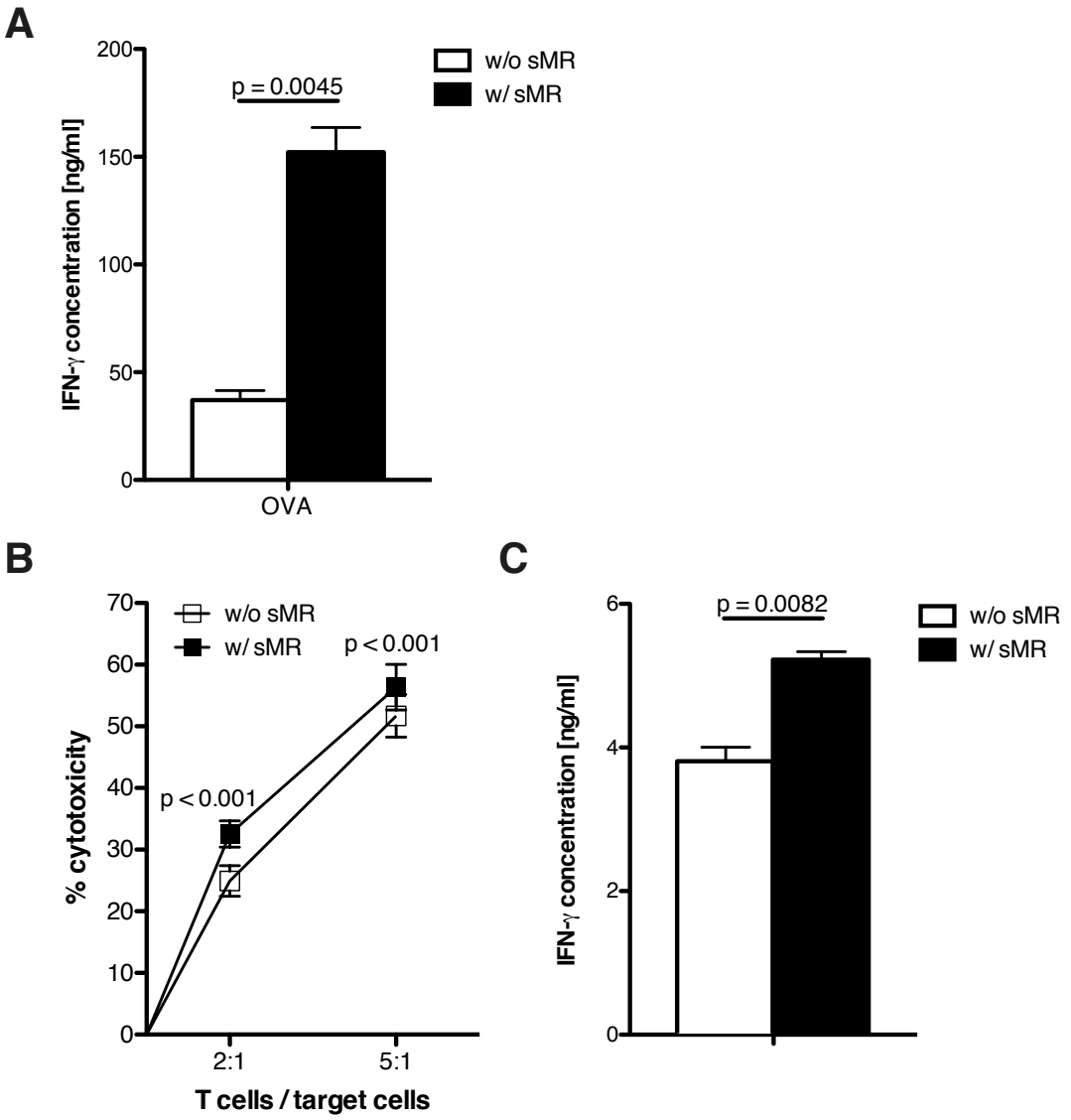

Figure 25: Treatment of BM(GM-CSF) cells with sMR-containing supernatant enhanced $CD4^+$ and $CD8^+$ T cell effector functions. $MR^{-/-}$ BM(GM-CSF) cells were stimulated O/N with sMR-containing (w/ sMR; black graphs/bars) or control (w/o sMR; white graphs/bars) supernatant. After stimulation, cells were either loaded with OVA antigen and co-cultured with antigen-specific $CD4^+$ OT-II T cells for 5 days (A) or co-culture with H-$2K^b$-specific $CD8^+$ DesTCR T cells for 3 days (B, C). Primed T cells were isolated by density gradient centrifugation and used for restimulation (A, C) or *in vitro* cytotoxicity assay (B). Data in the graphs represent (A, C) 1 experiment out of 3 independent experiments or (B) the mean of 3 independent experiments ± SEM. *P* values were calculated by student's t-test. (A, C) Isolated T cells were restimulated O/N with anti-CD3 antibody. Secretion of IFN-γ was analyzed by ELISA using cell supernatants. (B) Differently CFSE-labeled target (RMA) and control (RMA-S) cells were co-cultured with isolated T cells O/N in different T cell/ target cell ratios. Killing of target cells were analyzed by flow cytometry. Dead cells were stained with Hoechst.

In contrast to the pretreatment with recombinant MR, antigen-specific $CD4^+$ OT-II cells activated by $MR^{-/-}$ BM(GM-CSF) cells pretreated with sMR-containing supernatant secreted significantly higher amounts of IFN-γ (Figure 25A). Additionally, the cytotoxicity (Figure 25B) and secretion of IFN-γ (Figure 25C) by $CD8^+$ antigen-specific T cells were enhanced after priming by BM(GM-CSF) cells treated with sMR-containing supernatant

5.7. Altered T cell effector functions were not due to differences in T cell activation

Based on the results in Figure 21, Figure 22 and Figure 25, the recombinant FcMR seems to have a tolerogenic effect on BM(GM-CSF) cells whereas the sMR seems to have a immunstimulatory effect. To rule out differences in the activation capacity of BM(GM-CSF), surface marker, antigen uptake of BM(GM-CSF) cells and proliferation of T cells were analyzed.

5.7.1. Expression of surface molecules was not changed by FcMR or sMR

Binding of the MHC/peptide complex to the TCR is crucial for T cell priming. One additional signal to activate naïve T cells is the interaction of costimulatory molecules expressed by the APC with ligands on T cells surface [1,3,7]. This interaction promotes T cell activation. In contrast to activation, also inhibitory molecules are important to supress and terminate ongoing immune responses. To investigated if differences in T cell effector phase by FcMR and sMR-containing supernatant was due to altered activation by BM(GM-CSF) cells, first, the expression of MHC molecules (MHC I, MHC II), costimulatory molecules (CD40, CD80, CD86) as well as coinhibitory molecules (B7H1, B7DC) on the surface of BM(GM-CSF) cells were analysed after treatment with FcMR or sMR-containing supernatant.

BM(GM-CSF) cells were incubated in the presence of either FcMR and isotype control or supernatant of wt and $MR^{-/-}$ BM(GM-CSF) cells. Afterwards, surface molecules were stained with antigen-specific fluorescent-labeled antibodies and analyzed by flow cytometry (Figure 26).

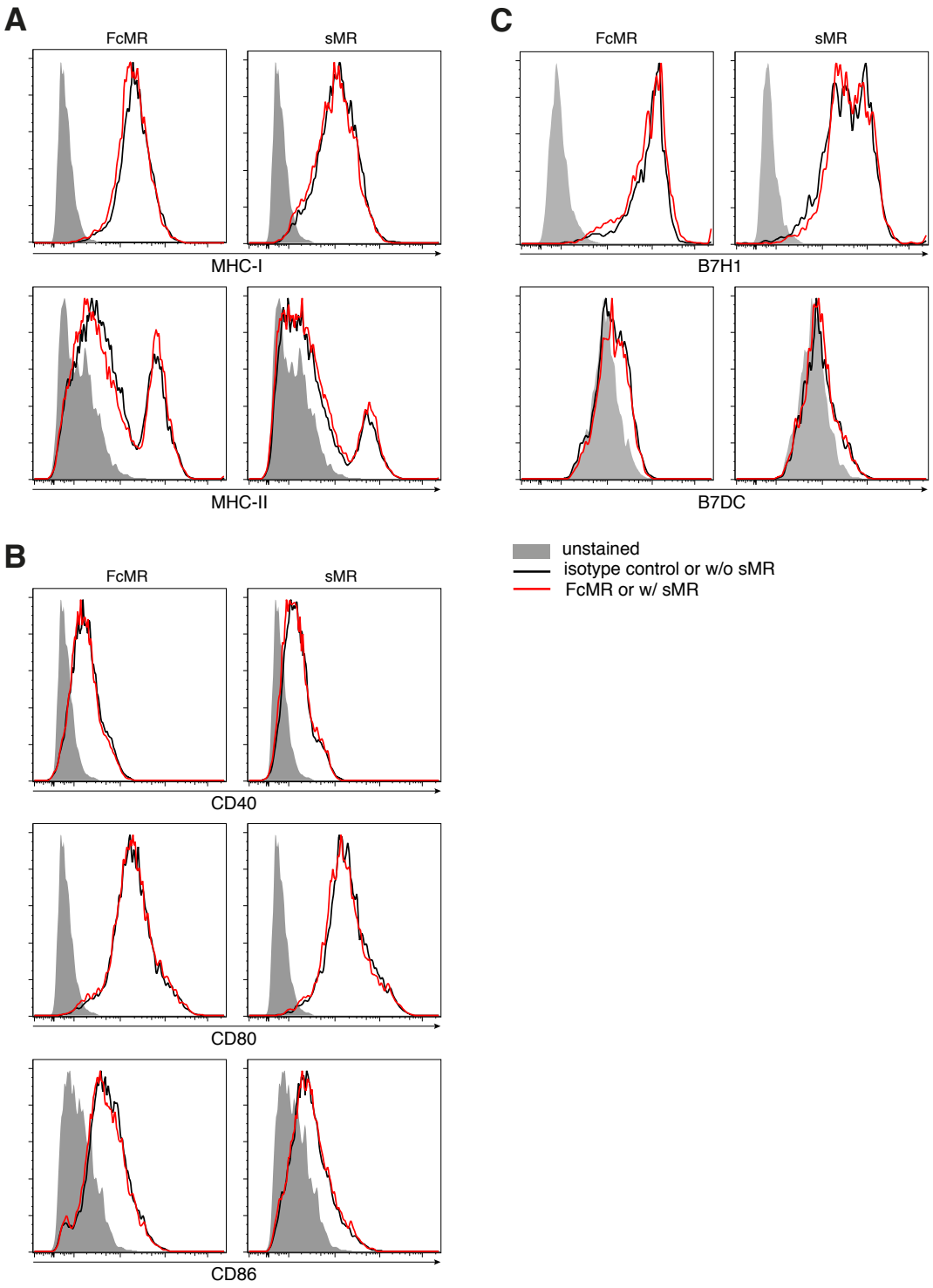

Figure 26: Expression of surface molecules on BM(GM-CSF) cells after FcMR or sMR-containing supernatant treatment was not changed. $MR^{-/-}$ BM(GM-CSF) cells were stimulated O/N with either complexed FcMR (red) and isotype control (black) or sMR-containing (red) and control supernatant (black). After stimulation, cells were scraped off and stained with fluorescent-labeled antibodies against (A) MHC molecules (MHC I, MHC II), (B) costimulatory molecules (CD40, CD80, CD86) or (C) coinhibitory molecules (B7H1, B7DC). Expression of surface molecules was analyzed by flow cytometry. Unstained cells were used as a control (filled grey). Representative graphs from 1 out of 9 independent experiments are shown.

BM(GM-CSF) cells expressed MHC I as well as MHC II molecules. Their expression was neither changed by FcMR nor by supernatant treatment (Figure 26A). The same was detected for costimulatory molecules. CD40, CD80, and CD86 were expressed but neither regulated by FcMR nor by sMR-containing supernatant (Figure 26B). The inhibitory molecules B7H1 (PD-L1) and B7DC (PD-L2) could be detected in BM(GM-CSF) cells but their expression was not influenced by treatment with FcMR or sMR-containing supernatant (Figure 26C).

Therefore, diminished and enlarged T cell effector functions by FcMR and sMR-containing supernatant treatment of BM(GM-CSF) cells, respectively, were not caused by differences in the expression of surface molecules.

5.7.2. MR treatment of BM(GM-CSF) cells do not provoke differences in antigen uptake

T cell activation is mainly based on the recognition of MHC/peptide complexes by TCRs. Therefore, peptides have to be processed and loaded on MHC molecules [8]. The surface expression of MHC molecules was not changed (see Figure 26A) whether BM(GM-CSF) cells were treated with recombinant MR or sMR-containing supernatant. Nevertheless, different peptides could be presented leading to a difference in effector cell activation. $CD8^+$ T cells in this system were activated by endogenous peptides of the BM(GM-CSF) cells and, thereby, independent of specific antigen uptake [80]. However, antigen-specific OT-II $CD4^+$ T cells were activated by an extracellular antigen (OVA) and, therefore, OVA had to be taken up by pinocytosis by the BM(GM-CSF) cells. To exclude a different activation of $CD4^+$ T cells due to altered antigen uptake by MR-treated BM(GM-CSF) cells the OVA uptake of $MR^{-/-}$ BM(GM-CSF) cells after treatment with FcMR or sMR-containing supernatant was analyzed. To validate the uptake mechanism also for receptor-mediated endocytosis, the uptake of transferrin (Trf) by the transferrin receptor, which is expressed by $MR^{-/-}$ BM(GM-CSF), was additionally analyzed.

$MR^{-/-}$ BM(GM-CSF) cells were stimulated with FcMR or supernatant containing sMR and the corresponding controls and pulsed with fluorescent-labeled OVA or Trf. Antigen uptake was analyzed by flow cytometry (Figure 27).

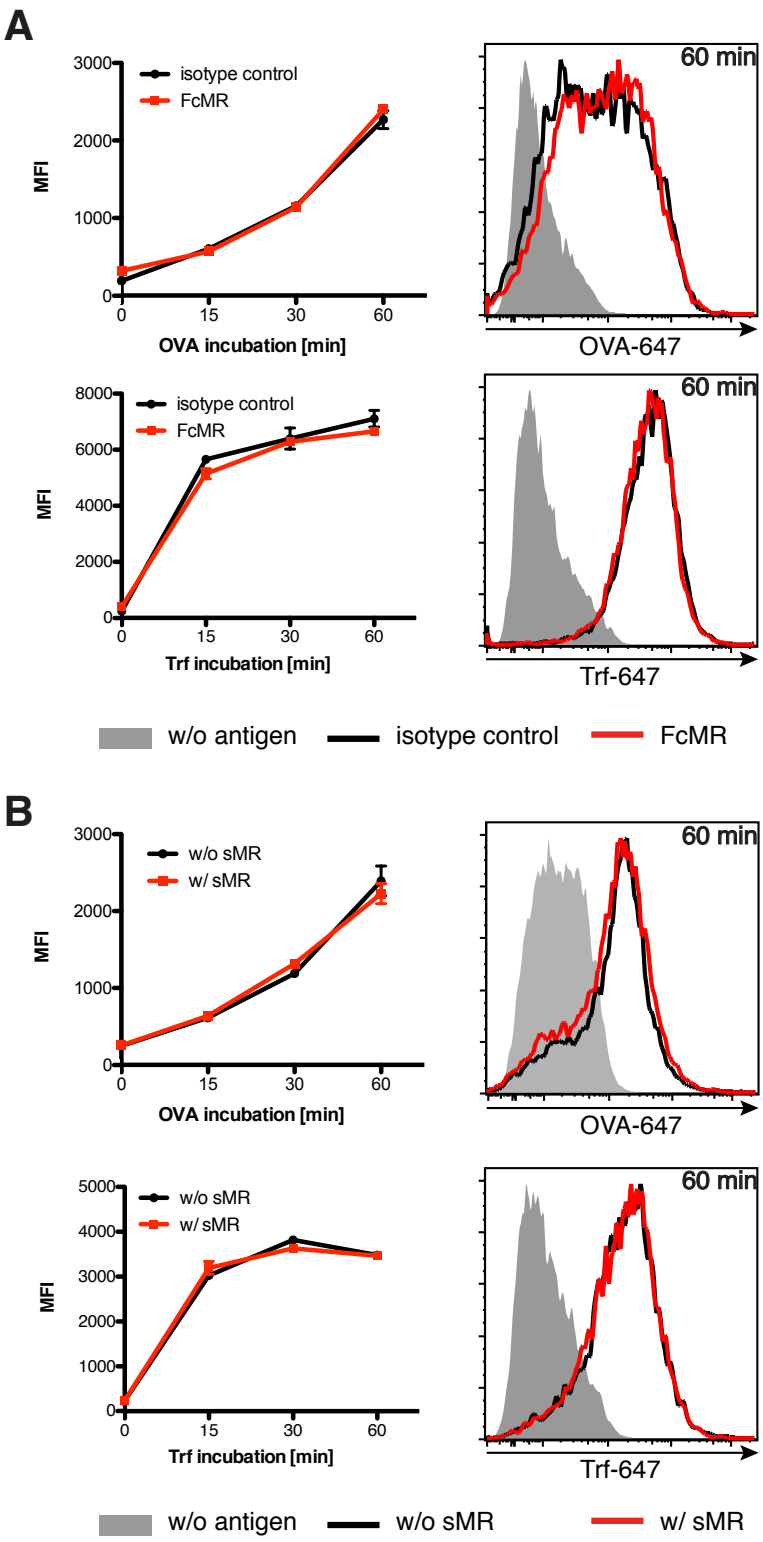

Figure 27: Pinocytosis and receptor-mediated endocytosis was not altered due to FcMR or sMR-conatining supernatant treatment of BM(GM-CSF) cells. $MR^{-/-}$ BM(GM-CSF) cells were stimulated with either (A) FcMR (red) and isotype control (black) or (B) sMR-containing (red) and control supernatant (black) O/N. Then, cells were replated and pulsed with 250 ng/mL OVA-Alexa Fluor® 647 or 5 µg/mL Trf-Alexa Fluor® 647 for 15, 30, or 60 min. Remaining antigen was washed away and uptake of antigen was analyzed by flow cytometry. Cells incubated in the absence of antigen were used as a control (filled grey). Representative graphs from 1 out of 4 independent experiments are shown.

The uptake of OVA by BM(GM-CSF) cells increased over time. Nevertheless no differences could be detected between cells stimulated with FcMR (red graph) and the isotype control (black graph) (Figure 27A, upper row). Also the incubation with supernatant (w/ sMR vs. w/o sMR) showed no influence on OVA uptake (Figure 27B, upper row). Transferrin was taken up within the first 15 minutes and its concentration only slightly increased over time. No differences in the receptor-mediated uptake of antigen were detected neither after FcMR, nor after supernatant treatment (Figure 27A and Figure 27B, bottom row).

5.7.3. IL-2 secretion and proliferation of T cells were not changed by MR treatment of BM(GM-CSF) cells

BM(GM-CSF) cells stimulated with the MR (FcMR or sMR-containing supernatant) take up antigens and express surface molecules in the same manner like control cells. However, T cells primed by MR-treated BM(GM-CSF) cells show altered activities. Therefore, it was analyzed whether the different activities of T cells were due to changed cytokine secretion or proliferation of the cells. Once activated by APCs, T cells start to secrete IL-2. IL-2 acts via an autocrine mechanism and facilitate the proliferation of T cells [4].

First, the IL-2 secretion of $CD4^+$ OT-II and $CD8^+$ DesTCR T cells was investigated. $MR^{-/-}$ BM(GM-CSF) cells were cultured in the presence of FcMR or sMR-containing supernatant (and corresponding controls) and co-cultured with antigen-specific T cells. 24 h after co-culturing, supernatants were isolated and IL-2 secretion was measured by ELISA (Figure 28).

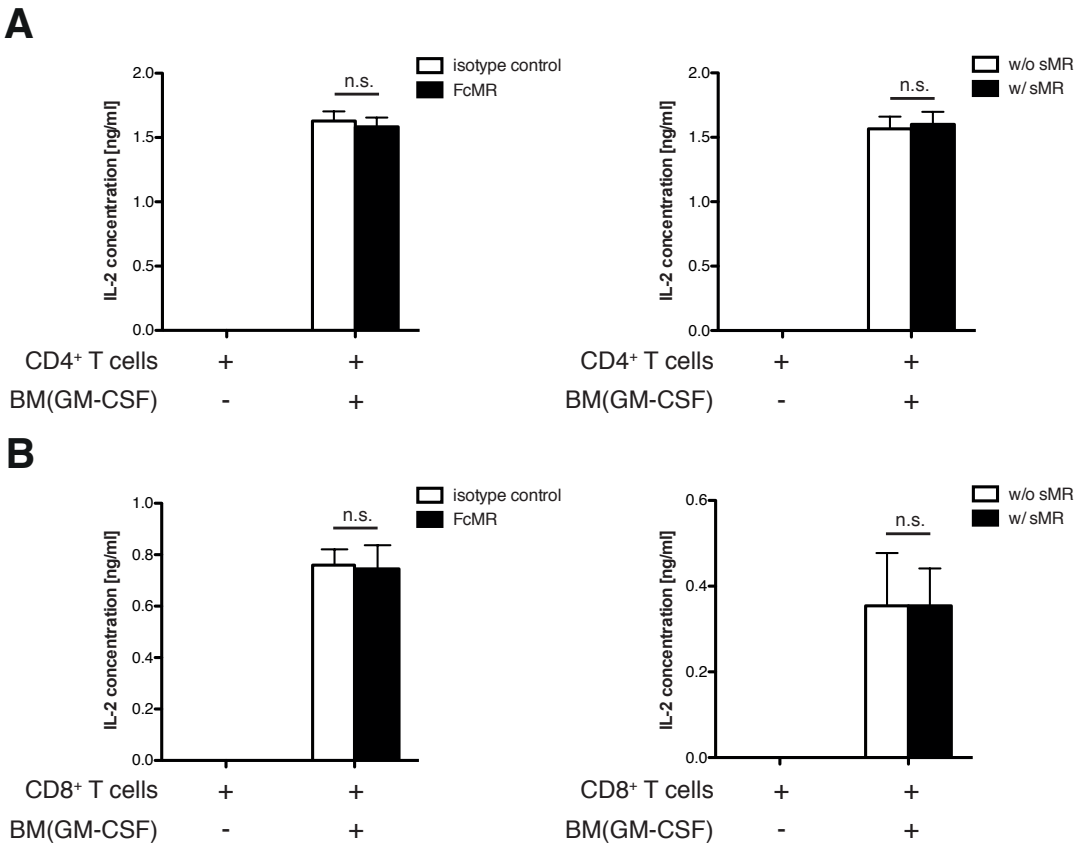

Figure 28: IL-2 secretion of primed antigen-specific T cells were not changed by MR treatment of BM(GM-CSF) cells. $MR^{-/-}$ BM(GM-CSF) cells were stimulated O/N with either complexed FcMR and isotype control (left panel) or sMR-containing and control supernatant (right panel). After stimulation, cells were loaded with OVA antigen (in case of $CD4^+$ T cells) and co-cultured with antigen-specific $CD4^+$ OT-II or $CD8^+$ DesTCR T cells for 24 h. Secretion of IL-2 by T cells were analzyed in the cell supernatant by ELISA. As a control, T cells were cultured without BM(GM-CSF) cells (left bars). Data in the graphs represent 1 experiment out of 4 independent experiments ± SEM. n.s.: not significant

T cells cultured without BM(GM-CSF) cells (Figure 28, left bars) as well as BM(GM-CSF) cells alone (data not shown) did not secrete measurable amounts of IL-2. When T cells were co-cultured with BM(GM-CSF) cells, IL-2 was secreted (Figure 28, right bars). However, no differences between MR-treated BM(GM-CSF) cells (Figure 28, black bars) and control cells (Figure 28, white bars) could be detected, neither for FcMR-treated cells, nor for sMR-containing supernatant-treated cells (Figure 28).

Next, we analyzed the proliferation rate of primed T cells. FcMR- or supernatant-prestimulated BM(GM-CSF) cells were co-cultured with CFSE-labeled antigen-specific $CD4^+$ OT-II and $CD8^+$ DesTCR T cells. Three days later, T cells were stained with fluorescent-labeled antibodies against CD4 or CD8 and cells were analyzed by flow cytometry. During proliferation CFSE is diluted equally between daughter cells with each new generation. Thus, the proliferation of T cells is depicted by a CFSE dilution profile in which each generation is represented through one peak. As a control, cells cultured in the absence of BM(GM-CSF) cells were used (Figure 29, filled grey).

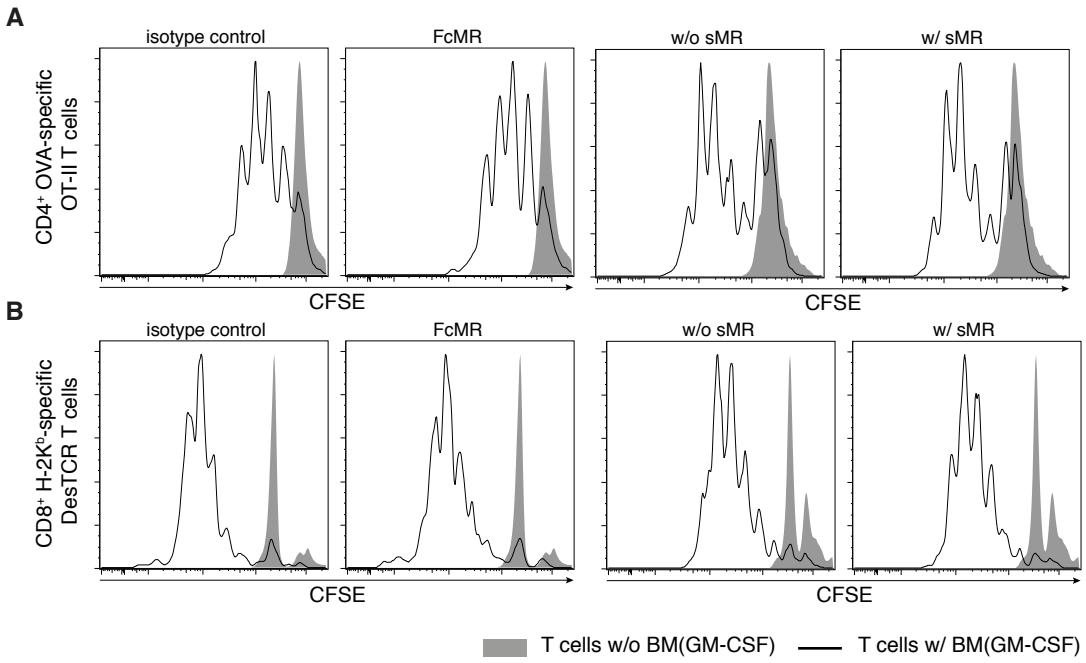

Figure 29: Proliferation of antigen-specific T cells was not changed due to MR treatment of BM(GM-CSF) cells. $MR^{-/-}$ BM(GM-CSF) cells were stimulated O/N with either FcMR and isotype control or sMR-containing (w/ sMR) and control (w/o sMR) supernatant. After stimulation, cells were either pulsed with OVA antigen and co-cultured with CFSE-labeled OVA-specific $CD4^+$ OT-II T cells (A) or co-culture with CFSE-labeled H-$2K^b$-specific $CD8^+$ DesTCR T cells directly (B) for 3 days. Antigen-specific T cells were stained by CD4 or CD8 antibody, respectively. Proliferation of T cells were analyzed by flow cytometry. T cells cultured in the absence of BM(GM-CSF) cells were used as a control (filled gray). Representative graphs from 1 out of 7 independent experiments are shown.

The experiment showed $CD4^+$ as well as $CD8^+$ T cells proliferate equally when primed by MR-treated or control BM(GM-CSF) cells (Figure 29, left panel). Furthermore, also the stimulation with sMR-containing supernatant compared to control did not influenced proliferation of antigen-specific primed $CD4^+$ and $CD8^+$ T cells (Figure 29, right panel).

5.8. *In vivo* sMR was upregulated after high-fat diet (HFD) in mice and in obese patients

In vitro, stimulation of BM(GM-CSF) cells with either FcMR or supernatant containing sMR resulted in different T effector functions of primed antigen-specific $CD4^+$ and $CD8^+$ T cells. I*n vivo*, sMR was found in murine [65] and human [68] serum offering the possibility that sMR can have an effect on cells via interaction with CD45 over distance. So far, the function of sMR is still unknown. In 2013, Rødgaard-Hansen et al. reported an upregulation of sMR in sepsis and liver disease in humans [68] and mentioned for the first time a disease-related sMR regulation. In cooperation with Bruno Guigas of the University Medical Center of Leiden we could show that analysis of adipose tissue (AT) of MR-deficient mice fed a high-fat diet (HFD) showed altered ratios of MΦ subpopulations and an increased recruitment of other immune cells like eosinophiles and neutrophiles. Furthermore, the $MR^{-/-}$ mice depicted a reduced fat accumulation of e.g. gonadal, visceral, and subcutaneous fat after HFD (unpuplished data). Further studies showed that in human AT a subpopulation of macrophages (ATM) highly expressing the MR is associated with less AT inflammation [102,103]. All these data proposed a direct correlation between MR expression and HFD induced obesity. To investigate this hypothesis the amount of sMR in serum samples of mice fed 12 weeks a low- or high-fat died and of lean and obese humans was analyzed.

First, an assay to identify sMR in serum samples was developed. sMR was immunoprecipitated with an anti-MR antibody and eluates were analyzed by SDS-PAGE and western blot (Figure 30).

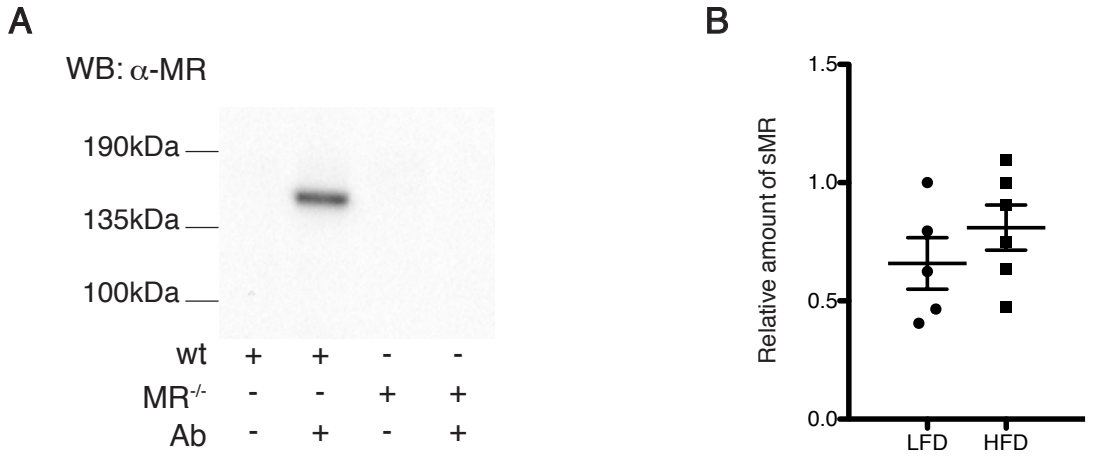

Figure 30: sMR was found in wt mouse serum and was elevated after HFD. (A) Serum samples of wildtype (wt) or $MR^{-/-}$ mice were precleared by protein A/G beads. An antibody specific for the extracellular part of the MR (clone MR5D3) was coupled to protein A/G beads. sMR of precleared samples were immunoprecipitated by antibody-coupled protein A/G beads. Beads without antibody were used as a control. Eluates were analyzed by SDS-PAGE and western blot. sMR were detected by an biotin-labelled antibody specific for the MR (clone MR5D3). Representative blot from 1 out of 4 independent experiments is shown. (B) Serum samples of 5 mice fed a low-fat died (LFD) or 6 mice fed a high-fat died (HFD) for 12 weeks were analyzed as described in (A). Relative intensities of MR bands on western blot were normalized to the mean of relative quantities of LFD samples. Data in the graphs represent the mean of 5 (LFD) or 6 (HFD) individual ± SEM.

We could specifically immunoprecipitated sMR from serum of wt mice but not from serum of $MR^{-/-}$ mice (Figure 30A). If no antibody was used in the precipitation sMR could not isolated neither in wt nor in $MR^{-/-}$ serum.

We used the established assay to immunoprecipitate sMR from serum samples of 5 low-fat diet (LFD) and 6 high-fat diet (HFD) mice. Increased amounts of sMR were detected in serum samples of mice fed HFD compared to LFD mice (Figure 30B).

In addition, sMR levels in the human serum samples were analyzed (Figure 31).

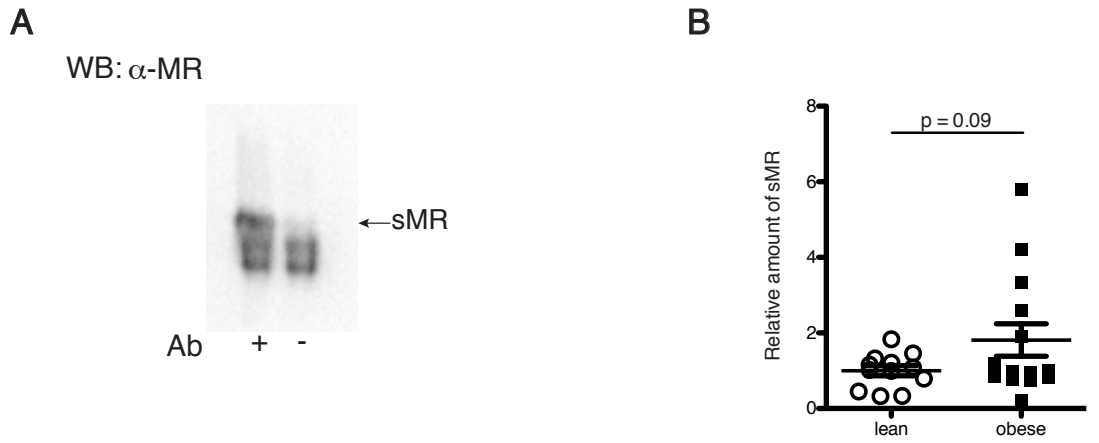

Figure 31: sMR was found in human serum and was elevated in obese patients. (A) A human serum sample was precleared by protein A/G beads. An antibody specific for the extracellular part of the MR (clone 7-450) was coupled to protein A/G beads. sMR of precleared samples were immunoprecipitated by antibody-coupled protein A/G beads. Beads without antibody were used as a control. Eluates were analyzed by SDS-PAGE and western blot. sMR were detected by an biotin-labelled antibody specific for the MR (clone 15-2). Representative blot from 1 out of 2 independent experiments is shown. (B) Serum samples of 12 lean and 14 obese patients were analyzed as described in (A). Relative intensities of MR bands on western blot were normalized to the mean of relative quantities of LFD samples. Data in the graphs represent the mean of 12 (lean) or 14 (obese) patients ± SEM. *P* values were calculated by student's t-test.

An immunoprecipitation of sMR from human serum sample was also possible. sMR was detected in western blot when an anti-human MR antibody was used in comparison to the same serum sample without antibody used in the precipitation (Figure 31A). Analysis of serum samples from 12 lean and 14 obese patients revealed enhanced sMR levels in obese humans compared to lean patients (Figure 31B).

6. Discussion

Antigen presenting cells (APCs) are essential to initiate an effective antigen-specific immune response when inflammatory processes were not completely eliminated by the innate immune system [8]. In addition, APCs are also important for the induction of immune tolerance [104,105]. Balancing immune response and tolerance, the intracellular signaling pathways leading to T cell activation versus T cell tolerance and involved receptor-proteins are still under investigation [106].

The mannose receptor (MR) is one of these receptors. It is expressed by a variety of cells including MΦs, non-vascular endothelium, a multitude of immune inhibitory cells and DCs, the major cell type at the cross talk between innate and adaptive immune response [54,55,76,78,107]. As an endocytic receptor on the cell surface of DCs, the MR induces immunity under inflammatory conditions through the uptake and processing of foreign extracellular antigens [54]. Under non-inflammatory conditions, the MR on DCs provokes $CD8^+$ T cell tolerance by binding to CD45 on T cells. The interaction between MR and CD45 inhibits CD45 phosphatase activity leading to T cell re-programming and the upregulation of CTLA-4, which in turn inhibits $CD8^+$ T cell cytotoxicitiy [79].

The present study demonstrates that CD45 on the surface of BM(GM-CSF) cells is bound by the MR, reducing its phosphatase activity and thereby altering BM(GM-CSF) cell behavior leading to changes in effector function of primed antigen-specific T cells. Additionally, this study presents a correlation of MR expression and HFD-induced obesity in mice and human.

6.1. The MR as binding partner of CD45

CD45 is a leukocyte-specific glycoprotein expressed in a cell-type specific pattern depending on differentially expressed exons and developmental stage of the cell [22]. The MR was discovered as a binding partner of CD45 by Martinez-Pomares et al. (1999). They observed a binding of the CR domain of the MR to two of the low molecular weight isoforms (~180 kDa) of CD45 expressed by marginal zone metallophilic MΦs and subcapsular sinus MΦs in secondary lymphoid organs and follicular DCs [53]. Schuette et al. (2016) showed an interaction of the MR with CD45 on $CD8^+$ T cells. Under non-inflammatory conditions, these cells express an intermediate molecular weight (~200 kDa) isoform of CD45 that was bound by the MR [79]. In this work, we were able to demonstrate that a recombinant MR construct comprising the CR, FN II and the CTLD1-2 domains of the MR (FcMR) also binds to CD45 of BM(GM-CSF) cells

expressing the lowest molecular weight isoform CD45R0 (Figure 16). Due to the fact that CD45 is expressed by all leukocytes in a cell-type specific pattern and the interaction of MR with CD45 was discovered in different cells expressing different isoforms, this raises the question which isoform is exactly bound by the MR and whether the expression of a specific isoform has an influence on the effect of the MR on the cell.

The extracellular part of CD45 differs in size, shape, and charge due to various isoforms. In BM(GM-CSF) cells no alternatively spliced exon could be detected neither in western blot analysis nor in flow cytometry (Figure 14 and Figure 15). This shows that BM(GM-CSF) cells express the lowest molecular isoform CD45R0. Although, Martinez-Pomares et al. [53] and Schuette et al. [79] showed an interaction of the CR domain of the MR with higher molecular weight isoforms of CD45, however, the FcMR binds to CD45R0 in BM(GM-CSF) cells (Figure 16). The domains common to all isoforms are the CR and FN III domain. An important function for these domains was already suggested based on the high variability of sequence divergence in rodents, cattle, and primates [108].
A disruption of the binding of MR to CD45 was observed after peptide N-glycanase F (PNGase F) treatment [53]. PNGase F releases intact N-glycans by cleavage between the innermost N-acetylglucosamine and asparagine. The CR and the FN III domains of CD45 are N-glycosylated, whereas the alternatively spliced exons A, B, and C are O-glycosylated [23]. These support the hypothesis that the MR might bind to the CR or FN III domain of CD45. Furthermore, this indicates that cell-specific glycosylation of CD45 is indeed responsible for the binding of MR.
The recognition of translational modifications of CD45 can explain why a binding of FcMR in BM(GM-CSF) cells was only detected with the upper of two CD45-specific bands (170-190 kDa) in our western blot analysis (Figure 16). The two bands in western blot might indicate two different glycosylated forms of CD45R0 because differences in size through glycosylation might result in a different migration in SDS-PAGE.
We also generated transient chinese hamster ovarian (CHO) cell lines expressing only one specific murine CD45 isoform and analyzed the binding of FcMR to CD45 (data not shown). Although, CD45 isoforms could be detected in CHO cells by isoform-specific antibodies in western blot analysis and flow cytometry, no interaction of FcMR with CD45 was detected. Due to cell type-specific expression of glycosylation enzymes these results further support the assumption that posttranslational modifications especially glycosylation of CD45 are recognized by the MR.

6.2. The importance of CD45 for APCs

The function of CD45 in lymphocytes has been intensely studied but in APCs the function is still elusive [109]. As a protein tyrosine phosphatase, CD45 has a pivotal role in signal transduction and has been linked to many autoimmune diseases [108].

In MΦs, CD45 is associated with adhesion [95,110]. It was reported that CD45-deficient mice have a defective β2-integrin-dependent adherence. CD45 co-localize with β2 integrin and Src kinases in focal contact sites [95] and was reported to be involved in two steps of integrin signaling. First, CD45 regulates paxillin degradation in MΦs [110]. Paxillin is essential in the signaling scaffold recruitment early in integrin adhesion [111]. Second, CD45 limits the activation of Src kinases by dephosphorylation of the autocatalytic site. In $CD45^{-/-}$ MΦs it has been described that the kinases Hck and Lyn are hyperphosphorylated and hyperactivated [95]. Our results show that the binding of FcMR to CD45 as well as stimulation with sMR-containing supernatant inhibits CD45 phosphatase activity in BM(GM-CSF) cells (Figure 17 and Figure 24) and indicates indeed an enhanced overall tyrosine phosphorylation of proteins (Figure 19 and Figure 24).

Antigen-specific T cells primed by FcMR- or sMR-containing supernatant-treated BM(GM-CSF) cells exhibit immune inhibitory or immune stimulatory capacity, respectively. The adhesion between APCs and T cells is important for the priming of T cells. A long-lasting interaction between APCs and T cells is necessary for efficient T cell priming whereas a short contact of APC and T cell has been postulated to induce tolerance [112,113]. A modified adhesion through MR-mediated inhibition of CD45 activity might be a reason for changed T cell effector function. Nevertheless it would not explain the opposed influence of FcMR and sMR-containing supernatant because both inhibited CD45 phosphatase activity in our experiments.

6.1. MR influence on priming capacity of APCs

Our data show that the binding of FcMR to CD45 in BM(GM-CSF) cells results in diminished $CD4^+$ and $CD8^+$ T cell effector function indicated by reduced IFN-γ secretion of primed antigen-specific T cells after restimulation (Figure 21) and decreased cytotoxic capacity of $CD8^+$ T cells (Figure 22A). In contrast, the treatment of BM(GM-CSF) cells with supernatant containing sMR increased the immunogenic phenotype of primed antigen-specific T cells. The cytokine secretion of $CD4^+$ T cells primed by BM(GM-CSF) cells treated with sMR-containing supernatant is elevated

(Figure 25A) and cytotoxicity of $CD8^+$ T cells is enhanced (Figure 25B). Thus, FcMR and sMR-containing supernatant seem to have opposing effects on BM(GM-CSF) cells which might be due to different priming of T cells.

The function of activated T cells regarding immunity versus tolerance is determined by the balance between immune stimulatory and inhibitory signals.
One important signal for the priming of T cells is the presentation of antigen on MHC molecules [7]. An altered antigen uptake might be causal for the differences between FcMR- and sMR-containing supernatant-mediated effector functions. Uptake of soluble protein and apoptotic cellular antigens is regulated by small GTPases that control vesicle trafficking in APCs. Inhibition of small GTPases correlates with defects in activating antigen-specific T cells [114,115]. Through integrin-mediated signaling chemical signals are transmitted into the cell (outside-in signaling). These signals provide a basis for responding to other inputs including those transmitted by growth-factor or G-protein-coupled receptors and thereby has an influence on regulation of immune system activity and inflammation [111]. In this study, an impact of the MR on antigen uptake and processing could not be observed. Neither pinocytosis nor receptor-mediated endocytosis were diminished or enhanced by FcMR or sMR-containing supernatant (Figure 27). Furthermore, the expression of MHC molecules remains the same after FcMR or sMR-containing supernatant treatment of BM(GM-CSF) cells (Figure 26A). These results additionally provide the evidence that an influence of the MR on CD45 in context of integrin-mediated adhesion might be unlikely. Nevertheless, the adhesion of MR-treated cell has to be considered.

Costimulatory signals provided by APCs are another critical determinant for T cell activation [7,116]. Signals arising from costimulatory and coinhibitory molecules dedicate activation of T cells. In correlation between CD45 and costimulation has been described by Thiel at al. (2015). It was reported that $CD45^{-/-}$ DCs are slightly pre-activated indicated by enhanced expression of costimulatory molecules [109]. We considered the expression of costimulatory (CD40, CD80, CD86) and coinhibitory molecules (B7H1, B7DC) on FcMR- or supernatant-treated BM(GM-CSF) cells determined however no up- or downregulation (Figure 26B and Figure 26C). According to that, MR-mediated inhibition of CD45 phosphatase activity has no influence on costimulation provided by APCs.

Other groups described an association of CD45 with cytokine secretion in myeloid cells [34–36]. Cytokines releases by APCs are important to dictate development of specialized T effector cells [7]. An increased secretion of pro-inflammatory cytokines (TNFalpha, IL-6) was reported for CD45-deficient BMDCs and splenic DCs upon TLR3 and TLR9 stimulation [36]. Montoya et al. (2006) demonstrate that $CD45^{-/-}$ splenic DCs offered a decreased type I IFN secretion (anti-inflammatory) in response to lymphocytic choriomeningitis virus [35]. This versatile effect of CD45 on the secretion of different cytokines was further supported by Cross et al. (2008) which described CD45 as negative regulator of MyD88-dependent TLR signalling and as positive regulator of MyD88-independent TLR signalling [34]. We hypothesized an relationship of cytokine secretion by MR-treated BM(GM-CSF) cells and the down-regulation of CD45 activity. It was investigated if FcMR and sMR-containing supernatant treatment facilitates different cytokine profiles in BM(GM-CSF) cells but TNFalpha was even less secreted by our cells and IL-6 secretion was not influenced under non-inflammatory conditions (data not shown). Even stimulation of BM(GM-CSF) cells by TLR1/2 (Pam3Csk4), TLR4 (LPS), and TLR9 (CpG) agonist did not altered TNFalpha and IL-6 secretion (data not shown).

Because both FcMR and sMR-containing supernatant stimulation did not influence antigen-uptake and –presentation, costimulation, and cytokine secretion of APCs the activation capacity of BM(GM-CSF) cells per se is not the reason for diverse effects on T effector function. This is additionally supported by the fact that proliferation (Figure 29) and IL-2 secretion of T cells primed by MR-stimulated BM(GM-CSF) cells (Figure 28) showed no variation at all.

6.2. Diverse effects of FcMR and sMR on BM(GM-CSF) cells

How FcMR and sMR-containing supernatant could have such opposing effects on BM(GM-CSF) cells remains elusive.

The phosphatase activity of CD45 is inhibited by dimerization [18]. CD45 is expressed at different developmental and activation stages in multiple, highly conserved isoforms [18]. The homodimerization efficiencies of all isoforms are different [117] but *in vitro* the various isoforms showed similar PTP activity [118]. For CD45R0, it was described that this isoform homodimerizes more easily than other isoforms [108].

Experiments in T cells with recombinant CD45 comprising the cytoplasmic domain of CD45 fused to the ligand-binding domain of epidermal growth factor receptor (EGFR) demonstrated that forced dimerization of an intracellular part of CD45 decreased TCR signaling [24]. Additional research revealed a specific juxtamembrane 'wedge' motif to be involved in dimerization of CD45 [18] Majeti et al. (2000) generated a constitutively active form of CD45 by inactivate the inhibitory wedge motif by an inactivating point mutation (CD45E613R). This point mutation leads to an autoimmune syndrome in mice resembling human systemic lupus erythematosus (SLE) [28]. These results suggest a mechanism that might regulate CD45 phosphatase activity by ligand-mediated dimerization.

At this point, one must focus on the addition of MR in our experiments. We used either purified recombinant MR (FcMR) or supernatant of cells generating a soluble form of the MR (sMR). In all experiments, FcMR had to be complexed by an anti-human antibody that binds to the fused human IgG1 Fc part in the recombinant protein. The complexation enables a multimerization of FcMR. If CD45 homodimerizes autonomous the binding of complexed FcMR might facilitate an enhanced dimerization of CD45 resulting in a strong decreased CD45 phosphatase activity (Figure 32, middle) similar to cell membrane-bound MR (cMR). Schuette et al. (2016) showed that interaction of cMR from wildtype BMDCs reduced CD45 phosphatase activity in $CD8^+$ T cells by direct interaction with CD45 compared to $CD8^+$ T cells that were co-cultured with MR-deficient BMDCs [79]. Membrane-associated proteins, such as the MR, clustere into "protein islands" in the cell [119]. Therefore, the clustered cMR binds to CD45, stabilizing the homodimerization and decreasing CD45 phosphatase activity (Figure 32, left).
In contrast to the purified FcMR, the sMR was applied as a component of cell supernatant. No further supplement was directly added to complex sMR in the supernatant. After independent homodimerization of CD45, which leads to an inhibition of CD45 phosphatase activity, the conformation might not be stabilized by sMR as it could be in case of complexed FcMR (Figure 32, right). Thus, the inhibition of CD45 phosphatase activity is neither enhanced nor prolonged.
The different inhibition of CD45 phosphatase activity concerning strength and duration of inhibition could influence the BM(GM-CSF) cells in different manner.

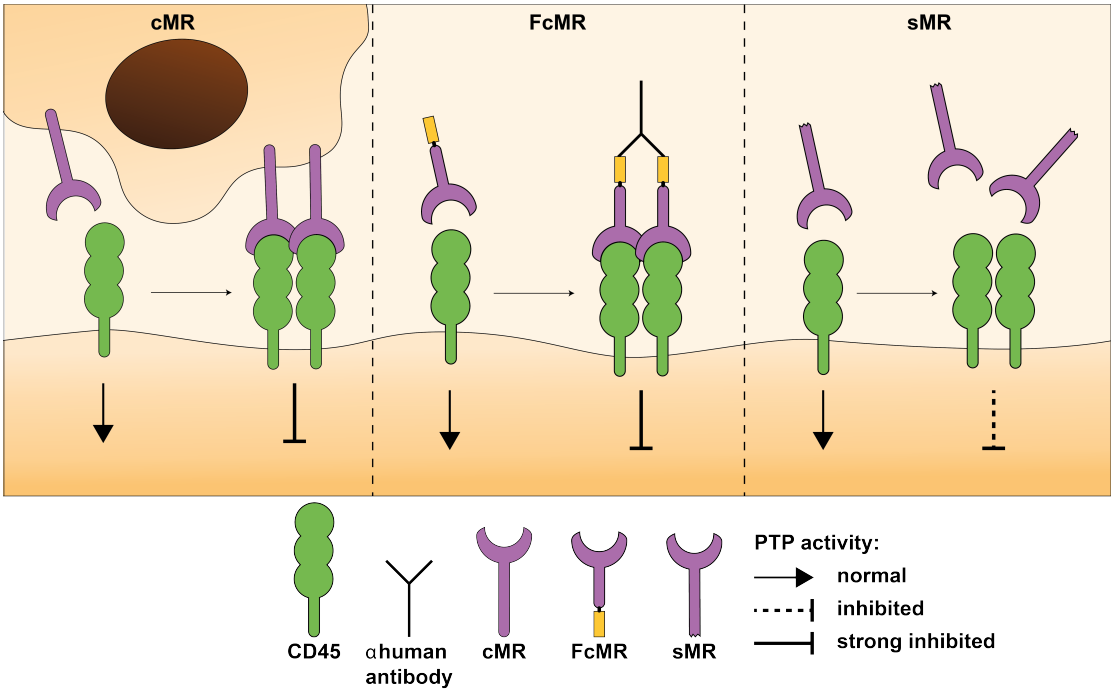

Figure 32: Hypothesis of dimerization of CD45 by cMR, FcMR, or sMR. Cell-bound MR (cMR), organized in protein clusters, binds to autonomous homodimerized CD45 and enables strong inhibition of CD45 phosphatase activity (left panel). Complexation of FcMR by an anti-human antibody that recognized fused human IgG1 Fc part of FcMR enables multimerization. Binding of this FcMR complexes to CD45 enhances autonomous homodimerization of CD45 also leading to strong inhibition of CD45 phosphatase activity (middle panel). sMR is added as component of cell supernatant and without a factor that facilitate complexation of sMR. Independent homodimerization of CD45 is not stabilized by sMR why inhibition of CD45 phosphatase activity is not increased (right panel).

Whereas FcMR contains the CR, FN II, and CTLD1-2 domain of the MR, the sMR comprises also CTLD3-8. CTLD4 and 5 have carbohydrate-binding ability [55]. This additional ligand-binding site of sMR can also have an impact on the interaction with CD45. Mannosylated oligosaccharides with more than one mannose residue might facilitate the clustering of sMR in cell supernatant as well as in serum. This may suggest that multiple soluble mannose receptor molecules cooperate in the ligand binding process to CD45 [120] comparable to complexed FcMR. In contrast, unpublished data from Dr. Verena Schütte showed that addition of OVA, a binding partner for CTLD4 of the MR, interrupts the interaction of MR with CD45 on $CD8^+$ T cells. This result shows that ligand binding by CTLDs and CR domain of the MR is competitively meaning that binding of mannosylated proteins to CTLDs can also interrupt interaction with CD45.

Another reason for the diverse effect of FcMR and sMR-containing supernatant could be the supernatant itself. sMR for our experiments was produced by BM(GM-CSF) cells that shed sMR by cleavage of metalloproteases [65]. After 4-5 days of culturing MR-positive BM(GM-CSF) cells sMR could be detected in the supernatant (Figure 23). Subsequently, this supernatant was used to stimulated MR-negative BM(GM-CSF) cells to analyze the influence of sMR on these cells.

The supernatant was collected from wildtype BM(GM-CSF) cells expressing the MR but also CD45. During culturing the amount of sMR increased continuously. Due to the expression of CD45 in sMR-producing BM(GM-CSF) cells, the sMR might bind in an autocrine manner to the MR-positive BM(GM-CSF) cells. Thereby, the sMR-producing MR-positiv BM(GM-CSF) cells might be altered by sMR/CD45 interaction as shown by altered phosphotyrosine levels of stimulated BM(GM-CSF) cells (Figure 24). Changed intracellular pathways in stimulated MR-positive BM(GM-CSF) cells might result in the production of additional soluble factors which influence MR-negative BM(GM-CSF) cells in a subsequent stimulation with supernatant (Figure 33).

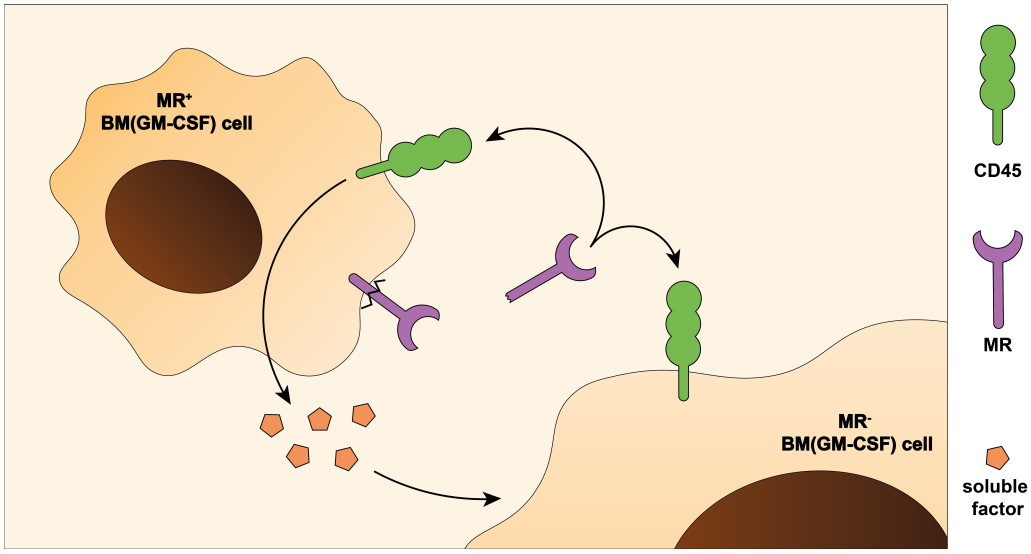

Figure 33: Model of the autocrine effect of sMR on sMR-producing MR-positive BM(GM-CSF) cells. sMR-containing supernatant was collected after culturing MR-positive BM(GM-CSF) cells for 4-5 days. In this time, MR-positive BM(GM-CSF) cells generated sMR by cleavage through metalloproteases. sMR within the supernatant binds to CD45 of sMR-producing MR-positive BM(GM-CSF) cells as well as to CD45 of MR-negative BM(GM-CSF) cells in subsequent stimulation. Interaction of sMR and CD45 on MR-positive BM(GM-CSF) cells influences sMR-producing MR-positive BM(GM-CSF) cells triggering the secretion of additional soluble factor. In turn, these factors together with sMR stimulate MR-negative BM(GM-CSF) cells in the subsequent incubation resulting in different effects compared to stimulation of MR-negative BM(GM-CSF) cells with recombinant MR.

Thus, subsequently, the MR-negative BM(GM-CSF) cells are not only influenced by sMR but also by additional soluble factor leading to the observed immunstimulatory capacity instead of the observed induction of immuntolerance caused by FcMR. The sMR-containing supernatant was tested for different cytokines (IFN-γ, IL-12, IL-6, IL-10) with no difference compared to the cytokine levels of supernatant from MR-deficient BM(GM-CSF) cells (data not shown). This analysis covers only a minimal proportion of soluble factors secreted by APCs. To circumvent additional effects of soluble factors, experiments with purified sMR are essential to verify its effects on BM(GM-CSF) cells without cofactors.

6.3. CD45 and JAK/STAT signaling in APCs

The Janus kinase/signal transducers and activators of transcription (JAK/STAT) pathway provides a mechanism to translate extracellular signal e.g. cytokines and growth factors, into a transcriptional response. Activation of this signal pathway stimulates cell proliferation, differentiation, cell migration, and apoptosis. Mutations that constitutively activate or inactivate players of this pathway cause inflammatory diseases [121]. For example, STAT3 has been indicated in several studies to suppress DC maturation and activation, and promotes tolerogenic function [106,122–125]. Increased STAT3 activation in c-fes$^{-/-}$ mice leads to impaired inflammatory responses [126]. Furthermore, the disruption of the *STAT3* gene in MΦ results in an abnormal activity concerning polarization of Th1 responses and increased amounts of secreted inflammatory cytokines in response to endotoxin [127]. Mice lacking STAT1 are highly sensitive to different viruses such as influenza virus, herpes simplex virus, and vesicular stomatitis virus [128–130].

CD45 is known to negatively regulate JAK/STAT pathway [48]. *In vitro* studies showed that CD45-deficient mast cells showed enhanced proliferation in response to IL-3 indicating a role of CD45 in the regulation of IL-3 signalling. Irie-Sasaki et al. (2001) revealed that CD45 directly interacts and dephosphorylates JAK2. In line with this, in CD45-deficient mice hyperphosphorylation of JAK2, STAT3 and STAT5 was detected [48].

In general, exogenous ligand binding to receptors induces multimerization of receptors, which allows transphosphorlyation of associated JAKs. Subsequently, JAK phosphorylates STAT molecules that dimerize, enter the nucleus, and activate or repress transcriptional processes [121]. The interaction of FcMR with CD45 leads to a diminished CD45 phosphatase activity (Figure 17) and elevated phosphotyrosine levels (Figure 19) in BM(GM-CSF) cells. This observation raised the question whether the MR has an

impact on JAK/STAT signaling in BM(GM-CSF) cells or not. We could show that mRNA levels of STAT1 were enhanced 4 h after MR stimulation (Figure 20) Target genes of STATs are among other suppressors of cytokine signaling (SOCS) proteins that act as negative regulator of JAK/STAT pathway [121]. In addition, translation of SOCS3 was strongly enhanced after MR stimulation of BM(GM-CSF) cells (Figure 20). This further indicates a correlation between the MR and JAK/STAT signaling. These hints of transcriptional regulation by MR has to be further investigated by transcriptome analysis in MR-deficient BM(GM-CSF) cells stimulated with FcMR or control. Thus, genes and other signaling pathways that facilitate the diminished effector functions of primed antigen-specific T cells might be discovered influencing BM(GM-CSF) cell activity. Additionally, this analysis can clarify what kind of other molecules or soluble factors are responsible for the divers effect of sMR-containing supernatant due to interaction of sMR with CD45 during production of the supernatant

6.1. sMR in disease states

The cell-bound form of the MR (cMR) binds a wide range of microbial antigens, e.g. *Candida albicans*, *Leishmania*, *Mycobacterium tuberculosis*, *HIV*, and *Pneumocytstis carniii,* and facilitates the clearance of these pathogens [131]. Additionally to the cMR, a functional soluble form (sMR) is shed by MR-positive cells [66]. This shedding is mediated by metalloproteases and enhanced during inflammation [65,66]. One postulated function of the sMR is to carry soluble ligand to areas of active immune response. Martinez-Pomares et al. (1996) detected the binding of a chimeric construct comprising the CR domain of the MR to cells in the germinal center of lymphoid organs in mice [59]. Confirming experiments with a chimeric construct of CTLD4-8 of the MR fused to human IgG1 showed improved binding of MR to *P. carinii* and enhanced uptake of the pathogen by phagocytic cells. However, the uptake was mediated by the interacting of the recombinant protein with cellular Fc-receptors [132].

Beside the function in pathogen clearance, an assisting function for pathogen to escape the immune response was observed. Shedding of sMR is enhanced by fungi (*P. carinii*, *Candida albicans*, *Aspergillius fumigatus*) through binding of β-glucans to dectin-1 [66]. Extracellular *P. carinii* is coated with sMR and circumvents phagocytosis by MΦs [67]. We detected the binding of a chimeric construct comprising the CR, FN II and CTLD1-2 domains of the MR dampen the immune response of T cells through binding to CD45

on APCs. This indicates a mechanism how pathogen-enhanced shedding may facilitate immune escape.

In contrast, the addition of supernatant containing sMR to BM(GM-CSF) cells promoted immunogenicity of primed T cells. This might be the underlying pathomechanism why sMR is enhanced in human serum in various disease states [68]. In general, sMR is found in serum of mice [65] and human [68] as we also showed in this work (Figure 30 and Figure 31). sMR is detectable both in healthy and diseased individuals, but levels are enhanced in diseased individuals [68]. Serum levels of human sMR correlate with other markers of infection and inflammation such as soluble CD136 [68]. Patients chronically infected with HCV and with cirrhosis has significantly higher amounts of sMR in serum than those with no or mild fibrosis [133]. Furthermore, Rødgaard-Hansen et al. (2014) predict sMR as a marker for several disease states such as sepsis and liver disease [68]. In fibrotic processes in the liver Kupffer cells have an important role [134]. They produce growth factors, cytokines, chemokines and metalloproteases that regulate pro- and anti-fibrotic processes [134,135]. Andersen et al. (2014) consider sMR as a marker for the activation of Kupffer cell during chronic inflammation [133].

Analysis of wildtype and MR-deficient mice fed a low-fat diet (LFD) or high-fat diet (HFD) revealed that in adipose tissue (AT) of MR-deficient mice subpopulations of MΦs were altered (unpublished data). Adipose tissue MΦs (ATMs) are responsible for obesity-linked inflammation due to secretion of pro-inflammatory cytokines [103]. The polarization state of ATMs is dynamic regarding the relationship of pro-inflammatory and anti-inflammatory MΦs. In general, in obese individuals, the amount of CD11c-positive pro-inflammatory MΦs exceeds the amount of Ym1-positive anti-inflammatory MΦs [136]. In HFD MR-deficient mice, the amount of CD11c-positiv MΦs is reduced compared to wildtype mice. Furthermore, HFD of MR-deficient mice resulted in an enhanced recruitment of other immune cells, e.g. eosinophils and neutrophils, in the AT and a reduced fat accumulation (unpublished data). We analyzed serum samples of LFD vs. HFD mice as well as of lean and obese humans to investigate a correlation of MR expression and HFD-induced obesity. Both mice and human sMR levels were enhanced after HFD and obesity, respectively (Figure 30 and Figure 31). *In vitro*, the sMR in cell supernatant may provoke an immunstimulatory effect on antigen-specific T cells primed by pre-stimulated BM(GM-CSF) cells. In AT, the populations that express high levels of MR are anti-inflammatory MΦs [136]. The expression of MR in these MΦs is decreased in chronically trained mice compared to sedentary mice on HFD [137]. The *in vivo* data

reinforce the assumption that sMR correlates to inflammatory processes. However, the shedding of sMR is correlated to the expression of cMR [65]. It cannot be excluded that sMR has no specific function and is rather a biomarker for several diseases due to enhanced expression of cMR during inflammation as proposed by Rødgaard-Hansen et al. [68].

7. Outlook

The results of the present study highlight a strong effect of the MR on BM(GM-CSF) cells by direct interaction with CD45. Still, there are many open questions to be answered.

The first question to be raised is whether a multimerization of MR is important for the interaction with CD45. To further elucidate if a crosslinking of MR molecules such as in case of cell-bound MR or complexed FcMR is necessary to provoke the observed effect on CD45 phosphatase inhibition it is essential to investigate the CD45 phosphatase activity in $MR^{-/-}$ BM(GM-CSF) cells stimulated with uncomplexed FcMR. If single FcMR molecules will reduce the CD45 phosphatase activity the priming capacity of stimulated BM(GM-CSF) cells need to be further analysed by detecting IFN-γ secretion and cytotoxicity of primed antigen-specific T cells.

The addition of supernatant containing sMR to BM(GM-CSF) cells reduced the CD45 phosphatase activity similar to complexed FcMR, nevertheless, antigen-specific T cells primed by these BM(GM-CSF) cells showed contrary effector functions. To investigate if these results are based on other molecules present in the supernatant the experiments need to be repeated with purified sMR. To this end, an assay needs to be established to isolate sMR from cell supernatant by affinity chromatography. If one is able to isolate sMR, experiments can be performed to further elucidate if incubation of BM(GM-CSF) cells with sMR results in diminished effector functions of primed antigen-specific T cells similar to complexed FcMR. Furthermore, sMR should be isolated from murine serum to investigate its influence on BM(GM-CSF) cells as a second source of naturally produced sMR and to further elucidate the function of sMR *in vivo*.

Beside the CR domain of MR that mediated the interaction with CD45 sMR also comprise CTLD4-8 and, thereby, has a second ligand-binding site. It is essential to perform competition experiments to investigate if the binding of a second ligand with CTLDs increase or inhibit binding capacity of MR to CD45. To this end, co-immunoprecipitation experiments need to be done with $MR^{-/-}$ BM(GM-CSF) cells stimulated with isolated sMR in the presence or absence of CTLD ligands (e.g. OVA or mannan). Furthermore, CD45 phosphatase activity assay with these stimulated BM(GM-CSF) cells should be performed.

The incubation of BM(GM-CSF) cells with either FcMR or sMR resulted in a slightly increase of total phosphotyrosine proteins in these cells indicating an influence of MR on

intracellular processes of BM(GM-CSF) cells. So, of extraordinary interest is the effect of MR on signalling pathways and metabolic processes in BM(GM-CSF) cells. Therefor, it is important to investigate transcriptional reprogramming in BM(GM-CSF) cells by transcriptome analysis of MR-stimulated BM(GM-CSF) cells. Thus, a MR-mediated influence on JAK/STAT pathway might be confirmed and connected or other involved intracellular processes can be discovered. To further clarify the role of serum sMR in HFD and obesity co-culture experiments should be performed with sMR-treated BM(GM-CSF) cells and adipocytes. Equally, it is essential to investigate a direct influence of sMR on adipocytes by analysing lipid metabolism of MR-treated adipocytes.

8. References

1. Medzhitov, R. & Janeway Jr., C. A. Innate immunity: impact on the adaptive immune response. *Curr Opin Immunol* **9,** 4–9 (1997).
2. Janeway Jr., C. A. The immune system evolved to discriminate infectious nonself from noninfectious self. *Immunol Today* **13,** 11–16 (1992).
3. Medzhitov, R. & Janeway Jr., C. A. Innate immunity: the virtues of a nonclonal system of recognition. *Cell* **91,** 295–298 (1997).
4. Parkin, J. & Cohen, B. An overview of the immune system. *Lancet* **357,** 1777–1789 (2001).
5. Hemmi, H. & Akira, S. TLR signalling and the function of dendritic cells. *Chem. Immunol. Allergy* **86,** 120–135 (2005).
6. Banchereau, J. *et al.* Immunobiology of dendritic cells. *Annu Rev Immunol* **18,** 767–811 (2000).
7. Palucka, K. & Banchereau, J. Dendritic cells: a link between innate and adaptive immunity. *J Clin Immunol* **19,** 12–25 (1999).
8. Banchereau, J. & Steinman, R. M. Dendritic cells and the control of immunity. *Nature* **392,** 245–252 (1998).
9. Guermonprez, P., Valladeau, J., Zitvogel, L., Thery, C. & Amigorena, S. Antigen presentation and T cell stimulation by dendritic cells. *Annu Rev Immunol* **20,** 621–667 (2002).
10. Blum, J. S., Wearsch, P. A. & Cresswell, P. *IY31CH16-Cresswell Pathways of Antigen Processing. Annu. Rev. Immunol* **31,** (2013).
11. Burgdorf, S., Lukacs-kornek, V. & Kurts, C. The Mannose Recepto Mediates Uptake of Soluble but Not ofCell-Associated Antigen for Cross-Presentation. *J. Immunol.* (2006).
12. Crotzer, V. L. & Blum, J. S. Autophagy and adaptive immunity. *Immunology* **131,** 9–17 (2010).
13. Bousso, P. T-cell activation by dendritic cells in the lymph node: lessons from the movies. *Nat. Rev. Immunol.* **8,** 675–84 (2008).
14. Mustelin, T. & Tasken, K. Positive and negative regulation of T-cell activation through kinases and phosphatases. *Biochem J* **371,** 15–27 (2003).
15. Kaplan, M. H., Hufford, M. M. & Olson, M. R. The development and in vivo function of T helper 9 cells. *Nat. Rev. Immunol.* **15,** 295–307 (2015).
16. Bettelli, E. *et al.* Reciprocal developmental pathways for the generation of pathogenic effector TH17 and regulatory T cells. *Nature* **441,** 235–238 (2006).
17. Hirahara, K. & Nakayama, T. CD4+ T-cell subsets in inflammatory diseases: Beyond the Th1/Th2 paradigm. *International Immunology* **28,** 163–171 (2016).
18. Stanford, S. M., Rapini, N. & Bottini, N. Regulation of TCR signalling by tyrosine phosphatases: from immune homeostasis to autoimmunity. *Immunology* **137,** 1–19 (2012).
19. Qian, D. & Weiss, A. T cell antigen receptor signal transduction. *Curr Opin Cell Biol* **9,** 205–212 (1997).
20. van Leeuwen, J. E. & Samelson, L. E. T cell antigen-receptor signal transduction. *Curr Opin Immunol* **11,** 242–248 (1999).
21. Weiss, a. & Littman, D. R. Signal transduction by lymphocyte antigen receptors. *Cell* **76,** 263–274 (1994).
22. Thomas, M. L. The leukocyte common antigen family. *Annu. Rev. Immunol.* **7,** 339–369 (1989).
23. Hermiston, M. L., Xu, Z. & Weiss, A. CD45: a critical regulator of signaling thresholds in immune cells. *Annu Rev Immunol* **21,** 107–137 (2003).

24. Desai, D. M., Sap, J., Silvennoinen, O., Schlessinger, J. & Weiss, A. The catalytic activity of the CD45 membrane-proximal phosphatase domain is required for TCR signaling and regulation. *EMBO J.* **13,** 4002–10 (1994).
25. Wang, Y., Liang, L. & Esselman, W. J. Regulation of the calcium/NF-AT T cell activation pathway by the D2 domain of CD45. *J. Immunol.* **164,** 2557–64 (2000).
26. Johnson, P., Ostergaard, H. L., Wasden, C. & Trowbridge, I. S. Mutational analysis of CD45. A leukocyte-specific protein tyrosine phosphatase. *J Biol Chem* **267,** 8035–8041 (1992).
27. Okumura, M. *et al.* Comparison of CD45 extracellular domain sequences from divergent vertebrate species suggests the conservation of three fibronectin type III domains. *J. Immunol.* **157,** 1569–75 (1996).
28. Majeti, R. *et al.* An inactivating point mutation in the inhibitory wedge of CD45 causes lymphoproliferation and autoimmunity. *Cell* **103,** 1059–1070 (2000).
29. Harvath, L., Balke, J. A., Christiansen, N. P., Russell, A. A. & Skubitz, K. M. Selected antibodies to leukocyte common antigen (CD45) inhibit human neutrophil chemotaxis. *J Immunol* **146,** 949–957 (1991).
30. Saunders, A. E. & Johnson, P. Modulation of immune cell signalling by the leukocyte common tyrosine phosphatase, CD45. *Cell Signal* **22,** 339–348 (2010).
31. Lorenz, H. M. *et al.* CD45 mAb induces cell adhesion in peripheral blood mononuclear cells via lymphocyte function-associated antigen-1 (LFA-1) and intercellular cell adhesion molecule 1 (ICAM-1). *Cell. Immunol.* **147,** 110–128 (1993).
32. Shenoi, H., Seavitt, J., Zheleznyak, A., Thomas, M. L. & Brown, E. J. Regulation of integrin-mediated T cell adhesion by the transmembrane protein tyrosine phosphatase CD45. *J Immunol* **162,** 7120–7127 (1999).
33. Prickett, T. C. & Hart, D. N. Anti-leucocyte common (CD45) antibodies inhibit dendritic cell stimulation of CD4 and CD8 T-lymphocyte proliferation. *Immunology* **69,** 250–256 (1990).
34. Cross, J. L., Kott, K., Miletic, T. & Johnson, P. CD45 regulates TLR-induced proinflammatory cytokine and IFN-beta secretion in dendritic cells. *J. Immunol.* **180,** 8020–8029 (2008).
35. Montoya, M. *et al.* CD45 is required for type I IFN production by dendritic cells. *Eur. J. Immunol.* **36,** 2150–2158 (2006).
36. Piercy, J., Petrova, S., Tchilian, E. Z. & Beverley, P. C. L. CD45 negatively regulates tumour necrosis factor and interleukin-6 production in dendritic cells. *Immunology* **118,** 250–256 (2006).
37. Trop, S., Charron, J., Arguin, C., Lesage, S. & Hugo, P. Thymic selection generates T cells expressing self-reactive TCRs in the absence of CD45. *J. Immunol.* **165,** 3073–9 (2000).
38. Kung, C. *et al.* Mutations in the tyrosine phosphatase CD45 gene in a child with severe combined immunodeficiency disease. *Nat Med* **6,** 343–345 (2000).
39. Tchilian, E. Z. *et al.* The exon A (C77G) mutation is a common cause of abnormal CD45 splicing in humans. *J. Immunol.* **166,** 6144–6148 (2001).
40. Kishihara, K. *et al.* Normal B lymphocyte development but impaired T cell maturation in CD45-Exon6 protein tyrosine phosphatase-deficient mice. *Cell* **74,** 143–156 (1993).
41. Mee, P. J. *et al.* Greatly reduced efficiency of both positive and negative selection of thymocytes in CD45 tyrosine phosphatase-deficient mice. *Eur. J. Immunol.* **29,** 2923–33 (1999).
42. Byth, K. F. *et al.* CD45-null transgenic mice reveal a positive regulatory role for CD45 in early thymocyte development, in the selection of CD4+CD8+

thymocytes, and B cell maturation. *J. Exp. Med.* **183,** 1707–18 (1996).
43. D'Oro, U., Sakaguchi, K., Appella, E. & Ashwell, J. D. Mutational analysis of Lck in CD45-negative T cells: dominant role of tyrosine 394 phosphorylation in kinase activity. *Mol. Cell. Biol.* **16,** 4996–5003 (1996).
44. D'Oro, U. & Ashwell, J. D. Cutting edge: the CD45 tyrosine phosphatase is an inhibitor of Lck activity in thymocytes. *J. Immunol.* **162,** 1879–83 (1999).
45. Burns, C. M., Sakaguchi, K., Appella, E. & Ashwell, J. D. CD45 regulation of tyrosine phosphorylation and enzyme activity of src family kinases. *J. Biol. Chem.* **269,** 13594–13600 (1994).
46. Baker, M. *et al.* Development of T-leukaemias in CD45 tyrosine phosphatase-deficient mutant lck mice. *EMBO J.* **19,** 4644–54 (2000).
47. Fecteau, S. *et al.* CTLA-4 up-regulation plays a role in tolerance mediated by CD45. *Nat. Immunol.* **2,** 58–63 (2001).
48. Irie-Sasaki, J. *et al.* CD45 is a JAK phosphatase and negatively regulates cytokine receptor signalling. *Nature* **409,** 349–354 (2001).
49. Penninger, J. M., Irie-Sasaki, J., Sasaki, T. & Oliveira-dos-Santos, a J. CD45: new jobs for an old acquaintance. *Nat. Immunol.* **2,** 389–396 (2001).
50. Yamada, T., Zhu, D., Saxon, A. & Zhang, K. CD45 controls interleukin-4-mediated IgE class switch recombination in human B cells through its function as a Janus kinase phosphatase. *J Biol Chem* **277,** 28830–28835 (2002).
51. Walzel, H., Schulz, U., Neels, P. & Brock, J. Galectin-1, a natural ligand for the receptor-type protein tyrosine phosphatase CD45. *Immunol. Lett.* **67,** 193–202 (1999).
52. van Vliet, S. J., Gringhuis, S. I., Geijtenbeek, T. B. H. & van Kooyk, Y. Regulation of effector T cells by antigen-presenting cells via interaction of the C-type lectin MGL with CD45. *Nat. Immunol.* **7,** 1200–1208 (2006).
53. Martínez-Pomares, L. *et al.* Cell-specific glycoforms of sialoadhesin and CD45 are counter-receptors for the cysteine-rich domain of the mannose receptor. *J. Biol. Chem.* **274,** 35211–35218 (1999).
54. Martinez-Pomares, L. The mannose receptor. *J. Leukoc. Biol.* **92,** 1177–86 (2012).
55. Stahl, P. D. & Ezekowitz, R. a. The mannose receptor is a pattern recognition receptor involved in host defense. *Curr. Opin. Immunol.* **10,** 50–55 (1998).
56. Sallusto, F., Cella, M., Danieli, C. & Lanzavecchia, A. Dendritic cells use macropinocytosis and the mannose receptor to concentrate macromolecules in the major histocompatibility complex class II compartment: downregulation by cytokines and bacterial products. *J. Exp. Med.* **182,** 389–400 (1995).
57. Taylor, P. R., Gordon, S. & Martinez-Pomares, L. The mannose receptor: Linking homeostasis and immunity through sugar recognition. *Trends in Immunology* **26,** 104–110 (2005).
58. Fiete, D. J., Beranek, M. C. & Baenziger, J. U. A cysteine-rich domain of the 'mannose' receptor mediates GalNAc-4-SO4 binding. *Proc. Natl. Acad. Sci. U. S. A.* **95,** 2089–2093 (1998).
59. Martínez-Pomares, L. *et al.* Fc chimeric protein containing the cysteine-rich domain of the murine mannose receptor binds to macrophages from splenic marginal zone and lymph node subcapsular sinus and to germinal centers. *J. Exp. Med.* **184,** 1927–37 (1996).
60. Martinez-Pomares, L. *et al.* Carbohydrate-independent recognition of collagens by the macrophage mannose receptor. *Eur. J. Immunol.* **36,** 1074–1082 (2006).
61. Madsen, D. H. *et al.* The non-phagocytic route of collagen uptake: A distinct degradation pathway. *J. Biol. Chem.* **286,** 26996–27010 (2011).
62. Malovic, I. *et al.* The mannose receptor on murine liver sinusoidal endothelial cells

is the main denatured collagen clearance receptor. *Hepatology* **45,** 1454–1461 (2007).
63. Kruskal, B. A., Sastry, K., Warner, A. B., Mathieu, C. E. & Ezekowitz, R. A. Phagocytic chimeric receptors require both transmembrane and cytoplasmic domains from the mannose receptor. *J. Exp. Med.* **176,** 1673–80 (1992).
64. Schweizer, A., Stahl, P. D. & Rohrer, J. A di-aromatic motif in the cytosolic tail of the mannose receptor mediates endosomal sorting. *J. Biol. Chem.* **275,** 29694–29700 (2000).
65. Martínez-Pomares, L. *et al.* A functional soluble form of the murine mannose receptor is produced by macrophages in vitro and is present in mouse serum. *J. Biol. Chem.* **273,** 23376–23380 (1998).
66. Gazi, U. *et al.* Fungal recognition enhances mannose receptor shedding through dectin-1 engagement. *J. Biol. Chem.* **286,** 7822–7829 (2011).
67. Fraser, I. P. *et al.* Pneumocystis carinii enhances soluble mannose receptor production by macrophages. *Microbes Infect.* **2,** 1305–1310 (2000).
68. Rødgaard-Hansen, S. *et al.* A soluble form of the macrophage-related mannose receptor (MR/CD206) is present in human serum and elevated in critical illness. *Clin. Chem. Lab. Med.* **52,** 453–461 (2014).
69. Andersen, M. N. *et al.* The novel biomarker of alternative macrophage activation, soluble mannose receptor (sMR/sCD206): Implications in multiple myeloma. *Leuk. Res.* **39,** 971–975 (2015).
70. Grønbæk, H. *et al.* Macrophage activation markers predict mortality in patients with liver cirrhosis without or with acute-on-chronic liver failure (ACLF). *J. Hepatol.* **64,** 813–822 (2016).
71. Burgdorf, S., Schölz, C., Kautz, A., Tampé, R. & Kurts, C. Spatial and mechanistic separation of cross-presentation and endogenous antigen presentation. *Nat. Immunol.* **9,** 558–66 (2008).
72. Stein, M., Keshav, S., Harris, N. & Gordon, S. Interleukin 4 potently enhances murine macrophage mannose receptor activity: a marker of alternative immunologic macrophage activation. *J. Exp. Med.* **176,** 287–92 (1992).
73. Martinez-Pomares, L. *et al.* Analysis of mannose receptor regulation by IL-4, IL-10, and proteolytic processing using novel monoclonal antibodies. *J. Leukoc. Biol.* **73,** 604–613 (2003).
74. Kel, J. *et al.* Soluble mannosylated myelin peptide inhibits the encephalitogenicity of autoreactive T cells during experimental autoimmune encephalomyelitis. *Am. J. Pathol.* **170,** 272–80 (2007).
75. Chieppa, M. *et al.* Cross-Linking of the Mannose Receptor on Monocyte-Derived Dendritic Cells Activates an Anti-Inflammatory Immunosuppressive Program. *J. Immunol.* **171,** 4552–4560 (2003).
76. Mascarell, L. *et al.* Oral macrophage-like cells play a key role in tolerance induction following sublingual immunotherapy of asthmatic mice. *Mucosal Immunol.* **4,** 638–647 (2011).
77. Allavena, P. *et al.* Engagement of the Mannose receptor by tumoral mucins activates an immune suppressive phenotype in human tumor-associated macrophages. *Clin. Dev. Immunol.* **2010,** (2010).
78. Höchst, B. *et al.* Liver sinusoidal endothelial cells contribute to CD8 T cell tolerance toward circulating carcinoembryonic antigen in mice. *Hepatology* **56,** 1924–33 (2012).
79. Schuette, V. *et al.* Mannose receptor induces T-cell tolerance via inhibition of CD45 and up-regulation of CTLA-4. *Proc. Natl. Acad. Sci. U. S. A.* **113,** (2016).
80. Schonrich, G. *et al.* Down-regulation of T cell receptors on self-reactive T cells as

a novel mechanism for extrathymic tolerance induction. *Cell* **65,** 293–304 (1991).
81. Lee, S. J. *et al.* Mannose receptor-mediated regulation of serum glycoprotein homeostasis. *Science* **295,** 1898–1901 (2002).
82. Shinkai, Y. *et al.* RAG-2-deficient mice lack mature lymphocytes owing to inability to initiate V(D)J rearrangement. *Cell* **68,** 855–867 (1992).
83. Hogquist, K. A. *et al.* T cell receptor antagonist peptides induce positive selection. *Cell* **76,** 17–27 (1994).
84. Barnden, M. J., Allison, J., Heath, W. R. & Carbone, F. R. Defective TCR expression in transgenic mice constructed using cDNA-based alpha- and beta-chain genes under the control of heterologous regulatory elements. *Immunol. Cell Biol.* **76,** 34–40 (1998).
85. Graham, F. L., Smiley, J., Russell, W. C. & Nairn, R. Characteristics of a human cell line transformed by DNA from human adenovirus type 5. *J. Gen. Virol.* **36,** 59–74 (1977).
86. Lundblad, A. *et al.* IMMUNOCHEMICAL STUDIES ON MOUSE MYELOMA PROTEINS WITH SPECIFICITY FOR DEXTRAN OR FOR LEVAN*. **9,** 535–544 (1972).
87. Ljunggren, H. G. & Kärre, K. Host resistance directed selectively against H-2-deficient lymphoma variants. Analysis of the mechanism. *J. Exp. Med.* **162,** 1745–59 (1985).
88. Watt, S. M., Gilmore, D. J., Davis, J. M., Clark, M. R. & Waldmann, H. Cell-surface markers on haemopoietic precursors. Reagents for the isolation and analysis of progenitor cell subpopulations. *Molecular and Cellular Probes* **1,** 297–326 (1987).
89. Pozzi, L.-A. M., Maciaszek, J. W. & Rock, K. L. Both Dendritic Cells and Macrophages Can Stimulate Naive CD8 T Cells In Vivo to Proliferate, Develop Effector Function, and Differentiate into Memory Cells. *J. Immunol.* **175,** 2071–2081 (2005).
90. Lutz, M. B. *et al.* An advanced culture method for generating large quantities of highly pure dendritic cells from mouse bone marrow. *J. Immunol. Methods* **223,** 77–92 (1999).
91. Lutz, M. B., Inaba, K., Schuler, G. & Romani, N. Still Alive and Kicking: In-Vitro-Generated GM-CSF Dendritic Cells! *Immunity* **44,** 1–2 (2016).
92. Helft, J. *et al.* GM-CSF Mouse Bone Marrow Cultures Comprise a Heterogeneous Population of CD11c+MHCII+ Macrophages and Dendritic Cells. *Immunity* **42,** 1197–1211 (2015).
93. Murray, P. J. *et al.* Macrophage Activation and Polarization: Nomenclature and Experimental Guidelines. *Immunity* **41,** 14–20 (2014).
94. Holmes, N. CD45: All is not yet crystal clear. *Immunology* **117,** 145–155 (2006).
95. Roach, T. *et al.* CD45 regulates Src family member kinase activity associated with macrophage integrin-mediated adhesion. *Current Biology* **7,** 408–417 (1997).
96. Trowbridge, I. S. & Thomas, M. L. CD45: An Emerging Role as a Protein Tyrosine Phosphatase Required for Lymphocyte Activation and Development - annurev.iy.12.040194.000505. *Annu. Rev. Immunol.* **12,** 85–116 (1994).
97. Parsons, S. J. & Parsons, J. T. Src family kinases, key regulators of signal transduction. *Oncogene* **23,** 7906–7909 (2004).
98. Babon, J. J., Lucet, I. S., Murphy, J. M., Nicola, N. A. & Varghese, L. N. The molecular regulation of Janus kinase (JAK) activation. *Biochem. J.* **462,** 1–13 (2014).
99. Bromberg, J. & Darnell Jr, J. E. The role of STATs in transcriptional control and their impact on cellular function.
100. Kazi, J. U., Kabir, N. N., Flores-Morales, A. & Rönnstrand, L. SOCS proteins in

regulation of receptor tyrosine kinase signaling. *Cell. Mol. Life Sci.* **71,** 3297–310 (2014).
101. Jordens, R., Thompson, A., Amons, R. & Koning, F. Human dendritic cells shed a functional, soluble form of the mannose receptor. *Int. Immunol.* **11,** 1775–1780 (1999).
102. Zeyda, M. & Stulnig, T. M. Adipose tissue macrophages. *Immunol Lett* **112,** 61–67 (2007).
103. Moreno-Navarrete, J. M. *et al.* The MRC1/CD68 Ratio Is Positively Associated with Adipose Tissue Lipogenesis and with Muscle Mitochondrial Gene Expression in Humans. *PLoS One* **8,** (2013).
104. Adler, A. J. *et al.* CD4+ T cell tolerance to parenchymal self-antigens requires presentation by bone marrow-derived antigen-presenting cells. *J. Exp. Med.* **187,** 1555–64 (1998).
105. Kurts, C., Kosaka, H., Carbone, F. R., Miller, J. F. & Heath, W. R. Class I-restricted cross-presentation of exogenous self-antigens leads to deletion of autoreactive CD8(+) T cells. *J. Exp. Med.* **186,** 239–45 (1997).
106. Cheng, F. *et al.* A Critical Role for Stat3 Signaling in Immune Tolerance. *Immunity* **19,** 425–436 (2003).
107. Linehan, S. A., Martínez-Pomares, L., Stahl, P. D. & Gordon, S. Mannose Receptor and Its Putative Ligands in Normal Murine Lymphoid and Nonlymphoid Organs: In Situ Expression of Mannose Receptor by Selected Macrophages, Endothelial Cells, Perivascular Microglia, and Mesangial Cells, but not Dendritic Cells. *J. Exp. Med* **189,** 1961–1972 (1999).
108. Tchilian, E. Z. & Beverley, P. C. L. Altered CD45 expression and disease. *Trends Immunol.* **27,** 146–153 (2006).
109. Thiel, N., Zischke, J., Elbasani, E., Kay-Fedorov, P. & Messerle, M. Viral interference with functions of the cellular receptor tyrosine phosphatase CD45. *Viruses* **7,** 1540–1557 (2015).
110. St-Pierre, J. & Ostergaard, H. L. A Role for the Protein Tyrosine Phosphatase CD45 in Macrophage Adhesion through the Regulation of Paxillin Degradation. *PLoS One* **8,** (2013).
111. Harburger, D. S. & Calderwood, D. A. Integrin signalling at a glance. *J. Cell Sci.* **122,** 159–163 (2009).
112. Hugues, S., Boissonnas, A., Amigorena, S. & Fetler, L. The dynamics of dendritic cell-T cell interactions in priming and tolerance. *Current Opinion in Immunology* **18,** 491–495 (2006).
113. Bakocević, N., Worbs, T., Davalos-Misslitz, A. & Förster, R. T cell-dendritic cell interaction dynamics during the induction of respiratory tolerance and immunity. *J. Immunol.* **184,** 1317–27 (2010).
114. Michelet, X. *et al.* MHC class II presentation is controlled by the lysosomal small GTPase, Arl8b. *J. Immunol.* **194,** 2079–88 (2015).
115. Luckashenak, N. *et al.* Constitutive Crosspresentation of Tissue Antigens by Dendritic Cells Controls CD8+ T Cell Tolerance In Vivo. *Immunity* **28,** 521–532 (2008).
116. Medzhitov, R. Innate immune recognition and control of adaptive immune responses. *Semin. Immunol.* **10,** 351–353 (1998).
117. Xu, Z. & Weiss, A. Negative regulation of CD45 by differential homodimerization of the alternatively spliced isoforms. *Nat. Immunol.* **3,** 764–71 (2002).
118. Ostergaard, H. L. *et al.* Expression of CD45 alters phosphorylation of the Ick-encoded tyrosine protein kinase in murine lymphoma T-cell lines (L-CA/T200/p56kk/phosphotyrosine phosphatase/lymphocyte growth regulation).

Immunology **86,** 8959–8963 (1989).
119. Lillemeier, B. F., Pfeiffer, J. R., Surviladze, Z., Wilson, B. S. & Davis, M. M. Plasma membrane-associated proteins are clustered into islands attached to the cytoskeleton. *Proc. Natl. Acad. Sci. U. S. A.* **103,** 18992–18997 (2006).
120. Biessen, E. A. L. *et al.* Lysine-based cluster mannosides that inhibit ligand binding to the human mannose receptor at nanomolar concentration. *J. Biol. Chem.* (1996). doi:10.1074/jbc.271.45.28024
121. Rawlings, J. S., Rosler, K. M. & Harrison, D. A. The JAK/STAT signaling pathway. *J. Cell Sci.* **117,** 1281–1283
122. Wang, T. *et al.* Regulation of the innate and adaptive immune responses by Stat-3 signaling in tumor cells. *Nat. Med.* **10,** 48–54 (2004).
123. Nefedova, Y. *et al.* Hyperactivation of STAT3 is involved in abnormal differentiation of dendritic cells in cancer. *J. Immunol.* **172,** 464–474 (2004).
124. Lunz, J. G., Specht, S. M., Murase, N., Isse, K. & Demetris, A. J. Gut-derived commensal bacterial products inhibit liver dendritic cell maturation by stimulating hepatic interleukin-6/signal transducer and activator of transcription 3 activity. *Hepatology* (2007). doi:10.1002/hep.21906
125. Lin, A., Schildknecht, A., Nguyen, L. T. & Ohashi, P. S. Dendritic cells integrate signals from the tumor microenvironment to modulate immunity and tumor growth. *Immunology Letters* **127,** 77–84 (2010).
126. Hackenmiller, R., Kim, J., Feldman, R. A. & Simon, M. C. response to GM-CSF signaling implicates Fes in the. *Immunity* **13,** 397–407 (2000).
127. Takeda, K. *et al.* Enhanced Th1 Activity and Development of Chronic Enterocolitis in Mice Devoid of Stat3 in Macrophages and Neutrophils. *Immunity* **10,** 39–49 (1999).
128. Meraz, M. A. *et al.* Targeted Disruption of the Stat1 Gene in Mice Reveals Unexpected Physiologic Specificity in the JAK–STAT Signaling Pathway. *Cell* **84,** 431–442 (1996).
129. Durbin, J. E. *et al.* Targeted disruption of the mouse Stat1 gene results in compromised innate immunity to viral disease. *Cell* **84,** 443–50 (1996).
130. Pasieka, T. J., Lu, B. & Leib, D. A. Enhanced pathogenesis of an attenuated herpes simplex virus for mice lacking Stat1. *J. Virol.* **82,** 6052–5 (2008).
131. Kerrigan, A. M. & Brown, G. D. C-type lectins and phagocytosis. *Immunobiology* **214,** 562–575 (2009).
132. Stehle, S. E., Rogers, R. A., Harmsen[3], [2] A G & Ezekowitz, R. A. B. A Soluble Mannose Receptor Immunoadhesin Enhances Phagocytosis of Pneumocystis carinii by Human Polymorphonuclear Leukocytes In Vitro.
133. Andersen, E. S. *et al.* Macrophage-related serum biomarkers soluble CD163 (sCD163) and soluble mannose receptor (sMR) to differentiate mild liver fibrosis from cirrhosis in patients with chronic hepatitis C: A pilot study. *Eur. J. Clin. Microbiol. Infect. Dis.* **33,** 117–122 (2014).
134. Wynn, T. A. & Barron, L. Macrophages: Master regulators of inflammation and fibrosis. *Seminars in Liver Disease* **30,** 245–257 (2010).
135. Heymann, F., Trautwein, C. & Tacke, F. Monocytes and macrophages as cellular targets in liver fibrosis. *Inflamm. Allergy Drug Targets* **8,** 307–18 (2009).
136. Goh, J., Goh, K. P. & Abbasi, A. Exercise and Adipose Tissue Macrophages: New Frontiers in Obesity Research? *Front. Endocrinol. (Lausanne).* **7,** 1–8 (2016).
137. Linden, M. A., Pincu, Y., Martin, S. A., Woods, J. A. & Baynard, T. Moderate exercise training provides modest protection against adipose tissue inflammatory gene expression in response to high-fat feeding. *Physiol. Rep.* **2,** 1–13 (2014).

9. Abbreviations

°C	Degree Celsius
4-NPP	4-Nitrophenyl phosphate disodium salt hexahydrate
ABTS	2,2'-azino-bis(3-ethylbenzothiazoline-6-sulphonic acid)
APC	Antigen presenting cell
APS	Ammonium persulfate
AT	Adipose tissue
ATM	Adipose tissue macrophage
BBS	Borate buffered saline
BCA	Bicinchoninic acid
Bcl-6	B-cell lymphoma 6 protein
BCR	B cell receptor
BM	Bone marrow
BSA	Bovine serum albumin
CD	Cluster of differentiation
CFSE	Carboxyfluorescein succinimidyl ester
CHO	Chinese hamster ovary
cMR	Cellular MR
CR	Cysteine-rich
Csk	C-src tyrosine kinase
CTL	Cytotoxic T cell
CTLA-4	Cytotoxic T-lymphocyte antigen 4
CTLD	C-type lectin-like domain
Ctrl	Control
DC	Dendritic cell
DMEM	Dulbecco's modified eagle's medium
DNA	Deoxyribonucleic acid
DTT	Dithiothreitol
EAE	Experimental autoimmune encephalomyelitis
ECL	Enhanced chemiluminescence
EDTA	Ethylenediaminetetraacetic acid
ELISA	Enzyme-linked immunosorbent assay
ER	Endoplasmatic reticulum
FACS	Fluorescence-activated cell sorting
FcMR	Recombinant MR construct comprising the CR, FN II, and CTLD1-2 domains of the MR
FCS	Fetal calf serum
FN	Fibronectin
GAPDH	Glyceraldehyde 3-phosphate dehydrogenase
GM-CSF	Granulocyte-macrophage colony-stimulating factor
h, min, sec	Hours, minutes, seconds
Hck	Tyrosine-protein kinase Hck
HCV	Hepatitis C virus

HEK	Human Embryonic Kidney
HEPES	4-(2-hydroxyethyl)-1-piperazineethanesulfonic acid
HFD	High-fat diet
HPRT	Hypoxanthine phosphoribosyltransferase
HRP	Horseradish peroxidase
IFN	Interferon
IgG, IgE	Immunoglobulin G, immunoglobulin E
IL	Interleukin
IMDM	Iscove's modified 87ulbecco's medium
IP	Immunoprezipitation
ITAM	Immunoreceptor tyrosine-base activation motif
JAK	Janus kinase
kDa	Kilodalton
LAT	Linker of activated T cells
LB	Laemmli buffer
Lck	Lymphocyte-specific protein tyrosine kinase
LFD	Low-fat diet
LPS	Lipopolysaccharide
LSEC	Liver sinusoidal endothelial cell
Lyn	Tyrosine-protein kinase Lyn
LYP	Lymphoid-tyrosine phosphatase
M-CSF	Macrophage colony-stimulating factor
mA	Milliampere
MAPK	Mitogen-activated protein kinase
MGL	Macrophage galactose-type lectin
MHC	Major histocompatibility complex
MIIC	MHC class II-rich compartment
MR	Mannose receptor
$MR^{-/-}$, $CD45^{-/-}$, $c\text{-}fes^{-/-}$	MR-, CD45-, c-fes-deficient
mRNA	Messenger RNA
MΦ	Macrophage
NAFLD	Non-alcoholic fatty liver disease
NaPOX	NeutrAvidin horseradish peroxidase
NASH	Non-alcoholic steatohepatitis
NF-κB	Nuclear factor kappa-light-chain-enhancer of activated B cells
NK	Natural killer
nm, μm, mm, cm	Nano-, micro-, milli-, centimeter
nM, μM, mM, M	Nano-, micro-, milli-, Molar
O/N	Overnight
OD	Optical density
OVA	Ovalbumin
PAGE	Polyacrylamide gel electrophoresis
PAMP	Pathogen-associated molecular pattern
PBS	Phosphate buffered saline

PBST	Phosphate buffered saline with Tween
PD-L1, PD-L2	Programmed death-ligand 1 and 2
pg, ng, µg, mg	Pico-, nano-, micro-, milligram
PNGase F	Peptide N-glycanase F
PPIA	Peptidylprolyl isomerase A
PRR	Pattern recognition receptor
PTK	Protein tyrosine kinase
PTP	Protein tyrosine phosphatase
qRT-PCR	Quantitative Real-time polymerase chain reaction
rcf	Relative centrifugal force
RNA	Ribonucleic acid
RPMI	Roswell park memorial institute medium
RT	Room temperature
SCID	Severe-combined immunodeficiency
SDS	Sodium dodecyl sulfate
SEE	Stable early endosome
SEM	Standard error of the mean
SFK	Src family protein tyrosine kinases
SH2	Src homology 2
SHP-1	Src homology region 2 domain-containing phosphatase-1
SLE	Systemic lupus erythematosus
SLIT	Sublingual immunotherapy
SLP-76	SH2 domain containing leukocyte protein of 76 kDa
sMR	Soluble MR
SOCS	Suppressor of cytokine signaling
STAT	Signal transducer and activator of transcription protein
TBP	TATA-box binding protein
TBS	Tris buffered saline
TBST	Tris buffered saline with Tween
TCR	T cell receptor
TEA	Triethanolamine
TEMED	Tetramethylethylenediamine
T_{FH}	T follicular-helper cell
Th1, Th2, Th9, Th17	T helper 1, T helper 2, T helper 9, T helper 17 cell
TLR	Toll-like receptor
TMB	3,3',5,5'-Tetramethylbenzidine
T_{reg}	T-regulatory cell
Trf	Transferrin
V	Volt
v/v	Volume to volume
W	Watt
w/, w/o	With, without
w/v	Weight to volume
wt	Wildtype

ZAP-70	Zeta-chain-associated protein kinase 70
μL, mL, L	Micro-, milli-, liter

10. Acknowledgments

This thesis and the whole work have greatly benefit from the support of various people, some of whom I would like to thank here.

First of all, I would like to thank Prof. Dr. Sven Burgdorf for the possibility to do my PhD thesis in his research group. It has been a privilege to work with him and to benefit from his assistance and support during the whole time of my thesis.

Furthermore, I would like to thank the examination board to spend the time on the evaluation of my thesis.

Special thanks got to the entire Burgdorf group for a wonderful teamwork, enjoyable moments, and instructive time in the lab. Verena Schütte, thank you for you help and answers to my questions and all the constructive conversations. Additionally, I have to thank all of my students I guided during my thesis. Especially, Frederike Harms, Jonas Schulte-Schrepping and Hannah Kemmer who not only spend many time and effort in my project but also awake my interest in apprenticeship.

I would also like to thank the other working groups of the LIMES institute. Without the helpful hand of so many people who provide me equipment and materials I could not realized important experiments as well as ideas I pursured.

And last but not least special thanks to my boyfriend Tom who always listened to me independent of talking about wonderful results as well as of complaining when everything went wrong again. Just listening was the best support you could give me.